Physiological Effects of Heterologous Expression of Proteorhodopsin Photosystems

by

Justin David Buck
Bachelor of Science, Chemical Engineering
Colorado School of Mines, 2004

Submitted to the Department of Biological Engineering
in partial fulfillment of the requirements for the degree of

Doctor of Philosophy in Biological Engineering

at the

Massachusetts Institute of Technology

February, 2012

Signature of Author: _____
Justin D. Buck
Department of Biological Engineering
January 6, 2012

Certified by: _____
Edward F. Delong
Professor of Civil and Environmental Engineering, and Biological Engineering
Thesis Advisor

Accepted by: _____
Forest White
Associate Professor of Biological Engineering
Course 20 Graduate Program Committee Chairperson

This doctoral thesis has been examined by a committee of the Biological Engineering Department as follows:

Chairperson, Graduate Thesis Committee: _____
John M. Essigmann
Professor of Chemistry, Toxicology and Biological Engineering

Thesis Advisor, Committee Member: _____
Edward F. DeLong
Department of Civil and Environmental, and Biological Engineering

Thesis Committee Member: _____
Kristala Jones Prather
Associate Professor of Chemical Engineering

Thesis Committee Member: _____
Michael Laub
Associate Professor of Biology

Physiological Effects of Heterologous Expression of Proteorhodopsin Photosystems

by

Justin David Buck

Submitted to the Department of Biological Engineering in partial fulfillment of the requirements for the degree of Doctor of Philosophy in Biological Engineering

Abstract

Proteorhodopsin (PR) phototrophy plays an important role in the marine ecosystem, harvesting energy from sunlight for a diverse community of hetertrophic organisms. The simple proteorhodopsin photosystem (PRPS) composed of six to seven genes is sufficient for producing a functional light-driven proton pump, capable of powering cellular processes. This thesis describes the functional characterization of a subcloned PRPS previously identified from a large insert metagenomic library (Martinez et al., 2007). Incorporation of the PRPS into a strain of *Pseudomonas putida* resulted in a light-dependent increase in viable cell yield of cultures grown in low carbon media. The light-dependent effect demonstrates a dependence on carbon, reducing at increasing carbon concentrations until no differential effect is observed. A survey of six PR-containing vectors from metagenomic libraries revealed PR transcription in two hosts, *P. putida* and *Pseudoalteromonas atlantica*, and of the three additional vectors with PRPS tested, two demonstrated the same qualitative light-dependent yield increase. This work illustrates the utility of a simple rhodopsin photosystem for supplementing the cellular energy system of a heterologous host, paving the way for future engineering applications in photoheterotrophy.

Advisor: Ed DeLong

Table of Contents

Chapter 1: Light Energy Harvesting and the Ecological Significance of Proteorhodopsin

Significance of Light Energy

The ability to harness the energy from solar radiation is an essential feature of building a sustainable society. Solar radiation is the greatest influx of energy to planet Earth. With an average flux in excess of 100 W/m^2 reaching the surface, the power available from the sun is more than 50,000 terrawatts, more than 10,000-fold greater than the current power usage of the United States (Brenner, 2006). As a result, the importance of solar energy as a renewable resource is unparalleled not only for human society but also for maintaining ordered biological systems and sustaining life.

Biological Light Capturing Mechanisms

Biology has been capturing the power of the sun for billions of years (Blankenship, 1992). Through this extensive period of history, a diverse range of biological components have evolved for the utilization of light energy. The most well-known group of these components are the oxygen-evolving photosynthetic pathways, found in plants as well as in many microbes, in which the energy of light is used to split water producing molecular oxygen and a high-energy source of reducing potential, which can be used for carbon fixation and biosynthesis (Voet and Voet, 2004). In addition to the oxygen-evolving systems, other related photosystems make use of alternate electron donors, such as hydrogen sulfide, as the source of reduction potential. A wide variety of these systems exist which have been tuned and modified to collect a wide spectrum of light wavelengths and to utilize the diversity of electron donors available in the various environments in which they evolved (Gottschalk, 1986). The key common feature to this class of photosystems, is the use of light energy for driving oxidation-reduction reactions. The storage of the energy in these photosystems is in two primary forms. The first is the energy contained in the high potential electrons of the reduced product which can be used for anabolic processes or

recycled for additional energy generation. The second form of energy conservation is in the generation of an electrochemical gradient across a lipid bilayer which can be used for chemiosmotic synthesis of the energy mediator adenosine triphosphate (ATP), driving transport processes, or powering flagellar motility. While the oxidative photosystems are energy-efficient and concomitantly generate usable reduction potential, these benefits come at the expense of complexity in these elaborate multi-protein structures.

An alternative light-harvesting mechanism is contained within a class of light-active proteins called opsins, rhodopsins, or retinylidene proteins. These proteins are broadly characterized as light-active transmembrane proteins which covalently bind a molecule of retinal (Spudich et al., 2000). Many of the proteins in this class behave as light-driven ion pumps (Oesterhelt and Stoeckenius, 1973; Beja et al., 2000b; Balashov et al., 2005). The pumping action of the protein allows the formation of an electrochemical gradient in which the absorbed radiation can be stored and used by the host, analogous to electrochemical potential produced by oxidative photosystems or respiratory chains. It is important to emphasize that in the case of rhodopsin-based light collection, the energy from the light is not used to drive any net oxidation-reduction reactions, and thus the light-harvesting process does not directly result in reduction potential for use in cellular metabolism. In contrast to the complex multi-protein complexes of the oxidative photosystems, rhodopsin-based photosystems are quite simple, often consisting of only the single rhodopsin protein and the retinal cofactor (Oesterhelt and Stoeckenius, 1971; Beja et al., 2000b).

Retinylidene Proteins (Rhodopsins)

Retinlylidene proteins, also known as rhodopsins, are integral membrane proteins which covalently bind a single cofactor retinal (vitamin A aldehyde) through the formation of a Schiff base with a lysine residue (Spudich et al., 2000). Rhodopsins fall into two categories based on primary sequence alignment, type I and type II (Spudich et al., 2000). Unlike the vast number of membrane proteins, the structure of rhodopsins is relatively well understood (Spudich et al.,

2000). Type I and type II rhodopsins have convergent secondary and tertiary structural homology, with several distinct differences still separating the two categories (Spudich et al., 2000). Type II rhodopsins contain significant hydrophilic loop regions which reside in the cytoplasm and serve to interact with other components of signaling (Spudich et al., 2000). No conclusive determination can be made as to the convergent or divergent evolutionary history of type I and type II rhodopsins, but the dramatic difference in primary sequence suggests a convergent evolution based the utility of retinal as a photoreceptor (Spudich et al., 2000).

Type II rhodopsins are found as the photoreceptors in eukaryotes, particularly as the pigments associated with vision (Spudich et al., 2000). Type II rhodopsins are also found as extra-ocular photoreceptor pinopsin, the retinal photoisomerase retinochrome, retinal G protein-coupled receptor (RGR), parapinopsin, VA opsin, melanopsin, peropsin, and encepalopsin (Spudich et al., 2000). An important feature of all rhodopsins is the formation of a salt bridge between the positive charge of the Schiff base and a nearby counterion residue, which plays a critical role in the photocycle (Spudich et al., 2000).

Type II rhodopsins bind the 11-cis form of retinal in the ground state; excitation of Type II rhodopsins results in a 11-cis to all-trans isomerization of the retinal, leading to structural changes in the protein (Spudich et al., 2000). Retinochrome and RGR are exceptions in which a light-dependent isomerization from all-trans to 11-cis serves to regenerate the 11-cis form of the chromophore (Hao and Fong, 1999). In contrast, type I rhodopsins bind all-trans retinal in the ground state with an isomerization leading the excited 13-cis form (Spudich et al., 2000). Another difference between type I and type II rhodopsins in the stereo chemistry of the active forms of retinal is the junction between the ring and the chain which takes the all-trans confirmation in type I rhodopsins and a cis confirmation in type II rhodopsins (Spudich et al., 2000).

The rest of this chapter will focus on the type I microbial rhodopsins found predominantly in archaea and bacteria.

Type I Rhodopsins

Type I rhodopsins, commonly known as microbial rhodopsins, encompass a wide range of physiological function from photosensing to ion transport (Spudich et al., 2000). Bacteriorhodopsin (BR) was the first type I rhodopsin identified (Oesterhelt and Stoeckenius, 1971). BR was isolated from the purple membranes of the extreme halophile *Halobacterium salinarum* (formerly known as *Halobacterium halobium*) (Stoeckenius and Kunau, 1968). Following the discovery of BR, three other rhodopsins were identified in *H. salinarum*, halorhodopsin (HR) (MacDonald et al., 1979), sensory rhodopsin I (SRI) (Bogomolni and Spudich, 1982) and sensory rhodopsin II (SRII) (Wolff et al., 1986). The various type I rhodopsins share a highly conserved protein structure and the retinal binding pocket and a moderate conservation of primary structure, but perform unique functions (Spudich et al., 2000). Bacteriorhodopsin is an outward proton pump (Oesterhelt and Stoeckenius, 1973); halorhodopsin is an inward chloride pump (Lanyi, 1986), and the sensory rhodopsins perform a sensory role associated with phototaxis (Spudich et al., 2000). Recently, additional type I proton-pumping rhodopsins have been discovered in bacteria including proteorhodopsin (PR) (Beja et al., 2000b), xanthorhodopsin (XR) (Balashov et al., 2005), and actinorhodopsin (Sharma et al., 2009). The phylogenetic relationship of type I rhodopsin amino acid sequences is depicted in the tree in Figure 1-1.

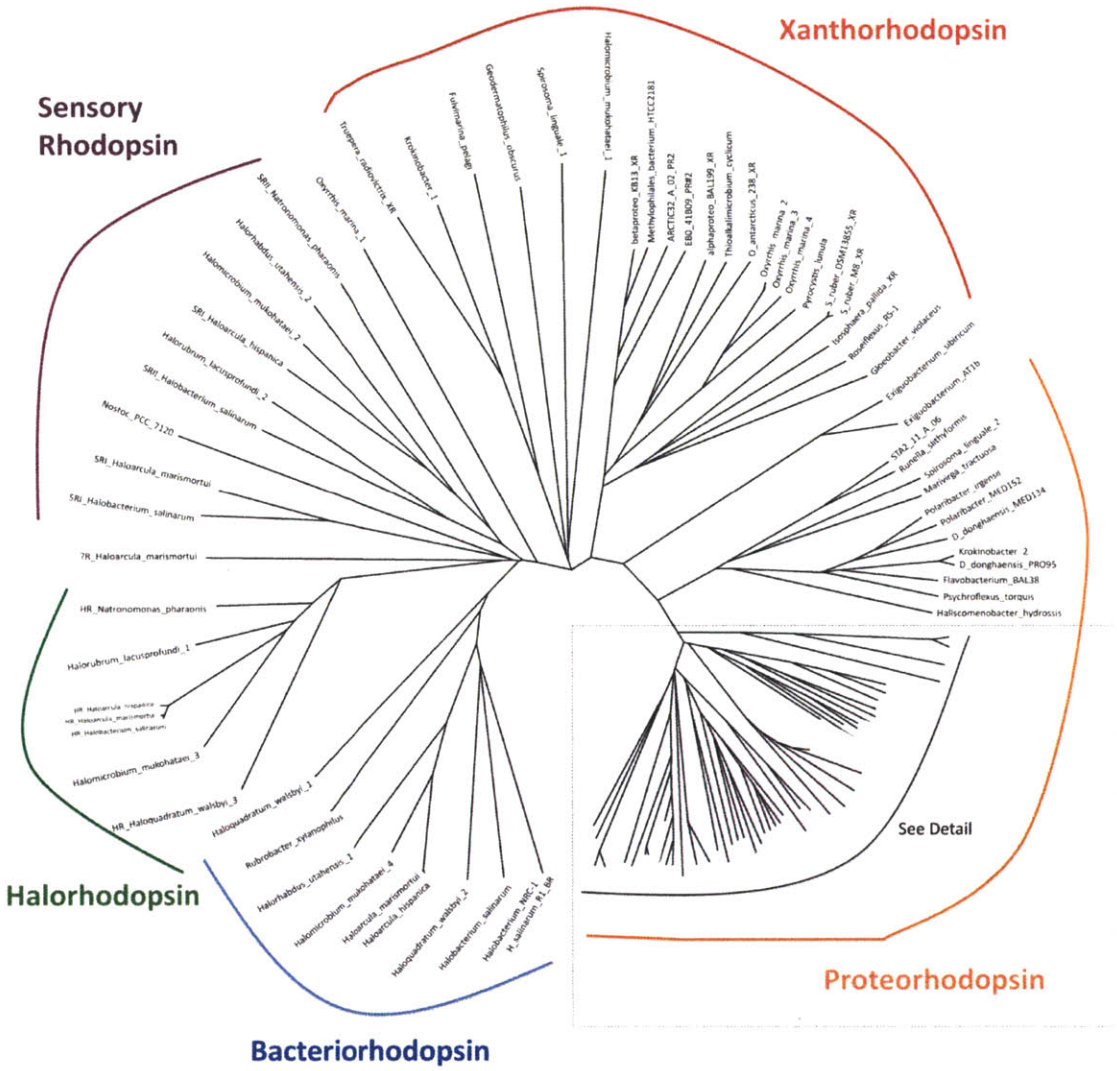

Figure 1-1: Phylogenetic Tree of Type 1 (Microbial) Rhodopsins from Inferred Amino Acid Sequences. Constructed with select sequences from GenBank from complete genome sequences containing rhodopsins. Tree constructed from a sequence alignment produced using ClustalX 2.0.10 with iteration at each step of alignment and a repeated iteration of the complete alignment, and the tree was drawn using the Drawtree program of Phylip 3.69. Major groupings include: Sensory Rhodopsins, Halorhodopsins, Bacteriorhodopsins, Xanthorhodopsins, and Proteorhodopsins. Detail box provided for proteorhodopsin generally corresponding to proteobacteria.

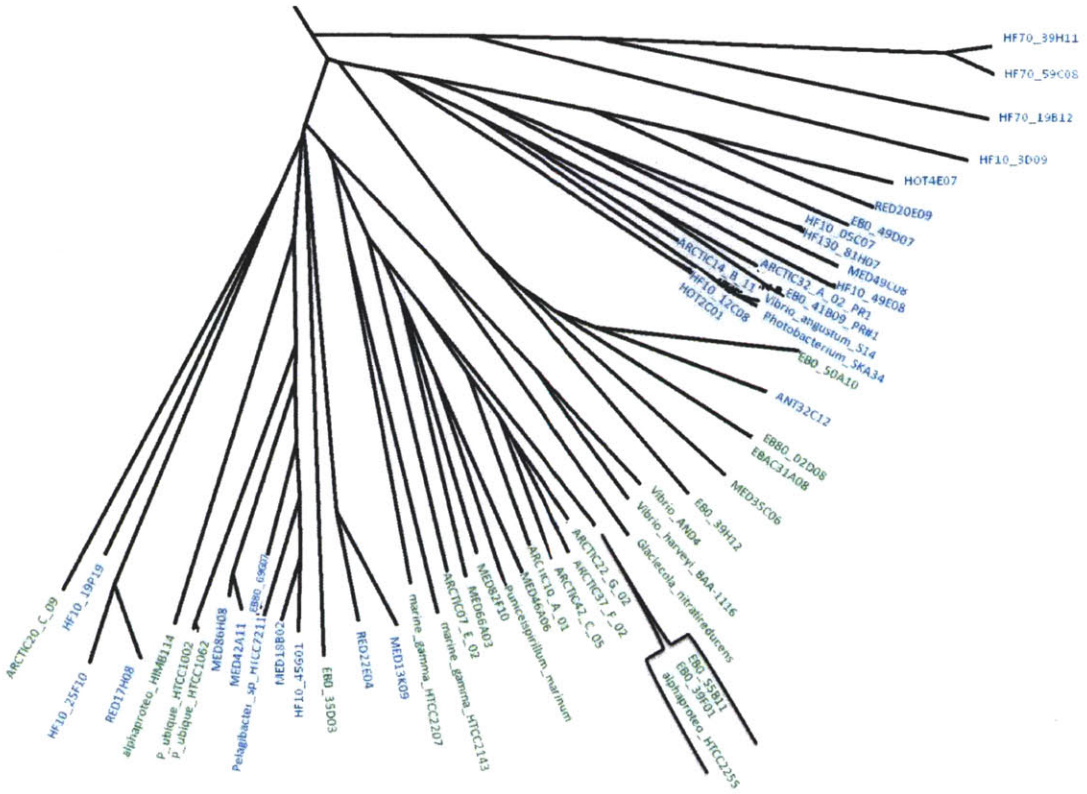

Continuation of Figure 1-1. Detail box of proteorhodopsin generally corresponding to proteobacteria. Text color indicates PR variant based either on experimental verification or predictation based on amino acid identity at the color tuning residue (position 105): green = green PR variants (leucine); blue = blue PR variants (glutamine).

Sensory Rhodopsins

The type I sensory rhodopsins, SRI and SRII, are photoreceptors which initiate a cascading phosphorylation event through the coupling of integral membrane transducer proteins, HtrI and HtrII (Spudich et al., 2000). The signaling resulting from the phosphorylation cascade is primarily related to phototaxis and control of the flagellar rotary motors (Hoff et al., 1997). SRI is an attractant receptor which directs cells toward longer wavelength light which can be used by the ion transporting rhodopsins during times of energy limitation (Spudich et al., 2000). SRII is a repellant receptor which directs cells away from short-wavelength blue light which potentially causes photooxidative damage (Spudich et al., 2000). In the absence of the HtrI transducer protein, SRI translocates protons across the membrane (Bogomolni et al., 1994; Haupts et al., 1995). Variants of SRII have also demonstrated proton pumping in the absence of HtrII (Iwamoto et al., 1999; Schmies et al., 2000). Sensory rhodopsins typically exhibit a photocycle which is on the time scale of hundreds of milliseconds to seconds (Spudich et al., 1995).

Halorhodopsin

Halorhodopsin is ion transporting type I rhodopsin which translocates a chloride ion from the periplasm across the plasma membrane into the cytoplasm (Lanyi, 1986). Halorhodopsin binds all-trans retinal (Alshuth et al., 1985) and has a peak absorbance around 580 nm (Greene et al., 1980). The chloride pumping action of halorhodopsin results in the formation of a trans-membrane electrical potential (MacDonald et al., 1979) which effects the mobility of other ions such as sodium (MacDonald et al., 1979) and hydrogen (Lanyi and MacDonald, 1979) across the membrane. The electrochemical potential-driven hydrogen ion transport can be used to generate ATP in a photophosphorylation process (Matsuno-Yagi and Mukohata, 1980).

Mechanistically, a chloride ion provides the counterion to the Schiff base opposed to a charged amino acid residue (Spudich et al., 2000). Halorhodopsin does not form the M

intermediate demonstrated by the other type I rhodopsins as the protonation of the Schiff base is stabilized by the chloride counterion (Varo et al., 1995). The proton-pumping bacteriorhodopsin can be transformed into a chloride pump through the mutagenesis of the aspartic acid residue at position 85 to a threonine (Sasaki et al., 1995). Switching the function of the two pumps (BR and HR) can also be accomplished by the addition of acidic solution to bacteriorhodopsin or azide to halorhodopsin (Bamberg et al., 1993; Varo et al., 1996).

Bacteriorhodopsin

The best characterized transport rhodopsin is the proton pump bacteriorhodopsin (BR). Proton pumps translocate protons across the cytoplasmic membrane creating proton motive force (PMF) for use in powering cellular machinery (Oesterhelt and Stoeckenius, 1973). BR was first identified in the purple membrane of *Halobacterium salinarum* (known as *Halobacterium halobium*) (Stoeckenius and Kunau, 1968) in which the microbial retinylidene protein was shown to be responsible for the pigmentation (Stoeckenius and Kunau, 1968; Oesterhelt and Stoeckenius, 1971). Following the identification of the retinal chromophore (Oesterhelt and Stoeckenius, 1971), it was identified that the all-trans and 13-cis forms were the isomers present in BR (Oesterhelt et al., 1973). It was shown that addition of hydroxylamine to whole cells removed the retinal chromophore (Oesterhelt et al., 1974) and that re-addition of exogenous retinal could reconstitute the BR (Oesterhelt and Schuhman, 1974). The binding site of retinal was revealed to be the lysine residue at position 216 (Lemke and Oesterhelt, 1981).

Observation of photobleaching of the BR and two distinct forms with absorbance maxima of 568 (dark adapted) and 412 (light adapted) began the study of the BR photocycle (Oesterhelt and Hess, 1973). The various intermediates in the photocycle, K, L, M, O were established through flash photolysis kinetic analysis of the BR absorbance spectrum (Kung et al., 1975; Lozier et al., 1975). The details of the photocycle and the proton transfer mechanism were pieced

together over the decades following the initial characterization of the BR photolysis (Lanyi, 2006).

The determination of the photocycle was enabled by structural information about the BR protein (Mendelsohn et al., 1974; Henderson, 1975; Henderson and Unwin, 1975). BR was one of the first integral membrane proteins crystallized (Michel and Oesterhelt, 1980), and it still remains one of the best structurally understood membrane proteins (Spudich et al., 2000) with structural resolution now available at the 1.55 angstrom level (Luecke et al., 1999). BR is often used as a reference to understand the mechanism of ion pumps and as an analogy to the proton translocation of the respiratory electron transport (Voet and Voet, 2004).

Proteorhodopsin

Proteorhodopsin (PR) was discovered through the sequencing of the large-insert marine metagenomic bacterial artificial chromosome (BAC) EBAC31A08 prepared from picoplankton DNA sampled from surface water in Monterey Bay (Beja et al., 2000b). A 16S small subunit rRNA sequence on the BAC identified the source organism as a gamma-proteobacterium of the SAR86 clade (Beja et al., 2000b). The function of the PR gene was predicted from the homology of the inferred amino acid sequence to BR and conservation of key structural residues supported the prediction (Beja et al., 2000b). The prediction of the PR gene as a member of the retinylidene protein family was confirmed by heterologous expression in *E. coli* in which the opsin protein successfully bound exogenous retinal (Beja et al., 2000b). In addition, the heterologously expressed protein demonstrated proton pumping behavior and fast photocycle kinetics expected of a bacteriorhodopsin homolog (Beja et al., 2000b). The peak absorbance wavelength was determined at 520 nm, in the green spectrum (Beja et al., 2000b). This discovery was the first observation of a rhodopsin from a bacterial source and the proton pumping function of the PR implied an new type of phototrophy in marine bacteria.

Xanthorhodopsin and Actinorhodopsin

Following the discovery of proteorhodopsin in marine bacteria (Beja et al., 2000b), the light-driven proton pump xanthorhodopsin (XR) was found in the extremely halophilic bacterium *Salinibacter ruber* (Balashov et al., 2005). A unique feature of xanthorhodopsin is the presence of a carotenoid antenna pigment, salinixanthin, in a 1:1 ratio with retinal (Balashov et al., 2005) which expands the action spectrum of the rhodopsin protein (Boichenko et al., 2006). Salinixanthin interacts with the retinal chromophore (Balashov et al., 2006) on a rapid timescale (Luecke et al., 2008; Polivka et al., 2009) due to a close proximity of the two chromophores (Balashov et al., 2008; Imasheva et al., 2008). XR contains many homologies to BR and PR, but the structural analysis reveals differences in the conformation and in the photocycles (Luecke et al., 2008).

In addition to the proton pumping type I rhodopsins found in the marine envionroment (PR) and hypersaline environment (BR and XR), sequences of PR and a rhodopsin with homology to PR called actinorhodopsin were discovered in brackish and fresh water bacteria (Atamna-Ismaeel et al., 2008; Sharma et al., 2009). This finding indicates the importance of rhodopsin in all aquatic environments regularly exposed to light.

Biophysical Characterization of Proteorhodopsin Structure, Photocycle, and Key Residues of the Proton Pumping Mechanism

While no crystalline structures of PR have yet been produced, the structure of PR has recently been determined using solid-state and solution nuclear magnetic resonance (NMR) techniques (Shi et al., 2009; Reckel et al., 2011). The results of the structural determination verify the heptahelical topology typical to rhodopsins (Figure 1-2AB) (Reckel et al., 2011). An interesting difference between PR and the other type I rhodopsins is the secondary structure between helices B and C, which forms a short loop sequence in PR and demonstrates anti-parallel beta-sheets in the other type I rhodopsins (Reckel et al., 2011). The loop between helices E and F is particularly short and constrained, providing a possible explaination to the spectral shift that is associated

with the A178R mutagenesis at this position (Yoshitsugu et al., 2008; Reckel et al., 2011). Beyond the tertiary structure of a single proteorhodopsin protein, the quaternary structure of PR in the membrane has been suggested to affect the photochemical properties (Klyszejko et al., 2008; Ranaghan et al., 2011).

Like other type I rhodopsins, PR binds retinal through a Schiff base at a lysine residue located in helix G (31A08-PR position K231) (Figure 1-2C) (Reckel et al., 2011). Retinal, vitamin A aldehyde, is a 20-carbon apocarotenoid with a six-carbon ring and backbone of conjugated single and double bonds. As with the other type I rhodopsins, PR binds all-trans retinal with a 13-cis isomerization upon photoexcitation (Dioumaev et al., 2002). Similar to the confirmation changes observed in the photocycle of BR, the retinal isomerization in PR leads to conformational changes of the helices, particularly an outward movement of the cytoplasmic half of helices E and F and an inward movement of the extra-cellular half of helix C (Andersson et al., 2009). The functional effect of the structural changes in the ion pumping rhodopsins is essentially the formation of two half-channels which enables the release and uptake of ions on opposing sides of the membrane (Lanyi, 1995).

The transport of protons through PR requires the specific function of several key residues lining the inner ion channel in the middle of the helical structure (Figure 1-2D). Analogous to the proton acceptor residue of BR, an aspartic acid residue (D97) acts as the Schiff base proton acceptor (Dioumaev et al., 2002). The Schiff base proton donor residue in PR is a glutamic acid (E108) which differs slightly from aspartic acid donor residue in BR (Dioumaev et al., 2002). Several residues in the retinal binding pocket provide important functions as counterions stabilizing the various forms of the Schiff base including an aspartic acid residue (D227) (Imasheva et al., 2004) and an arginine residue (R94) (Partha et al., 2005). A histidine residue (H75) affects the photocylce by interacting with D97 during the proton transfer process (Bergo et al., 2009; Hempelmann et al., 2011). A glutamic acid (E142) on the periplasmic side blue PR also seems to play an important role in the transfer of protons for these variants (Kralj et al., 2008b).

The photocycle of PR is very similar to the photocycle of BR (Dioumaev et al., 2002). The absorption of a photon results in the photocycle which includes a variety of spectrally unique intermediates which are observed on time-scales ranging from femtoseconds to milliseconds (Dioumaev et al., 2002; Varo et al., 2003; Xiao et al., 2005; Neumann et al., 2008). The absoption of a photon initiates the initial isomerization event converting the all-trans retinal to 13-cis retinal (Dioumaev et al., 2002; Lenz et al., 2006). The high specificity of the 13-cis isomerization is dependent on the anionic aspartic acid counterion (D227) (Imasheva et al., 2004); the D227N mutant produces a 9-cis isomerization form of retinal (Imasheva et al., 2004).

After the isomerization event, a red-shifted intermediate (the K state) is produced in the 10-100 microsecond timeframe (Dioumaev et al., 2002). This K state is not observed in BR which instead accumulates an L state before the M state (Dioumaev et al., 2002). An L intermediate for PR has been observed (Xiao et al., 2005), but an accumulation of the L intermediate between the K and M states is not explicitly observed in PR as in the photocycle of BR (Dioumaev et al., 2002). This may be the result of the slow rate of K decay and a fast rate of M formation (Varo et al., 2003).

The second intermediate is the blue-shifted M state (Dioumaev et al., 2002) well known in microbial rhodopsisn as a critical state for the proton pumping stage of BR and the signal transducing stage of SR (Spudich et al., 2000). However, the M-like state in PR does not constitute the primary release of the proton to the periplasm in PR (Dioumaev et al., 2002; Varo et al., 2003). The K to M transition is entropy driven (Varo et al., 2003). The M state is characterized by the deprotonated Schiff base following transfer of the proton to D97 acceptor residue and prior to the reprotonation from the E108 donor residue (Dioumaev et al., 2002). The M state of PR is well-represented by two forms M_1 and M_2 which are spectrally identical but can be resolved kinetically (Varo et al., 2003). The overall rise of the M state occurs over approximately 10 milliseconds (Dioumaev et al., 2002). The E108Q mutants shows an extended duration for decay of the M state due a lack of ability to reprotonate the Schiff base (Dioumaev et

al., 2002). A D227N mutant results in the formation of a long-lived (30 minute) blue-shifted intermediate with a 362 nm absorbance indicating a deprotonated Schiff base (Imasheva et al., 2005).

Following the M state, a late red-shifted N state is formed (Dioumaev et al., 2002). The growth of the N state occurs in about 2 milliseconds toward the end of the M state, and the slow decay of the N and following states is on the order of 10-100 milliseconds (Dioumaev et al., 2002). The N state still maintains the 13-cis form of retinal, even during the proton uptake step which is in contrast to BR (Dioumaev et al., 2002). The N state is a low-enthapy state and the transition from N to the PR'(O) state is driven by entropy (Varo et al., 2003).

The final state of the photocycle, PR'(O), is indistinguishable from the PR ground state in the visible spectrum, however it resembles the O state of bacteriorhodopsin and halorhodopsin based on fourier transform infrared spectroscopy and is kinetically distinguishable from the PR ground state (Varo et al., 2003). The PR'(O) state of PR relaxes back to the ground state to complete the photocycle (Varo et al., 2003). The proton translocation across the membrane is initiated during the M_2 to N transition and completed during the transition between the N, PR'(O), and PR ground states (Varo et al., 2003). The proton uptake step precedes the release step (Dioumaev et al., 2002). The slow decay of the PR'(O) state to the ground state has been attributed to the lack of charged residues (analogs of Glu-194 and Glu-204 from BR) which are transiently protonatable (Dioumaev et al., 2002).

The nature and rate of the photocycle of the proton pump are highly dependent on the pH (Friedrich et al., 2002; Lakatos et al., 2003; Verhoefen et al., 2011), which is expected to have significant modifications to the protonation state, and thus charge, of residues in the retinal binding pocket (Huber et al., 2005). At low pH, the directionality of the proton pumping action has been reported to be reversed (Friedrich et al., 2002) and the M-like intermediate with deprotonated Schiff base is not formed (Friedrich et al., 2002; Dioumaev et al., 2003; Lakatos et

al., 2003). At pH greater than 9.5, a fast (10-50 microsecond) release of a proton occurs during the rise of the M stage similar to BR (Krebs et al., 2002; Xiao et al., 2005)

Residues in the binding pocket affect the retinal chromophore. The most striking example of this is the residue located at position 105. PR with a leucine residue at position 105 exhibit a green absorption maximum around 525 nm, while those with a glutamine residue have a blue absorbance maximum around 490 nm (Man et al., 2003). The difference between the hydrophobic leucine residue and the hydrophilic zwitterionic glutamine results in changes to both water molecules in the retinal binding pocket (Amsden et al., 2008) as well direct interactions with the C13-methyl group of the retinal chromophore (Kralj et al., 2008a). Blue variants originally found from deeper water and Antarctic samples (Beja et al., 2001; de la Torre et al., 2003) displayed slow photocycle kinetics (200+ milliseconds) typically associated with sensory rhodopsins (Spudich et al., 2000). However, the discovery of blue variants with fast photocycle kinetics indicates that spectral tuning is not strictly related to the speed of the photocycle (Sabehi et al., 2005).

Other residues affect the spectral properties of the PR. Several PR variants contain a hydrophobic methionine residue at this critical position which results in a green absorbance maximum (535 nm) similar to the leucine residue (Gomez-Consarnau et al., 2007). Also in the retinal binding pocket, an asparagine residue near the Schiff base (N230) affects the absorbance spectrum and the stability of the K intermediate following the initial isomerization (Bergo et al., 2004). In addition, residues outside the binding pocket (P65 and D70) have been found to affect the absorbance spectrum (Man-Aharonovich et al., 2004). Replacement of an alanine residue in the loop between the E and F helices is responsible for major changes in the positions of the helices and the changes in the spectral properties of the PR (Yoshitsugu et al., 2008; Yamada et al., 2010).

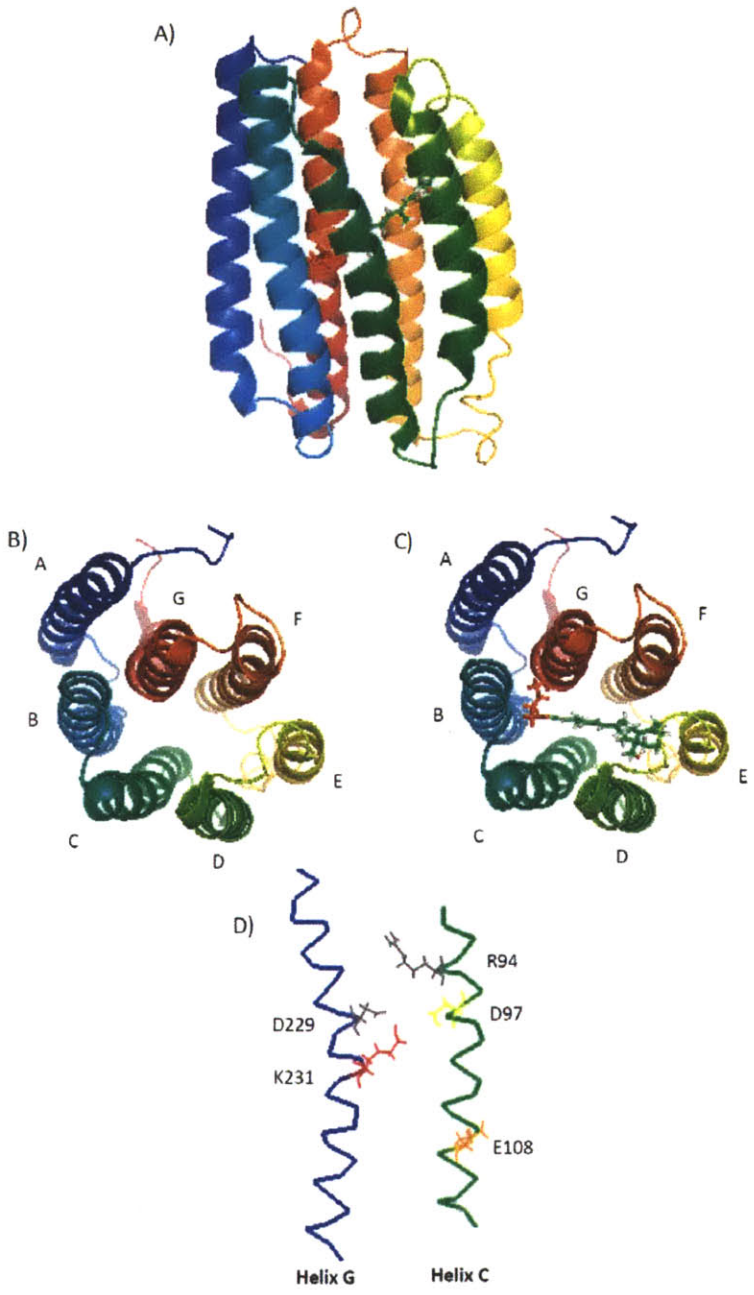

Figure 1-2: Structure of Proteorhodopsin. Structural position data from solution NMR of EBAC31A08 Green PR data available in the protein database (PDB 2L6X) (Reckel et al., 2011). Images generated using PyMOL v1.1. A) Membrane cross-sectional view of PR and bound retinal. B) Top view without retinal. C) Top view with bound retinal. D) Cross section view of helices C and G and key residues of the proton pumping mechanism.

Protorhodopsin Diversity

Since the discovery of PR (Beja et al., 2000b), a diverse range of PR variants have been found (Beja et al., 2001; de la Torre et al., 2003; Sabehi et al., 2003; Sabehi et al., 2004; Venter et al., 2004; Sabehi et al., 2005; Frigaard et al., 2006; McCarren and DeLong, 2007). PR are primarily categorized by the color of light at the peak of the absorbance spectrum; green PR have a peak absorbance around 525 nm, and blue PR have a peak absorbance around 490 nm (Beja et al., 2001). However, variations throughout the PR primary amino acid structure do not necessarily correspond to two major groupings by the absorbance spectrum (Figure 1-1).

Grouping of PR by sequence alignment reveals distinct groupings (Figure 1-1)(Sabehi et al., 2003; Sabehi et al., 2005; McCarren and DeLong, 2007). Divergence of these sequences seems potentially related to geographical isolation, speciation, and gene transfer processes (de la Torre et al., 2003; Sabehi et al., 2003). In addition to the divergence in PR sequence across microbial phyla, divergent PR sequences within closely related groups demonstrated that PR variants are not tightly associated with taxonomic lineage (Sabehi et al., 2004).

Interestingly, two rhodopsins predicted to contain proton pumping function have been discovered adjacent to one another on two metagenomic environmental library clones (McCarren and DeLong, 2007; Henn et al., 2008). In both cases, one of the rhodopsins aligns closely with XR and the other is predicted to be a blue PR based on the presence of a glutamine at the residue primarily responsible for color tuning (McCarren and DeLong, 2007; Henn et al., 2008). The activity of these rhodopsins has not yet been confirmed and the missing residues for the highly conserved, Schiff base-forming lysine in the XRs (McCarren and DeLong, 2007; Henn et al., 2008) raises questions about the rhodopsin functionality.

The Proteorhodopsin Photosystem

Proteorhodopsin is an attractive system for studying the effects of proton pumping on host physiology and for biotechnological applications because of its simplicity. Only two components are required for the fully functional proton pump capable of translating the energy

from light into electrochemical potential, the opsin membrane protein and the apocarotenoid cofactor retinal (Oesterhelt and Stoeckenius, 1973). The proteo-opsin protein is encoded by a single gene and the assembly in the membrane does not require any specific chaperones (Beja et al., 2000b). Thus, in a retinal producing background, only one gene is required for a functional proton pump.

The production of retinal can be accomplished from the common central metabolite isopentenyl diphosphate (IPP) using as few as six genes (Sabehi et al., 2005; Martinez et al., 2007). IPP is a common isoprene-donating compound found at the beginning of isoprenoid (a.k.a. terpenoid) biosynthetic pathways (Kuzuyama and Seto, 2003). The first step of isoprenoid synthesis is the condensation of IPP with its isomer dimethylallyl diphosphate (DMAPP), which can be formed by IPP isomerase (encoded by the *idi* gene). The enzymes required for the biosynthesis of retinal from IPP and DMAPP and the [gene encoding the enzyme] include: farnesyl diphosphate (FPP) synthase [*ispA*], geranylgeranyl diphosphate (GGPP) synthase [*crtE*], phytoene synthase [*crtB*], phytoene desaturase [*crtI*], lycopene cyclase [*crtY*], and 15,15' β-carotene dioxygenase [bacteriorhodopsin-related protein (*brp*) / bacteriorhodopsin-related-protein-like homolog (*blh*)] (Sabehi et al., 2005; Martinez et al., 2007). *E. coli*, like numerous other bacteria, contains the *idi* and *ispA* genes on the chromosome and only requires *crtEIBY* and *blh* in order to synthesize retinal (Sabehi et al., 2005; Martinez et al., 2007).

The *crtEIBY* and *blh* genes have been found adjacent to the gene encoding PR on several bacterial artificial chromosomes (BACs) from large insert marine metagenomic libraries (Sabehi et al., 2005; Martinez et al., 2007; McCarren and DeLong, 2007). The overall gene cluster encompassing the PR and biosynthetic pathway for retinal constitutes a proteorhodopsin photosystem (PRPS) (Sabehi et al., 2005; Martinez et al., 2007; McCarren and DeLong, 2007). A functional screen of fosmid libraries which identified two PRPS gene clusters confirmed the function of the genes in the PRPS and demonstrated that only six genes were required for a completely functional system in *E. coli* (Martinez et al., 2007). Evidence from surrounding genes

on the BACs indicates that PRPSs are harbored by a wide range of taxa (McCarren and DeLong, 2007). Similarities in the PRPS found across taxonomic divisions indicates widespread horizontal transfer of the PRPS attributed to the small size (8 kb) and modular nature of the PRPS (Sabehi et al., 2005; Martinez et al., 2007; McCarren and DeLong, 2007).

Evidence for Ecological Significance of Proteorhodopsin

Proteorhodopsins have been identified in oceans all around the world (Beja et al., 2000b; Beja et al., 2001; de la Torre et al., 2003; Sabehi et al., 2003; Venter et al., 2004; Rusch et al., 2007; Atamna-Ismaeel et al., 2008; Campbell et al., 2008; Jung et al., 2008; Cottrell and Kirchman, 2009; Zhao et al., 2009; Koh et al., 2010). It has been estimated that 13% of bacteria (Sabehi et al., 2005) and 10% of euryarchaea (Frigaard et al., 2006) in the photic zone of the ocean contain a PR. In the oligotrophic nutrient-limited marine environment where genome streamlining appears to be a common occurance (Giovannoni et al., 2005b), the widespread abundance of PR strongly suggests an important physiological function.

The distribution of PR color variants has been found to be associated with the light conditions in the environment from which they were isolated (Beja et al., 2001). This agreement indicates an evolutionary selective pressure for matching the spectral tuning to light availability with high precision (Beja et al., 2001; Bielawski et al., 2004).

The phylogenetic diversity of strains harboring PR suggests the simple photosystem provides an advantage for a wide range of organisms (Beja et al., 2000b; de la Torre et al., 2003; Giovannoni et al., 2005a; Sabehi et al., 2005; Frigaard et al., 2006; Gomez-Consarnau et al., 2007; McCarren and DeLong, 2007; Atamna-Ismaeel et al., 2008; Giovannoni et al., 2008; Gomez-Consarnau et al., 2010; Slamovits et al., 2011). What appears to be a high incident rate of horizontal gene transfer of PR further supports the versatility and utility of PR phototrophy (Sabehi et al., 2005; Frigaard et al., 2006; Sharma et al., 2006; Martinez et al., 2007; McCarren and DeLong, 2007)

Diversity of Strains Harboring Proteorhodopsin

A phylogenetic tree of 16S small subunit rRNA of hosts of microbial rhodopsins demonstrates the diversity of organisms which utilize rhodopsins (Figure 1-3). The type(s) of rhodopsins contained in the genome of these organisms can be seen in Figure 1-1. Taxonomic assignment based on genes located adjacent to the PR revealed hosts ranging from gamma- (Beja et al., 2000b), alpha- (de la Torre et al., 2003) and beta-proteobacteria (McCarren and DeLong, 2007) to *Planctomycetales* (McCarren and DeLong, 2007) and *Euryarchaea* (Frigaard et al., 2006). As expected from the diversity represented in PR-containing clones from large insert metagenomic libraries, PR have been recently found in a wide range of cultured isolates (Giovannoni et al., 2005a; Gomez-Consarnau et al., 2007; Stingl et al., 2007; Giovannoni et al., 2008; Gonzalez et al., 2008; Lami et al., 2009; Gomez-Consarnau et al., 2010; Oh et al., 2010; Riedel et al., 2010).

The first PR in a cultured isolate was discovered in *Pelagibacter ubique* HTCC1062, a member of the SAR11 clade of alpha-proteobacteria abundant throughout the world ocean (Giovannoni et al., 2005a). While this species demonstrates light-dependent differences in respiration rate, ATP content, and stationary phase morphology, no observed differences in growth rate or yield have been observed in this strain (Giovannoni et al., 2005a; Steindler et al., 2011). PR has also been identified in other cultured alpha proteobacteria including SAR116 isolate Candidatus *Puniceispirillum marinum* IMCC1322 (Oh et al., 2010), strain HIMB114 (Rappe et al., 2009) and Rhodobacterales bacterium HTCC2255 (Giovannoni et al., 2006b). To date, none of these strains have reported function of PR.

Isolates possessing PR have been cultivated from other divisions of proteobacteria as well. A methylotrophic beta proteobacterium, strain HTCC2181, was found to harbor both a proteorhodopsin-like sequence (high similarity to xanthorhodopsin) as well as genes associated with retinal biosynthesis (Giovannoni et al., 2008). The first gamma proteobacterium isolated with proteorhodopsin was strain HTCC2207 of SAR96 clade (Stingl et al., 2007), followed by

marine gamma proteobacterium HTCC2148 (Amann et al., 2008). Several strains of cultured *Vibrionaceae* contain proteorhodopsin including *Vibrio harveyi* ATCC BAA-1116 (Bassler et al., 2007), *Vibrio* sp. AND4 (Gomez-Consarnau et al., 2010), and closely related *Photobacterium angustum* S14 (Lauro et al., 2009) and *Photobacterium* sp. SKA34 (Hagstrom et al., 2006).

Proteorhodopsin has been found in several species of bacteroides (Bowman et al., 2006; Gomez-Consarnau et al., 2007; Hagstrom et al., 2007; Gonzalez et al., 2008; Lail et al., 2010; Riedel et al., 2010; Klippel et al., 2011; Lucas et al., 2011).

A similar species *Dokdonia donghaensis* PRO95 has been discovered to possess a PR, but no light-dependent effects were observed in the conditions tested (Riedel et al., 2010); however, these only included carbon concentrations at which no effect was observed for MED134 (Gomez-Consarnau et al., 2007).

Proteorhodopsin and similar rhodopsins have even been found in the Eukaryotic dinoflagellate protists *Oxyrrhis marina*, *Karlodinium micrum*, *Pyrocystis lunula*, and *Alenandrium tamarense* (Slamovits et al., 2011). Antibodies raised to the dinoflagellate PR of *O. marina* demonstrated expression of the PR in what appeared to be the endomembrane system (Slamovits et al., 2011). While no clear function was indicated for the rhodopsin, it seems likely to serve a proton pumping function due to similarity to other proton pumping proteorhodopsin (Slamovits et al., 2011).

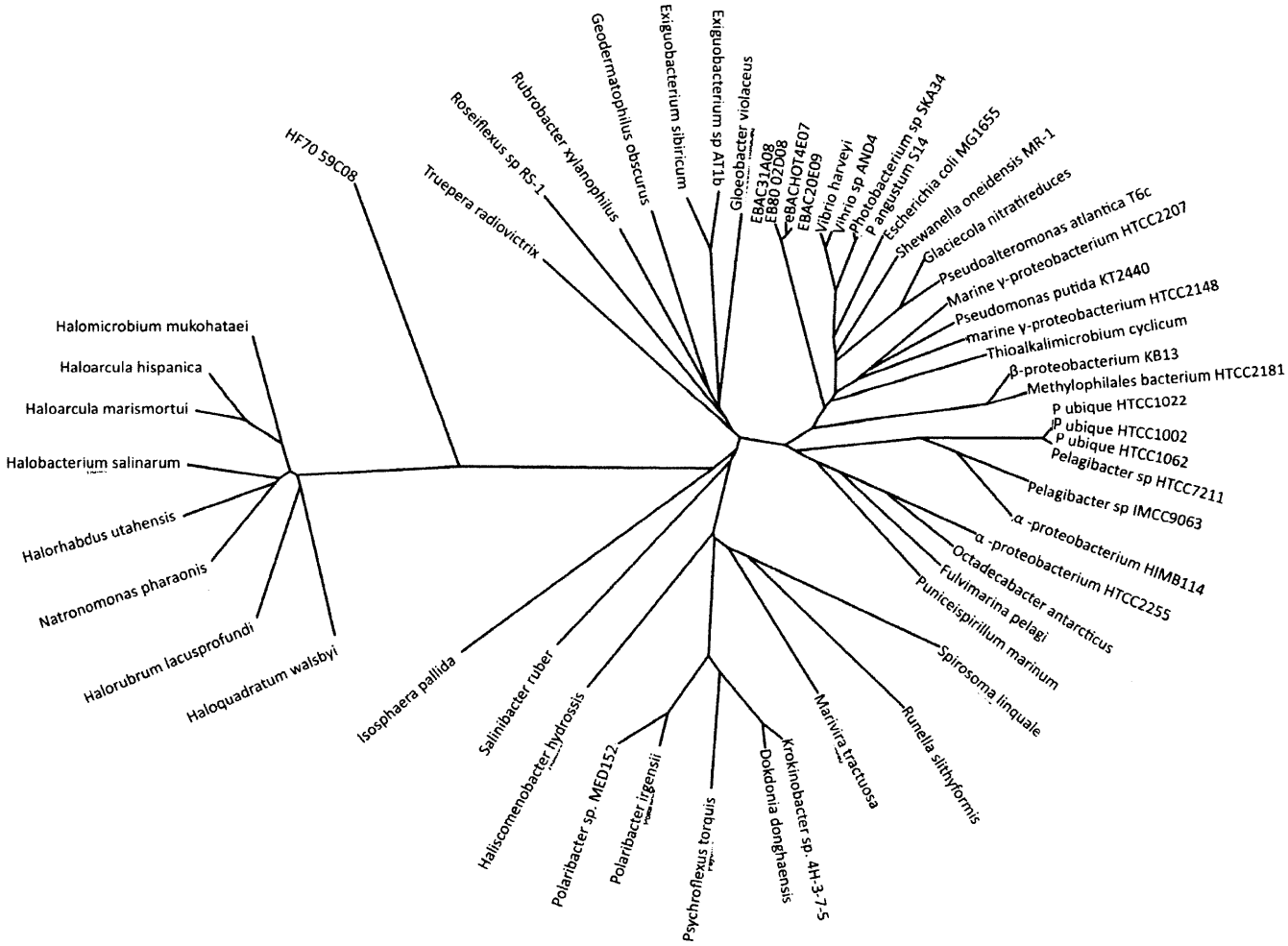

Figure 1-3: Phylogenetic Tree of 16S SSU rRNA of Selected Organisms Containing Type-1 Rhodopsins. 16S rRNA sequences were taken from GenBank for representative species possessing rhodopsins depicted in Figure 1-1. Large-insert BACs and Fosmids with 16S sequences contiguous with PR sequences are added for reference. Tree constructed from a sequence alignment produced using ClustalX 2.0.10 with iteration at each step of alignment and multiple iterations of the complete alignment, and the tree was drawn using the Drawtree program of Phylip 3.69.

Physiological Effects Associated with Proteorhodopsin

As an integral membrane protein which transports protons from the cytoplasm to the periplasm, PR interacts directly with the electrochemical potential of the membrane and the proton motive force (PMF). The most direct effect observed from the function of proton pumps is a change in membrane potential and an acidification of the periplasmic and extra-cellular spaces (Oesterhelt and Stoeckenius, 1973; Beja et al., 2000b; Balashov et al., 2005). Secondary effects of the function of proteorhodopsin occur via components interacting with the membrane potential. Thus, any system interacting directly with the PMF is potentially altered by the action of PR. The major systems in consideration are the F-type ATP synthase (Capaldi and Aggeler, 2002), rotary flagellar motor (Berg, 2003), electron transport chain (ETC) (Ingledew and Poole, 1984), and the PMF-powered plasma membrane active transport systems (Simoni and Postma, 1975). Finally, effects which are downstream of the secondary effects of PR would be tertiary effects of PR and could include physiological phenotypic responses such as growth rate, survival, lag time, yield of biomass from substrates, and other fitness advantages which confer a selective advantage for the host. Because the PR interacts with a critical component of central metabolism and bioenergetics, the implications of its function are widespread and encompassing many aspects of the host physiology (Figure 1-4).

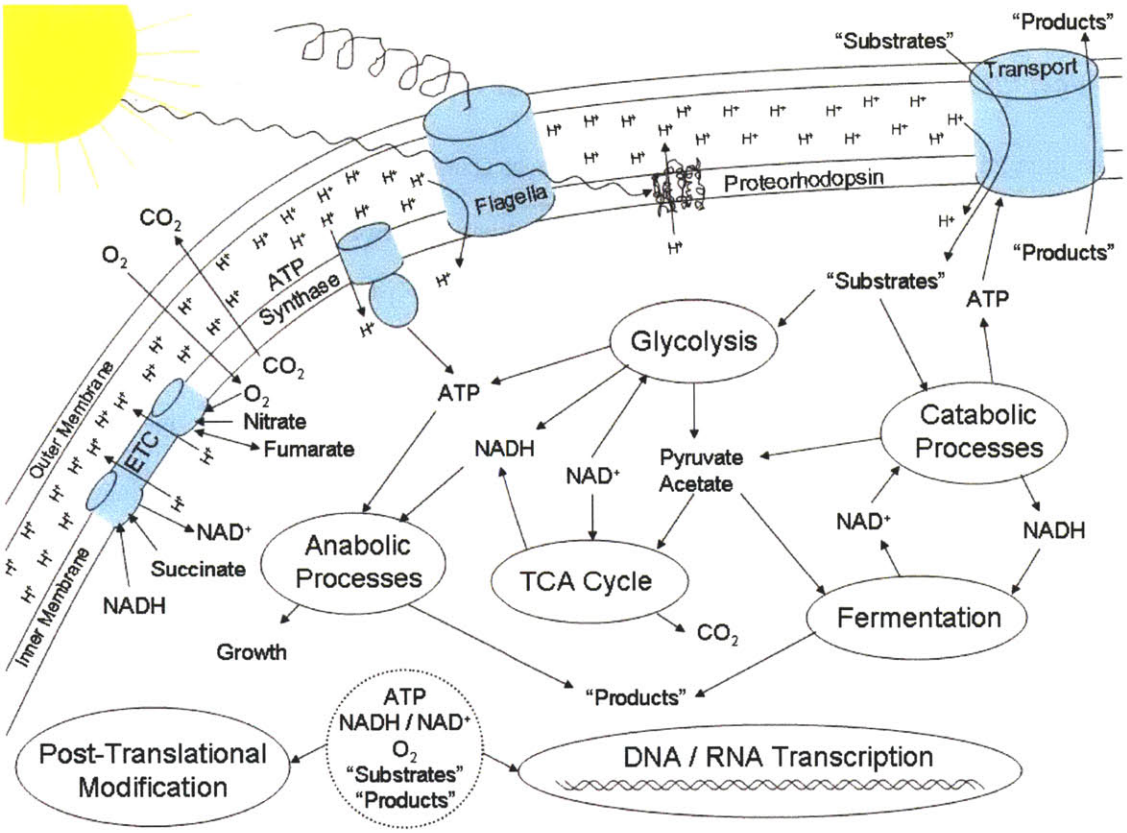

Figure 1-4: Interaction of Proteorhodopsin with Host Physiology

Physiological Effects of Proton-Pumping Rhodopsins in Native Hosts

The importance of rhodopsins as a source of cellular energy have been thoroughly documented for the BR of *Halobacterium salinarum*. The function as an outward driven proton pump was identified as the means of energy conservation (Oesterhelt and Stoeckenius, 1973). The ability of the PMF generated by BR to drive photophosphorylation was demonstrated shortly after (Danon and Stoeckenius, 1974). The observed decrease in respiration rate of *H. salinarum* in the presence of light (Oesterhelt and Krippahl, 1973) was linked to action spectrum of BR and PMF generated by the proton pumping activity (Litvin et al., 1977). Light-driven transport of amino acids using the PMF from BR was demonstrated in vesicles (MacDonald and Lanyi, 1975) and in whole cells (Hubbard et al., 1976). The effect of light-driven proton pumping on the PMF of whole cells was determined with various inhibitors and uncouplers (Michel and Oesterhelt, 1976). Most importantly from a physiological standpoint, *H. salinarum* demonstrates an increase in survival under anaerobic conditions in the light (Brock and Petersen, 1976) and increased growth rate and yield in the light during continuous cultivation (Rogers and Morris, 1978; Rodriguez-Valera et al., 1983).

The purple membrane containing BR is produced during conditions of low oxygen and in the presence of light (Stoeckenius and Kunau, 1968). Quantitative analysis of gene expression confirmed the increased transcription in conditions of low oxygen and light (Oesterhelt and Stoeckenius, 1971). The expression of BR and the light-driven increase in growth was shown to be dependent on the dilution rate, and thus the growth rate, in continuous culture (Shand and Betlach, 1991).

Consistent with the implied bioenergetic role, expression of the XR from *Salinibacter ruber* is induced in conditions of low aeration and the presence of light (Rogers and Morris, 1978). The proton pumping function of XR has been confirmed using membrane vesicles (Balashov et al., 2005). At low levels of respiration, XR results in a photoinhibition of oxygen uptake (Balashov et al., 2005). *S. ruber* is

a rod-shaped obligate aerobe (Boichenko et al., 2006). Little has been reported about the metabolic capabilities *S. ruber* and the physiological effects of light despite the complete genome sequence available (Anton et al., 2002).

Pelagibacter ubique HTCC1062 was the first isolated strain found harboring a PR gene (Mongodin et al., 2005). The strain also posses all of the genes required to produce retinal from the precursors isopentenyl diphosphate and dimethylallyl diphosphate (Giovannoni et al., 2005a). The expression level of PR in *P. ubique* does not show strong dependency on the presence of light and was estimated to be around 10,000 PR per cell (Giovannoni et al., 2005a). The PR was demonstrated to exhibit fast photocycle kinetics in *P. ubique* and demonstrated proton pumping behavior when heterologously expressed in *E. coli* (Giovannoni et al., 2005a). In conditions of limited carbon, *P. ubique* demonstrated a light-dependent decrease in respiration rate, increase in ATP concentration, and increase in taurine uptake (Giovannoni et al., 2005a). The decreased respiration associated with incubation in the light appeared to minimize the use of endogenous carbon thus enabling cells to maintain a larger size during the initial phases of carbon starvation (Steindler et al., 2011). Studies with this strain have not demonstrated any light-dependent increases to growth rate or yield (Steindler et al., 2011).

Complete genome sequencing of *Vibrio* sp. AND4 revealed a PR gene (Giovannoni et al., 2005a; Steindler et al., 2011). The PR of this strain was confirmed to display fast photocycle kinetics in *E. coli* and to contain all of the conserved residues required for proton pumping function (Gomez-Consarnau et al., 2010). The PR of *Vibrio* AND4 is found adjacent to the genes *crtEIBY* and *blh* associated with the synthesis of retinal which appear to have been acquired by horizontal gene transfer (Gomez-Consarnau et al., 2010). While *Vibrio* AND4 did not demonstrate any light-dependent increases in growth rate or yield, the survival of the strain during starvation was improved in the presence of light as was the recovery of the strain after short periods of starvation (Gomez-Consarnau et al., 2010). Notably, the light-dependent response was eliminated by a deletion of the PR gene and recovered with the addition a plasmid carrying

PR (Gomez-Consarnau et al., 2010). This represents the first light-based physiological effect in a native host which can de directly attributed to the PR.

The only heterotrophic strain harboring a PR to demonstrate a light-dependent increase in growth to date is the flavobacterium *Dokdonia donghaensis* MED134 (Gomez-Consarnau et al., 2010). The PR from *Dokdonia* MED134 contains a methionine residue at the color tuning position which results in a green absorbance maximum of 535 nm, a feature common to the PR identified in bacteroides group (Gomez-Consarnau et al., 2007). The PR displayed fast photocycle kinetics typical of proton pumps when expressed in *E. coli* (Gomez-Consarnau et al., 2007). As with other PR-containing isolates, the genes for retinal synthesis are also located in the genome (Gomez-Consarnau et al., 2007).

The light-dependent increase in growth rate and yield observed with *Dokdonia* MED134 is dependent on a low concentration of dissolved organic carbon in the growth media (Gomez-Consarnau et al., 2007). This light-based growth effect was attributed to PR based on the agreement between the absorbance spectrum of the PR and a crude action spectrum indicating dramatically improved growth with green light and moderate to low increases with blue or red light (Gomez-Consarnau et al., 2007). Inhibition of lycopene cyclase, an enzyme in the carotenoid synthesis pathway, eliminated the light-dependent growth effects and provided further support for the role of PR (Gomez-Consarnau et al., 2007). Transcriptomic analysis of *Dokdonia* MED134 grown in the light and the dark revealed differential expression of numerous genes including the PR and transport systems and indicated an important role of sodium transport (Kimura et al., 2011).

A related species of flavobacteria which harbors a PR, *Polaribacter* sp. MED152, does not demonstrate light-dependent increases in growth (Kimura et al., 2011), but a light-dependent increase in carbon dioxide uptake may indicate a shift in the metabolic profile for carbon utilization (Gomez-Consarnau et al., 2007).

Proteorhodopsin Effects in Heterologous Hosts

The proton motive force generated by the proton pumping action of PR has previously been demonstrated to be suitable for powering cellular processes in *E. coli* (Gonzalez et al., 2008). The flagellar motor of *E. coli* is powered directly by PMF (Martinez et al., 2007; Walter et al., 2007), and the rotational frequency of the flagella is linearly related to the magnitude of the PMF and can be controlled across a wide range speeds (Berg et al., 1982; Berg, 2003). The expression of a green PR in *E. coli* with the addition of exogenous retinal was demonstrated to drive flagellar rotation in a fashion dependent on illumination with green light (Fung and Berg, 1995; Gabel and Berg, 2003). This work demonstrated the importance of limiting respiratory PMF for producing an observable effect from PR; the use of the respiratory inhibitor azide or experimentation in anaerobic conditions were required to demonstrate light-dependent increases in swimming speed and rate of flagellar rotation (Walter et al., 2007). This work presented a circuit-based model of PMF generation and consumption which explains the inability of PR to increase flagellar rotation rates under conditions of high respiratory activity by comparing PR and respiration to power-sources operating in parallel; no "current" is produced by the PR proton pumping until the "voltage" produced by respiration falls below a threshold value (Walter et al., 2007).

The PMF generated by PR can be used to drive chemiosmotic phosphorylation in *E. coli* (Walter et al., 2007). Using a complete proteorhodopsin photosystem discovered in a large insert environmental fosmid library, *E. coli* was shown to create a functional retinal-bound PR capable of pumping protons without the addition of exogenous retinal (Martinez et al., 2007). The necessity of five genes of the photosystem for the production of retinal was demonstrated, confirming the function of the genes in the retinal synthesis pathway located adjacent to the PR (Martinez et al., 2007). Disruption to the retinal synthesis pathway or the PR gene eliminated the proton pumping ability (Martinez et al., 2007). Further, it was demonstrated that the PMF generated by the PR was capable of driving ATP synthesis in a photophosphorylation process (Martinez et al., 2007). This work also clearly demonstrated the

importance of limited respiratory activity for the observation of PR generated ATP (Martinez et al., 2007).

Heterologous expression in *Shewanella oneidensis* has also demonstrated a physiological role for the PMF resulting from PR (Martinez et al., 2007). Expression of PR resulted in the successful formation of the integral membrane protein, and the addition of exogenous retinal resulted in membranes with the characteristic absorbance spectrum of the retinylidene protein (Johnson et al., 2010). A light-dependent increase in the membrane potential resulted from the PR indicating successful proton pumping activity (Johnson et al., 2010). While growth was not appreciably affected by the PR, survival was higher in the light than in the dark (Johnson et al., 2010). Interestingly, in contrast to the photoinhibition of respiration results observed for *Halobacterium salinarum* and *Salinibacter ruber*, *S. oneidensis* demonstrated a light-dependent increase in respiration rate as measured through current production from respiration to an electrode in a microbial fuel cell (Johnson et al., 2010). This increase was proposed to be the result of an increased uptake rate of the substate, lactate, from the media caused by the PMF supplied by the PR (Johnson et al., 2010). Additionally, the PMF produced by PR was shown to recover an anaerobic growth defect of an *S. oneidensis* F-type ATPase mutant growing anaerobically on lactate (Johnson et al., 2010).

Biotechnology applications of PR

While the role of proton-pumping rhodopsins in the natural environment is still being elucidated (Hunt et al., 2010), the utility of the photoactive proteins is already being considered for a number of biotechnological applications. The interest in using proton pumping rhodopsins in biotechnology applications is clearly illustrated by the number of patents which have been filed surrounding the various uses of PR (Fuhrman et al., 2008).

Optimization for the expression and assembly of PR in membranes has been undertaken for the purpose of biotechnological applications (Delong and Beja, 2003; Jensen et al., 2004; Jensen and Kelemen, 2005; Bott et al., 2008; Jensen et al., 2008; Stuart, 2008; Delong and Beja, 2009; Devroe et al., 2009; Jensen et al., 2009; Martinez and Delong, 2009). BR has been evaluated in the construction of

photoelectric devices for the production of electricity from light in a form of a biological solar cell (Gourdon et al., 2008; Ranaghan et al., 2011). Potential applications for BR also include data processing (Drachev et al., 1974b; Drachev et al., 1974a; Kayushin and Skulachev, 1974) and storage (Oesterhelt et al., 1991; Juchem et al., 2002). Likewise, PR has been evaluated for similar application. PR has been considered for the production of optical devices and bioelectronics (Bae et al., 1999; Yao et al., 2005a; Yao et al., 2005b). PR has also been adapted to function as a fluorescent indicator of membrane potential (Ranaghan et al., 2010).

The use of proton pumping rhodopsins for bioenergy applications has also been suggested (Kralj et al., 2011). The universality of the PRPS and its widespread utilization suggest an ability to supplement a range of metabolisms with the relatively small and simple photosystem (Walter et al., 2010). Using the energetic boost from the PMF generated from the PRPS, it may be possible to improve the production of a broad range of energy-limited products using energy derived from light (Sabehi et al., 2005; Martinez et al., 2007; McCarren and DeLong, 2007).

Thesis Overview

The objective of this thesis project was to increase our understanding of how heterologous expression of proteorhodopsin (PR) affects energy metabolism of the host organism, particularly pertaining to carbon utilization and yield. The ultimate goal of this work was the demonstration of an increased production of a carbon compound (in this case biomass) as a proof of principle for utilization of proteorhodopsin photosystems in engineered metabolic systems.

Chapter 2 presents the subcloning of the PRPS from the previously characterized metagenomic fosmid HF10_19P19 (Martinez and Delong, 2009) and the subsequent functional characterization of the subcloned photosystem (clone J2B6) in *Escherichia coli* using two different vector expression system. This work confirmed that the seven genes of the PRPS, identified previously (Martinez et al., 2007), are sufficient for the formation of the functional integral membrane retinylidene protein with the associated biosynthesis of the retinal chromophore. The absorbance spectrum confirmed the PR as a blue variant.

Proton pumping and photophosphorylation assays confirmed the functionality as previously reported (Martinez et al., 2007).

Chapter 3 presents the conjugation and integration of a modified vector containing the subcloned PRPS into the chromosome of the engineered host strain *Pseudomonas putida* MBD1. Evidence for successful transconjugation of the vector into *P. putida* and transcription of the PR gene from the photosystem is provided. Growth of the PRPS-contain strain *P. putida* pSJ2B6 demonstrated a light-dependent increase in yield under conditions of low dissolved organic carbon (DOC) concentration. The light-dependent growth effect was not observed for a control strain (*P. putida* pSCCFOS) lacking the PRPS, attributing the difference observed between light and dark conditions to the seven genes of the PRPS. Growth in the dark demonstrated a decreased yield for strain *P. putida* pSJ2B6 compared to *P. putida* pSCCFOS which is hypothesized to potentially be the result of burden or toxicity of gene expression and retinal synthesis. The light-dependent increase in growth yield observed in *P. putida* pSJ2B6 diminished with increasing concentrations of DOC. This result is similar to the finding of the proteorhodopsin-containing strain *Dokdonia* MED134 which exhibited a DOC concentration dependent increase in growth (Martinez et al., 2007), and reinforces previous observations about the utility of proton-pumping rhodopsins under conditions of limiting carbon and respiration (Gomez-Consarnau et al., 2007; Kimura et al., 2011).

Chapter 4 presents a survey for expression of six PR-containing vectors in two host organisms, *P. putida* and *Pseudoalteromonas atlantica*. The PR-containing constructs were derived from large insert environmental metagenomic libraries and harbor a variety of PR and retinal synthesis genes. Evidence is presented for the successful construction of strains with five of the six PR-containing vectors in both host organisms. Reverse-transcriptase polymerase chain reaction results suggest transcription of the PR gene in all strains during late exponential phase growth on rich media. Growth of three additional *P. putida* stains under low DOC conditions was evaluated. Two strains, *P. putida* pSHF10_19P19 and *P. putida*

pS41B09, demonstrated the same qualitative light-dependent growth yield increase observed for *P. putida* pSJ2B6.

Chapter 5 provides a summary of the findings from the thesis and concluding remarks about the prospects for using the PRPS in heterologous hosts for scientific exploration and engineering applications.

Chapter 2: Functional Characterization of a Subcloned Proteorhodopsin Photosystem in *Escherichia coli* Abstract

Proteorhodopsin photosystems (PRPS), composed of the retinylidene protein and genes encoding the biosynthetic pathway for the cofactor retinal, were discovered on large-insert environmental BAC and fosmid libraries (Rogers and Morris, 1978; Martinez et al., 2007; Walter et al., 2007; Gomez-Consarnau et al., 2010; Steindler et al., 2011). Functional characterization of the PRPS directly from the large-insert fosmid HF10_19P19 demonstrated successful proton pumping activity and photophosphorylation in *E. coli* dependent on six genes, *crtE*, *crtI*, *crtB*, *crtY*, *blh*, and PR (Sabehi et al., 2005; Martinez et al., 2007; McCarren and DeLong, 2007). These six genes (with an optional seventh gene, *idi*) represent a minimal PRPS which is predicted to form a functional light-capturing system in a broad range of hosts (Martinez et al., 2007).

The work presented here includes the subcloning of the seven gene PRPS from fosmid HF10_19P19 (Sabehi et al., 2005; Sharma et al., 2006; Martinez et al., 2007; McCarren and DeLong, 2007) and functional characterization of the PRPS expressed using two vectors, pCC1FOS and pMCL200. Transformation of *E. coli* with the cloned genes resulted in successful expression of the PRPS from each of the two different vectors, in a fashion consistent with expression from vector-based promoters. HPLC analysis of cultures overexpressing the PRPS verified the production of retinal, and spectral analysis of membrane preparations confirmed the successful formation an integral membrane retinylidene protein with an absorbance spectrum characteristic of a blue variant PR as predicted (Martinez et al., 2007). The functionality of the photosystem expressed from both vectors was established through assays of light-dependent proton pumping and ATP formation. The results demonstrated that the seven subcloned genes were sufficient for producing a functional photosystem, confirmed the predicted absorbance properties of the HF10_19P19 PR, and demonstrated light-dependent proton translocation and

ATP formation with overexpression in two inducible vector systems, setting the stage for experiments on physiological effects of the PRPS in heterologous hosts.

Introduction & Background

Functional Arrangement of Proteorhodopsin Photosystems

Two components are required for a functional proteorhodopsin capable of light-driven proton pumping, the retinylidene protein and the covalently-bound cofactor retinal (Martinez et al., 2007). When PR was first discovered, it was postulated that the ability to synthesize retinal is likely contained within the host organism (Beja et al., 2000b; Spudich et al., 2000). The discovery of β-carotene hydroxylase (*crtR*), responsible for the conversion of β-carotene to zeaxanthin, on a large-insert environmental library clone provided the first supporting evidence for carotenoid biosynthetic genes and the production of β-carotene in organisms possessing the PR gene (Beja et al., 2000b). While the beta-carotene hydroxylase is not directly involved in the production of retinal, its presence was circumstantial evidence for the production of β -carotene, the precursor of retinal (Sabehi et al., 2004). The beta-carotene hydroxylase also provides a potential pathway for the production of 3-hydroxyretinal (Sabehi et al., 2004) which serves as a chromophore for other opsins (Seki et al., 1998; Sabehi et al., 2004). The discovery of *crtEIBY*, *blh*, and *idi* adjacent to the PR gene on a large-insert environmental BAC clone provided direct evidence of retinal biosynthesis associated with proteorhodopsin, marking the discovery of the first PRPS (Seki et al., 1998). In a similar fashion, additional PRPS gene arrangements were discovered through the sequencing of PR-containing clones from large-insert environmental libraries (Sabehi et al., 2005).

The discovery of *blh* adjacent to the genes for carotenoid synthesis marked the first discovery of this protein in bacteria (McCarren and DeLong, 2007). Analysis of the function of *blh* and bacteriorhodopsin-related protein (*brp*) indicated the role of these products in the cleavage of β-carotene to the apocarotenoid retinal (Sabehi et al., 2005). The β-carotene cleavage function of bacterial *blh* and the successful binding of the produced retinal to produce a functional PR were confirmed establishing a functional role for this gene in the retinal synthesis gene cluster (Peck et al., 2001).

A phenotypic color screen of a fosmid library (HOT_10m) (Sabehi et al., 2005) prepared with marine genomic DNA collected from a depth of ten meters below the surface at the ALOHA station of the Hawaii Ocean Time series (22°45' N, 158°W) (DeLong et al., 2006) revealed two fosmids which cause a bright orange color change in colonies of the host *E. coli* strain (Karl and Lukas, 1996). DNA sequence analysis revealed that the color change caused by both of these fosmids was the result of proteorhodopsin photosystems (Martinez et al., 2007). Through transposon insertion and sequencing, it was discovered that these fosmids, HF10_19P19 and HF10_25F10, contain analogous PRPS clusters of seven genes arranged in identical configurations (PR, *crtEIBY*, *blh*, *idi*) (Martinez et al., 2007). Aside from these seven genes, the two fosmids did not share any other genes in common (Martinez et al., 2007). The relative orientation of the PRPS gene cluster from HF10_19P19 is depicted in Figure 2-1.

The work of Martinez et al. clearly established the functionality of the photosystem components. One of the seven genes encodes the integral membrane protein proteorhodopsin, which based on the glutamine residue at the color tuning position and the orange color of the *E. coli* colonies and culture pellets was hypothesized to be a blue variant (Martinez et al., 2007). The disruption of the PR gene by transposon mutagenesis resulted in the loss of the orange color and functionality of the proton pumping PR (Martinez et al., 2007).

The other six genes of the HF10_19P19 PRPS, *crtE*, *crtI*, *crtB*, *crtY*, *blh*, and *idi*, encoded enzymes involved in the biosynthesis of retinal (Figure 2-1). The function of these genes on the HF10_19P19 fosmid was confirmed by disruption of each gene by transposon mutagenesis, and subsequent observation of the accumulation of specific intermediates in the carotenoid biosynthetic pathway (Martinez et al., 2007).

The *idi* gene encodes isopentenyl diphosphate isomerase which catalyzes the isomerization between isopentenyl diphosphate (IPP) and dimethylallyl diphosphate (DMAPP) (Martinez et al., 2007). DMAPP is used as an isoprene donor for initiating the isoprenoid biosynthetic pathway (Agranoff et al., 1959). IPP can be formed directly through the mevalonate pathway from acetyl-CoA (Kuzuyama and

Seto, 2003). Alternatively, DMAPP and IPP can be created via a non-mevalonate pathway as is the case in *E. coli* (Beytia and Porter, 1976). *E. coli* contains an endogenous variant of the *idi* gene (Rohmer et al., 1996). As an isomerase, the *idi* gene product can also convert DMAPP to IPP, which is required for the addition of subsequent isoprene units in the retinal biosynthetic pathway (Hahn et al., 1999). Regardless of the pathway used for DMAPP and IPP production, the *idi* gene of the PRPS is not required for the production of retinal for *E. coli* or the formation of a functional proton-pumping PR (Kuzuyama and Seto, 2003). However, studies have shown more efficient production of carotenoids in *E. coli* with the inclusion of *idi* gene (Martinez et al., 2007).

The first step in the isoprenoid pathway is the formation of farnesyldiphosphate (FPP) from IPP and DMAPP by the action of FPP synthase (Kajiwara et al., 1997). As with the *idi* gene, the *ispA* gene encoding FPP synthase does not need to be supplied to *E. coli* for the successful production of carotenoids (Fujisaki et al., 1989). The *ispA* gene has not been found associated with any PRPS (Sabehi et al., 2005; Martinez et al., 2007).

The metabolic pathway between FPP and β-carotene is encoded by four genes found in the photosystem, *crtEIBY* (Figure 2-1) (Sabehi et al., 2005; Martinez et al., 2007; McCarren and DeLong, 2007). Verification of the function of these genes in the PRPS of fosmid HF10_19P19 had been previously demonstrated (Sabehi et al., 2005; Martinez et al., 2007). The *crtE* gene product, geranylgeranyl diphosphate (GGPP) synthase, synthesizes GGPP from the precursors FPP and IPP (Martinez et al., 2007). Disruption of the *crtE* gene on HF10_19P19 eliminated the metabolic branch into carotenoid synthesis and results in the loss of pigmentation and the lack of accumulation of carotenoid/apocarotenoid products (Sandmann and Misawa, 1992).

Phytoene synthase, the gene product of *crtB*, catalyzes the production of phytoene from two molecules of GGPP (Martinez et al., 2007). Subsequently, phytoene is converted to lycopene by the action of the phytoene desaturase (*crtI*) (Sandmann and Misawa, 1992), and lycopene cyclase (*crtY*) then transforms lycopene to β-carotene (Giuliano et al., 1986). In confirmation of the anticipated function of

each gene, transposon mutagenesis of *crtB*, *crtI*, and *crtY* on fosmid HF10_19P19 resulted in the loss of the PR-based orange pigmentation. The *crtY* disruption resulted in a pink pigment which was confirmed to be lycopene with high performance liquid chromatography (HPLC) (Misawa et al., 1990).

In the final step, the cleavage of β-carotene into two molecules of retinal is achieved by the gene product of *blh*, a 15,15'- β-carotene dioxygenase (Martinez et al., 2007). The function of this enzyme from HF10_19P19 was verified by the observation of β-carotene accumulation by HPLC after the disruption of this gene (Sabehi et al., 2005). No other gene disruptions on the HF10_19P19 fosmid effected the formation of a functional photosystem (Martinez et al., 2007). The previous work to date has clearly established the necessity of six genes (*crtEIBY*, *blh*, and PR) on HF10_19P19 for the formation of a functional PR and retinal biosynthesis pathway, and suggests that these six gene are sufficient for a complete PRPS (Martinez et al., 2007).

The functionality of the photosystem contained on the HF10_19P19 fosmid was confirmed using several methods (Martinez et al., 2007). First, the ability to translocate protons across the cytoplasmic membrane was confirmed by monitoring the pH of an unbuffered cell suspension (Martinez et al., 2007), which had been previously established as a method for observing proton pumping behavior of rhodopsins (Martinez et al., 2007). In addition to the classical proton pumping experiments, light-dependent production of ATP was demonstrated for the first time with a PRPS (Oesterhelt and Stoeckenius, 1973; Beja et al., 2000b; Balashov et al., 2005). The change in the extra-cellular pH and the light-dependent ATP production were confirmed to be dependent on proton-motive force and chemiosmotic phosphorylation through the use of the inhibitors CCCP (carbonylcyanide m-chlorophenylhydrazone, a proton ionophore uncoupling agent) and DCCD (N',N'-dicyclohexylcarbodiimide, an inhibitor of the F-type ATP synthase) (Martinez et al., 2007). Just as with any disruptions to the necessary photosystem genes, CCCP eliminated the observed proton pumping response (Martinez et al., 2007). DCCD did not affect the proton pumping behavior but did eliminate the photophosphorylation in agreement with the CCCP treatment and PR gene disruption (Martinez et al., 2007). Together, these results demonstrated the

functionality of native PRPS contained within a contiguous set of genes on a single vector, when expressed in a heterologous host. This work also provided the first direct evidence that the energy captured by PR could be used for the production of ATP in a heterologous host (Martinez et al., 2007). The results obtained with the six gene PRPS (Martinez et al., 2007) also provided support for the hypothesis that PRPS constitute a mobile photosystem capable of autonomous function after transfer to a broad range of hosts through horizontal gene transfer (Martinez et al., 2007).

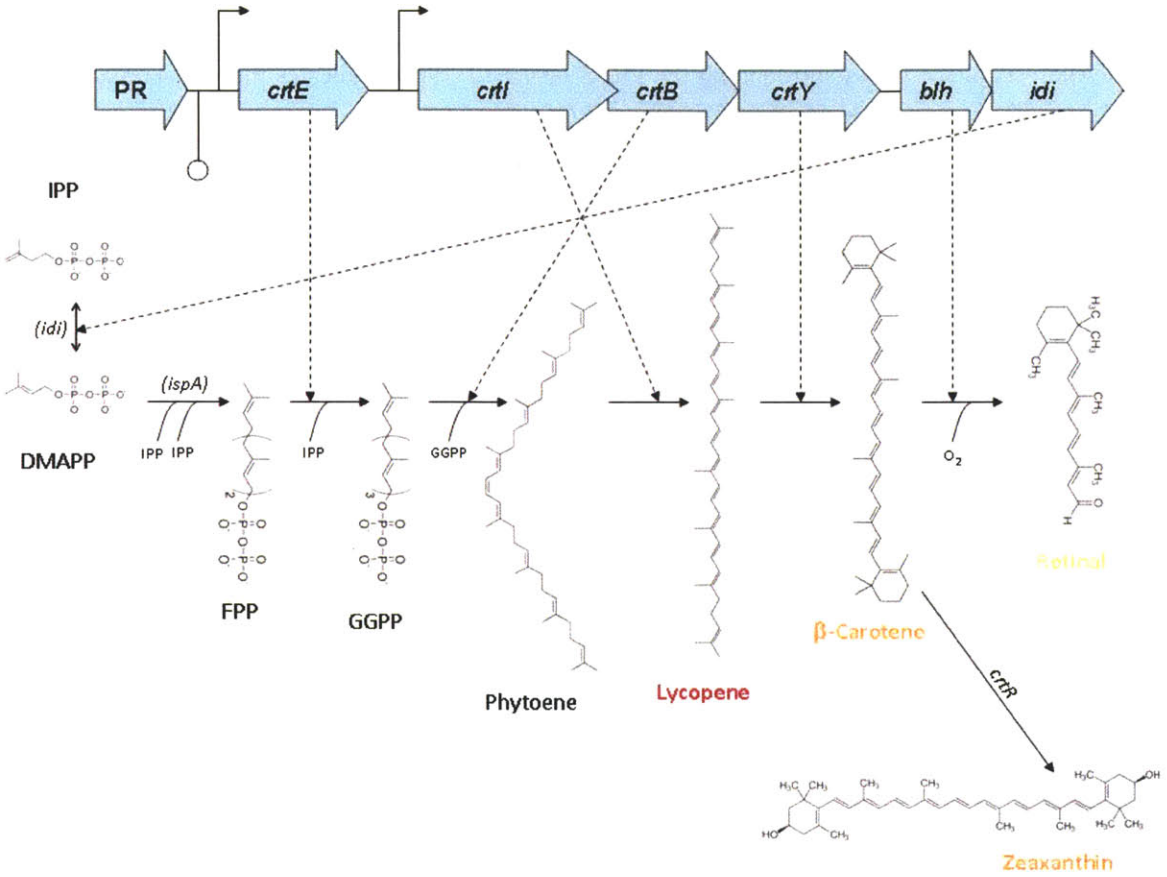

Figure 2-1: Proteorhodopsin Photosystem and Retinal Biosynthetic Pathway. Pathway and gene cluster described by Martinez et al., 2007. Biosynthetic pathway for the production of retinal is shown in the middle from left to right. Starting point for the pathway shown is isopentenyl disphosphate (IPP) which is produced in *E. coli* via a non-mevalonate pathway (Sabehi et al., 2005; Frigaard et al., 2006; Sharma et al., 2006; McCarren and DeLong, 2007). Intermediates and substrates along the pathway include: dimethylallyl diphosphate (DMAPP), farnesyl diphosphate (FPP), geranylgeranyl pyrophosphate (GGPP), phytoene, lycopene, and beta-carotene. Enzymes and genes responsible for the catalysis of the various steps are shown above the arrows; genes naturally occurring in *E. coli*, FPP Synthase (*ispA*) and IPP Isomerase (*idi*), are in parenthesis. Structure of products is shown with product name below. Production of zeaxanthin from β-carotene by β-carotene hydoxylase (*crtR*) shown for reference. The cluster of the seven genes comprising the PRPS of HF10_19P19 is shown above. The photosystem contains the gene for the proteorhodopsin (PR) as well as six genes associated with the cofactor retinal; *crtE* (GPP synthase), *crtI* (phytoene dehydrogenase), *crtB* (phytoene synthase), *crtY* (lycopene cyclase), *blh* (bacteriorhodopsin-related-protein-like homolog), *idi* (IPP isomerase). Dashed arrows indicate the reactor catalyzed by the corresponding gene product. The photosystem has predicted sites for transcriptional promotion and termination at the indicated locations. Figure adapted from Martinez et al., 2007.

Phylogenetic Origin of the HF10_19P19 PRPS

Analysis of the genes surrounding the PRPS on HF10_19P19 indicates that the 41,802 bp insert DNA was derived from an alpha proteobacterium (Rohmer et al., 1996). Aside from the genes for the PRPS, other predicted genes on the HF10_19P19 fosmid which were used to make the taxonomic assignment based on annotation of BLAST results include: flagellar motility motor proteins (motA and motB), molybdenum cofactor and molybdopterin biosynthesis proteins, anaerobic dehydrogenase and cytochrome C family protein, protease and peptidase, sulfate/tungstate ABC transporter, aminotransferase, methyltransferase, ATPase, 3-hydroxybutyryl-CoA dehydrogenase, phosphoribosyl-AMP cyclohydrolase, an RNA polymerase, a ribosomal protein, an iron-sulfur cluster binding protein, and a cytoplasmic chaperone protein along with many hypothetical proteins with unknown function (Martinez et al., 2007; McCarren and DeLong, 2007).

The PR found on the HF10_19P19 PRPS contains a glutamine residue at the tuning position (Martinez et al., 2007) which is indicative of a blue variant proteorhodopsin (Martinez et al., 2007). As noted previously (Man et al., 2003), blue variants often display slow photocycle kinetics which often correlate with lower light availability in the regions from which they were isolated (Martinez et al., 2007). However, blue variants with fast photocycle kinetics have been identified (Beja et al., 2001; Wang et al., 2003; Bielawski et al., 2004). The PR found onMedeBAC66A03 is the closest aligning to the PR on HF10_19P19 (Sabehi et al., 2005), and it has demonstrated fast photocycle kinetics and proton translocation in *E. coli* (Martinez et al., 2007). However, MedeBAC66A03 is a green variant (Sabehi et al., 2005), and site-directed mutagenesis to change the absorbance spectrum of green variants has also been associated with changing of the photocycle kinetics (Sabehi et al., 2005), so the photocycle kinetics of the HF10_19P19 PR remain highly speculative.

DNA sequence reference databases have grown since HF10_19P19 was first reported by Martinez et al., 2007. Performing a BLASTn analysis using the entire nucleotide sequence of the HF10_19P19 fosmid as the query against the National Center for Biotechnology Information (NCBI)

Genomes database reveals similarity (17% query coverage, e-value 5e-169) to a newly sequenced organism, Candidatus *Puniceispirillum marinum* IMCC1322 an alpha proteobacterium of the SAR116 clade (Man et al., 2003). The primary region of homology between the HF10_19P19 fosmid and the *P. marinum* genome is within the PRPS region, and when the BLASTn query is refined to only the PRPS the query coverage improves (29% query coverage, e-value 1e-124), and *P. marinum* is the top organism result for the PRPS from HF10_19P19 on the nucleotide level.

Evaluating the inferred amino acid sequence of the genes of the PRPS from HF10_19P19 (Oh et al., 2010) individually using tBLASTn against the NCBI Genome database, several species are repeatedly in the top three hits as demonstrated in Table 2-1 below. For all of the species with more than one top hit on the table [Candidatus *Puniceispirillum marinum* IMCC1322 (Martinez et al., 2007), *Vibrio harveyi* ATCC BAA-1116 (Oh et al., 2010), Rhodobacterales bacterium HTCC2255 (Bassler et al., 2007), and gamma proteobacterium HTCC2207 (Giovannoni et al., 2006b)], the genes for retinal synthesis and PR are arranged in a contiguous gene cluster in the same PRPS arrangement as seen in HF10_19P19 and other PRPS (Giovannoni et al., 2006a). These results provide further evidence for the likely lateral transfer and retention of PRPS genes among a variety of taxonomically diverse marine bacteria.

Table 2-1 tBLASTn Results for HF10_19P19 PRPS Gene Queries Against the NCBI Genome Database

	Hit #1		Hit #2		Hit #3	
ene	Species	-Val	Species	-Val	Species	-Val
R	Alpha proteobacterium HTCC2255	E-96	Vibrio harveyi ATCC BAA-1116	E-91	Candidatus Puniceispirillum marinum IMCC1322	E-91
rtE	Candidatus Puniceispirillum marinum IMCC1322	E-81	Alpha proteobacterium HTCC2255	E-70	Marine Gamma Proteobacterium HTCC2207	E-40
rtI	Candidatus Puniceispirillum marinum IMCC1322	E+00	Alpha proteobacterium HTCC2255	E+00	Marine Gamma Proteobacterium HTCC2207	E+00
rtB	Alpha proteobacterium HTCC2255	E-57	Candidatus Puniceispirillum marinum IMCC1322	E-54	Vibrio harveyi ATCC BAA-1116	E-44
rtY	Alpha proteobacterium HTCC2255	E-85	Candidatus Puniceispirillum marinum IMCC1322	E-76	Marine Gamma Proteobacterium HTCC2207	E-51
lh	Candidatus Puniceispirillum marinum IMCC1322	E-27	Alpha proteobacterium HTCC2255	E-26	Marine Gamma Proteobacterium HTCC2207	E-18
di	Candidatus Puniceispirillum marinum IMCC1322	E-97	Pseudomonas fulva 12-X	E-74	Xanthobacter	E-74

This chapter will describe the subcloning and characterization of a minimal, seven-gene PRPS from the previously characterized HF10_19P19 fosmid including the *idi* gene and all six genes previously shown to be necessary for the synthesis of a functional PRPS capable of generating proton motive force (PMF) and ATP from light (Sabehi et al., 2005; Martinez et al., 2007; McCarren and DeLong, 2007). In this work, I confirmed that these seven genes are sufficient for forming a fully functional photosystem in *E. coli*. The isolation of the functional photosystem in the copy-controlled pCC1FOS vector and the subsequent movement into pMCL200, a Lac-inducible plasmid expression system is described. The functionality of the retinal biosynthetic pathway and the expression of the integral membrane retinylidene protein from the photosystem were verified. Proton pumping activity and the ability to perform photophosphorylation using the produced proton motive force was demonstrated in the PRPS overexpressed using both vector systems. This work extends the initial characterization of this photosystem (Martinez et al., 2007), and sets the stage for experiments discussed in Chapter 3 and 4 describing the growth effects and expression of this minimal PRPS and other PRPS-containing large insert vectors in heterologous hosts.

Methods

Cloning and Constructs Made

PCR Amplification of the Photosystem from HF10_19P19

The PRPS from fosmid HF10_19P19 (Martinez et al., 2007) was amplified for subcloning by PCR (Martinez et al., 2007). Due to the length of the PRPS (7.6 KB) and early difficulties with obtaining a successful reaction, the high fidelity polymerase PfuUltra Hotstart (Agilent Technologies) was used for the amplification of the PRPS. The 50 µL PCR reaction contained 2.5 units polymerase in the 1X PfuUltra buffer (Agilent Technologies). Purified HF10_19P19 fosmid was added at approximately 1 ng purified as the template. Primers HF10_19P19_PRPS-5' (GGACGTTCTAGAACGCGACGTTTGGGGAG, Proligo) and HF10_19P19_PRPS-3'd (GCCTAGATTGCAGAATTGCAAGTGGAATTGGTC, Proligo) were added at 500 nM, and dNTPs (New England Biolabs) were supplied at 200 nM. The hotstart enzyme was activated with a 2-minute denaturing step at 93°C followed by 25 cycles of 40 seconds at 93°C, 30 seconds at 62°C, and 8 minutes at 72°C. The PCR program concluded with a 10 minute polishing step at 72°C followed by a hold step at 4°C.

Verification of PCR by gel electrophoresis of product and restriction pattern

One microgram of the PCR product was restriction digested with Hind III to verify the amplification product. Hind III digestions were performed in 15 uL volumes in 1X final concentration of New England Biolabs Buffer NE2 using 1 unit of Hind III. The restriction digestion was performed at 37°C overnight to allow complete digestion of DNA. The restriction enzyme was heat inactivated at 65°C for 20 minutes. The uncut and the Hind III digested PCR products were run on a gel 0.75% agarose (EMD CAS No: 9012-36-6) in 0.5X TBE buffer [5.4 g/L tris base (Calbiochem CAS No: 77-86-1), 2.75 g/L boric acid (Mallinckrodt Chemicals CAS No: 10043-35-3), 0.1 mM EDTA (Mallinckrodt Chemicals CAS No: 6381-92-6), pH 8.0] (Mullis et al., 1986) to verify product lengths (Ausubel, 1987). Gel was

run at 85 V for 1 hour and 15 minutes. The gel was stained with 1X SYBR Gold (Molecular Probes) for 20 minutes and imaged on an FLA 5100 (Fugifilm) with excitation at 473 nm and emission filter LPB.

Preparation of PCR Product for Blunt-End Ligation

Remaining PCR product was purified using a PCR Clean-Up Kit (Qiagen). Product was eluted in 50 uL buffer EB (Qiagen). The purified PCR product was treated with end-repair kit (Epicentre CCFOS110) to facilitate blunt-end cloning. End-repair reaction was 80 uL in volume in 1X end-repair buffer using 4 uL end-repair enzyme and final concentrations of 250 uM and 100 uM for dNTPs and ATP, respectively. Reaction was incubated at room temperature for 1 hour followed by heat inactivation at 70°C for 10 minutes. The product DNA was purified using gel electrophoresis (0.75% agarose, 0.5X TBE) run for 3 hours at 85 V. The gel was stained with SYBR gold for 15 minutes. Bands of the correct length (7.6 kb) were cut from the gel with the aid of a UV lamp. DNA was recovered from the gel pieces using a gel purification kit (Qiagen). DNA was eluted from purification columns using 50 uL buffer EB (Qiagen) and stored at -20°C until use in ligation.

Ligation and Transformation

The blunt-ended PCR product was ligated (Sambrook et al., 1989) into the pCC1FOS vector (Epicentre) at a molar ratio of approximately 1:1 (insert:vector); 2.5 uL insert (7650 nt) at 18.6 ng/uL was added to 10 uL vector (8139 nt) at 5 ng/uL. Ligation was performed in 30 uL 1X T4 ligase buffer with 1 uL (400 units) T4 DNA ligase (New England Biolabs) at 16°C overnight.

The ligation product was dialyzed against 20 mL 18.2 MOhm deionized water on a 0.025 um pore size filter (V series Millipore) to remove residual salts prior to transformation (Sambrook et al., 1989). 10 uL of the dialyzed ligation product was transformed into 15 uL electrocompetent Epi300 (Epicentre) at 2000V, 200 ohm, and 25 uF. Transformations were grown in 800 uL SOC media (Sambrook et al., 1989) at 37°C for 1 hr shaking at 175 rpm to build antibiotic resistance. 100 uL of the transformation was plated on LB-agar plate with 12.5 ug/mL chloramphenicol and grown overnight at

37°C. 192 colonies were picked from the plate into two 96-well blocks with Luria-Bertani (LB) media [BD Biosciences, 10 g/L tryptone, 5 g/L yeast extract, 10 g/L sodium chloride, (Hanahan, 1983)] supplemented with 15% glycerol (BDH/VWR) and 12.5 ug/mL chloramphenicol (Sigma). Blocks were grown overnight at 37°C and preserved at -80°C (Revco Legaci).

Selection and Verification of Proteorhodopsin Photosystem Clone

Following the approach used to identify the HF10_19P19 fosmid (Sambrook et al., 1989), potential clones were screened for color change from the expression of the proteorhodopsin photosystem. A white membrane filter (Pall #60305 Supor-200 0.2 um pore size, 142 mm diameter) was placed on top of a plate containing LB, 15 g/L bactoagar (BD Biosciences) and 12.5 ug/mL Cam and 0.001% L-arabinose (Sigma CAS No: 5328-37-0) to provide a suitable background for observing color change. Potential clones were transferred from the stock cultures to the plate using a 96-pin stamp. The plate was grown at 37°C overnight. One colony from the two plates (plate #2, well B6) exhibited an orange colored pigment characteristic of the expression of the photosystem on the HF10_19P19 fosmid (Martinez et al., 2007). A negative control strain was selected from the plate of colonies which did not show any color change (plate #2, well C9). The photosystem positive (J2B6) and photosystem negative (J2C9) clones were restreaked to ensure monoclonal populations, and glycerol stocks (LB + 15% glycerol) were prepared for five of the monoclonal colonies and cryopreserved for subsequent verification and use.

Fosmid was isolated from an overnight culture of clone J2B6 grown in 3 mL LB using the following protocol. Cell pellets were resuspended in 250 uL buffer P1 (Qiagen) with RNase. 250 uL of P2 lysis buffer (Qiagen) was added and mixed by repeated inversion. Within 5 minutes, 350 uL of N3 neutralization buffer (Qiagen) was added and immediately mixed by repeated inversion. The sample was centrifuged for 10 minutes at 13,200 rpm (Eppendorf 5415D). Supernatant was transferred to a clean microcentrifuge tube, mixed with 500 uL isopropanol and allowed to precipitate for 5 minutes. The sample was centrifuged for 5 minutes at 10,000 rpm (Eppendorf 5415D). Liquid was discarded and the

DNA pellet was washed with 500 uL 70% ethanol. Sample was centrifuged again for 5 minutes at 10,000 rpm. Liquid was discarded and pellet was dried of remaining ethanol before resuspension with 50 uL deionized water. Purified fosmid was analyzed on a NanoDrop 1000 spectrophotometer (Thermo Scientific) to determine DNA concentration and stored at -20°C.

Isolated plasmid was restriction digested with Hind III (New England Biolabs) for identification of the correct insert and to determine orientation in the vector. 500 ng of DNA was digested with 1 uL enzyme in 25 uL reaction of 1X buffer (NEB #2 for Hind III). Digestions were performed at 37°C overnight followed by heat inactivation at 65°C for 20 minutes. Digested fosmid was analyzed by gel electrophoresis (0.75% agarose in 0.5X TBE) at 85 V for 2 hours alongside 1 KB+ ladder followed by 15 minutes of SYBR Gold staining and imaging.

PCR was used to confirm orientation of the insert in the vector using the sequencing primers for pCC1FOS (Invitrogen, forward primer GGATGTGCTGCAAGGCGATTAAGTTGG, location 230-265; reverse primer CTCGTATGTTGTGTGGAATTGTGAGC, location 476-501; cloning site location 361-362) along with the primer for the amplification of the PR oriented from the inside toward the end of the gene cluster (Invitrogen, TTACTTTGCCGCTTCAGATTGTGA) to result in amplification of the PR with one of the two sequencing primers. PCR of 1 ng template fosmid DNA was performed with 0.5 uL Taq polymerase (New England Biolabs) 50 uL in 1X thermopol buffer. Primers and dNTPS were added to final concentrations of 200 nM and 200 uM respectively. The thermocycle program consisted of a 2-minute denaturing step at 95°C, followed by 25 cycles of 15 seconds at 95°C, 30 seconds at 61°C, and 1 minute at 72°C, and concluding with a 10 minute polishing step at 72°C and holding at 4°C. PCR products were analyzed with gel electrophoresis (1% agarose in 0.5X TBE with 1X SYBR Safe stain) at 125V for 1 hour and imaged on a Fugifilm FLA 5100 with excitation at 473 nm and emission filter LPB.

Transfer of the Photosystem to pMCL200 Vector

Isolated fosmid from the J2B6 clone (6 ug) was digested with 20 units BamHI in 20 uL of 1X NEB Buffer #2 supplemented with BSA for 1 hour at 37°C (New England Biolabs). pMCL200 vector was prepared simultaneously with BamHI digestion (20 units) and calf intestinal alkaline phosphatase (CIP, New England Biolabs) treatment (10 units) in 60 uL of NEB buffer #2 supplemented with BSA for 1 hr and 37°C. BamHI digested vectors were purified using 0.75% agarose gel electrophoresis at 100V for 2 hours. The gel was stained for 15 minutes in 1X SYBR gold. The bands corresponding to the PRPS from the J2B6 vector (7.7 kb) and the linearized pMCL200 vector (2.5 kb) were cut from the gel with the aid of a UV lamp and recovered from the gel using a gel extraction kit (Qiagen).

BamHI digested pMCL200 vector and PRPS insert were ligated at an approximate molar ratio of 5:1 (insert:vector, 2.4 ng vector + 52 ng insert) in 20 uL of 1X T4 ligase buffer overnight at 16°C. The ligation product was dialyzed against 20 mL 18.2 MOhm deionized water on a 0.025 um pore size filter (V series Millipore) before transformation. Transformation was performed using 5 uL of the dialyzed ligation product and 20 uL of electrocompetent Top10F' (Invitrogen) at 2000V, 200 ohm, and 25 uF in a 1 mm gap electrophoration cuvette. Transformed cells were incubated at 37°C in 800 uL SOC media + 0.2% glucose with shaking at 150 rpm for 1 hour. 100 uL of the transformed culture was plated on LB with 12.5 ug/mL chloramphenicol, 10 ug/mL tetracycline, 0.5 mM IPTG (Sigma, CAS No: 367-93-1), and 40 ug/mL X-Gal. 20 colonies with disruptions in the lacZ alpha gene (colonies not displaying the blue color in the blue-white screening process) were restreaked on LB-agar plates with chloramphenicol and 1 mM IPTG and grown overnight in 1.5 mL LB with chloramphenicol. Liquid cultures were pelleted for plasmid isolation which was performed as with the J2B6 fosmid described above.

Colonies were verified for the presence and orientation of the PRPS through color change on the IPTG induction plates and with a characteristic banding pattern produced from gel electrophoresis of Hind III (New England Biolabs) and Sca I (New England Biolabs) restriction digestion products. Restriction digestion was performed at 37°C overnight in 20 uL 1X NEB buffer (#2 for HindIII and #3

for ScaI) using 20 units of the restriction endonuclease and approximately 300 ng purified vector, followed by heat inactivation for 20 minutes at 80°C. Digestion products were separated with gel electrophoresis (0.75% agarose containing ethidium bromide) at 100V for 2 hours and imaged using the Fugifilm FLA-5100 with 532 nm excitation and LPG emission filter.

Plasmid DNA from the pMCL200 PRPS clone #5 was transformed into 20 uL of electrocompetent Epi300 (Epicentre) at 2000V, 200 ohm, and 25 uF. Transformed cells were grown in 800 uL SOC at 37°C at 175 rpm for 1 hour followed by plating of 10 uL on LB-agar with 0.5 mM IPTG and 12.5 ug/mL chloramphenicol. 5 replicate colonies were picked from the plate, grown in LB media supplemented with 15% glycerol, and cryopreserved at -80°C.

End-sequencing of the PRPS in both directions from either side of the cloning site of the pMCL200 vector was performed using the Sanger dideoxynuclotide termination method (Martinez et al., 2007) to confirm the identity and orientation of the PRPS in the vector. pUC sequencing primers matching the pMCL200 vector and primers used for the amplification of the PRPS from HF10_19P19 were used for the sequencing: pUC forward (CTTTACACTTTATGCTTCC), pUC reverse (GCAAGGCGATTAAGTTGG), HF10_19P19_PRPS-5' (GGACGTTCTAGAACGCGACGTTTGGGGAG), and HF10_19P19_PRPS-3'd (GCCTAGATTGCAGAATTGCAAGTGGAATTGGTC). The 10 uL reaction mix (BigDye V3 Terminator Kit, Applied Biosystems) for the primer extension contained: 0.5 uL BigDye Mix, 2.0 uL 5X buffer, 0.32 uL of primer (10 uM), and approximately 100 ng template DNA. The thermocycling program for the extension was: 1 minute at 96°C, followed by 30 cycles of 96°C for 10 seconds, 50°C for 5 seconds, and 60°C for 4 minutes. Following the primer elongation step, the products were treated with 2.5 uL of 125 mM EDTA and 35 uL of 96% ethanol and incubated at room temperature for 30 minutes. DNA was pelleted at 3000xg for 30 minutes and the supernatant was discarded. 70 uL of 70% ethanol was added to each reaction followed by pelleting for 15 minutes at 1650xg. The DNA pellets were drained onto a paper towel and spun at 185xg for 1 minute to remove residual liquid. Purified elongation

products were resuspended in Hi Di formamide (Applied Biosystems). Sequencing was performed using the ABI 3730 system (run module XLRSeq50_POP7). Sequence analysis was performed using Applied Biosystems sequence analysis software method 3730BDTv3-KB-DeNovo_v5.2. Sequence was analyzed using Sequencher (Gene Codes Corporation) and BLASTn (NCBI) was used to align the sequences from HF10_19P19 (Sanger et al., 1977) to the sequencing results.

The pMCL200 vector without an insert in the cloning site was transformed into Top10F' (Invitrogen) and Epi300 (Epicentre) strains using the same techniques described for the PRPS to serve as both a control for transformations and a subsequent negative control for experiments determining the function of the photosystem.

Transfer of the Photosystem Vectors into E. coli BW25113

Electrocompetent *E. coli* BW25113 (Martinez et al., 2007) was prepared using the following protocol provided by Tracy Mincer [adapted from a protocol from the Knight Lab at MIT (Baba et al., 2006)] An overnight culture was grown from monoclonal cryogenic stock in 3 mL LB at 37°C shaking at 250 rpm. The starter culture was diluted 1:1000 into 250 mL of LB-Lennox (10 g/L tryptone, BD Biosciences; 5 g/L, yeast extract, BD Biosciences; 5 g/L sodium chloride, Sigma) and grown at 37°C with shaking at 250 rpm for 2-1/2 hours. The culture was poured into a 250 mL centrifuge bottle and placed on ice for 15 minutes before pelleting for 10 minutes at 5,000 x g at 4°C using JA14 rotor. The pellet was washed twice by resuspending in 100 mL cold autoclave-sterilized deionized water followed by pelleting as before. The pellet was then washed twice by resuspending in 20 mL cold sterilized 15% glycerol with centrifugation for 10 minutes at 5,000 x g in 25 mL oakridge tubes using JS13 rotor. The final pellet was resuspended with 1 mL 15% glycerol, and 100 uL aliquots were flash frozen in cryotubes using a dry ice ethanol bath. Electrocompetent cells were stored at -80°C.

Plasmids prepared from Epi300 strains containing pFOS-PRPS, pMCL-PRPS, pMCL200, and pCC1FOS by the method described above were ethanol precipitated (Che et al., 2008) by the addition of

200 uL 100% ethanol and 10 uL of 3M sodium acetate to 50 uL of plasmid. Ethanol precipitations were incubated at -20°C for greater than 1 hour followed by pelleting at 13,200 rpm for 5 minutes in an Eppendorf 5415D microcentrifuge. The DNA pellet was washed with 200 uL cold 70% ethanol followed by another centrifugation step at 13,200 rpm for 5 minutes. The supernatant was discarded, and the pellet was allowed to dry before being resuspended in 30 uL sterilized deionized water.

Approximately 300 ng each plasmid (5 uL) was transformed (Sambrook et al., 1989) into 30 uL electrocompetent *E. coli* BW25113 at 2000V, 200 ohm, and 25 uF. Transformed cells were grown at 37°C for 45 minutes at 150 rpm in 800 uL SOC to build antibiotic resistance before plating 10 uL on LB-agar plates with 12.5 ug/mL chloramphenicol. Colonies were selected and stored cryogenically as described above.

Production of Retinal

For the purpose of verifying retinal production from the PRPS, an overnight starter culture of *E. coli* Epi300 pFOS-PRPS grown in LB with 12.5 ug/mL chloramphenicol was diluted 1:100 into 20 mL cultures of LB with chloramphenicol containing 0, 10, 40, or 160 uM 2-(4-methylphenoxy)triethylamine hydrochloride (MPTA, generous gift from Buddy Cunningham) and an equivalent associated methanol vehicle (Sigma CAS No: 67-56-1). After 3 hours of growth at 37°C, copy-up induction of the fosmid was performed at a final concentration of 0.02% L-arabinose. The cultures were grown for an additional 14 hours and pelleted at 5,000 rpm for 5 minutes (Sorvall Legend RT, Heraeus #3046 Rotor). The pellets were frozen at -80°C until extraction of the carotenoids.

Carotenoids were extracted from the cell pellets using a 7:2 mixture of acetone (Sigma CAS No: 67-64-1):methanol. 300 uL of solvent was added to the cell pellet in a 15 mL conical bottom centrifuge tube. The mixture was sonicated for a total duration of 15 minutes with cycles of 20 seconds on and 20 seconds off on high power using a Bioruptor sonication system (Diagenode) with ice water bath including 15 mL centrifuge tube sonication resonating chip. Following the extraction, the mixture was pelleted for 5

minutes at 7,000 rpm (Sorvall Legend RT, Heraeus #3046 Rotor) and the extract was transferred to a clean microcentrifuge tube. The pellets contained residual color after the first extraction and were extracted a second time with the same sonication program using 500 uL of 7:2 acetone:methanol solvent mixture. The extract was separated from the cell debris using another centrifugation step and the two extraction fractions were combined and stored at -80°C until being run on the HPLC.

Extract samples were analyzed with reverse phase gradient HPLC using modified Tokyo solvents (Sambrook et al., 1989); Solvent A was composed of 62.5% water, 21% methanol, 16.5% acetonitrile, and 10 nM ammonium acetate, and Solvent B was composed of 50% methanol, 30% ethyl acetate, and 20% acetonitrile. The gradient profile is summarized in the following table:

Table 2-2: Reverse Phase Gradient HPLC Program

Time (min)	%B	Flow (mL/min)
0	70	0.8
6	90	0.8
19	100	0.8
32	100	0.8
35	70	0.8

The program contained a 15 minute post-time to provide a sufficient period of the initial conditions prior to the injection of the next sample. HPLC was run on Agilent 1100/1200 system [degasser (G1379A), pump (G1312A), injector (G1367B), thermostatted column compartment (G1316A), diode array detector (G1315D)]. Sample injection was handled by an autosampler and was 100 uL in volume. The column for separation was a Zorbax C-18 column (Agilent, 150 x 4.6 mm column size, 3.5 μm particles, 80-100 angstrom pore size). A blank of 7:2 acetone:methanol was run prior to the first sample.

Data was collected using Chemstation for LC 3D Systems (Rev. B.03.01 Agilent) from continuous measurement of chromatograph traces at 370 nm and 475 nm for the detection of elution of retinal and carotenoids, respectively. In addition, the diode array detector (DAD) was set to record the spectrum from 200-600 nm in 1 nm increments at all times for spectral analysis of elution products. Analysis of absorbance spectra was performed with Chemstation.

Standards of all-trans retinal (Sigma CAS# 116-31-4) and lycopene (Sigma CAS# 502-65-8) were run under the same gradient conditions dissolved in the same 7:2 acetone:methanol mixture.

Absorbance Spectrum of Protorhodopsin in Membrane Preparations

Starter cultures of *E. coli* Epi300 containing pCC1FOS and pFOS-PRPS were inoculated from frozen stock into LB with 12.5 ug/mL chloramphenicol and incubated at 37°C and 250 rpm overnight. Starter cultures were diluted 1:1000 into 1 L LB with chloramphenicol and 0.001% L-arabinose and grown at 37°C and 250 rpm in 2 L Erlenmeyer flasks for 14 hours. Cultures were pelleted in 50 mL aliquots and washed twice in 10 mM Tris-HCl. Pellets were stored frozen at -20°C.

Sample pellets for membrane preparation were resuspended in 5 mL of a resuspension solution (20% sucrose, 30 mM Tris HCl, pH 8.0). 550 uL of a 10X lysozyme solution (5 mg/mL lysozyme, 100 mM EDTA, 50% glycerol, pH 7.5) was added to resuspended cells and incubated at room temperature for 30 minutes. The resulting spheroplasts were pelleted at 8,000 rpm for 10 minutes in a Sorvall Legend RT (Heraeus #3046 Rotor), and resuspended in 4 mL sterile deionized water. Disruption of cells was performed by sonication on ice in round bottom tubes with a Sonicator 3000 (Misonix) for 2 minutes total sonication time with cycles of 10 seconds on and 5 seconds off using a power setting of 4.0. Samples were centrifuged at 35,000 rpm using a SW 60 Ti rotor in a Beckman-Couter Optima-L-90K for 30 minutes at 4°C in 4 mL thinwall polyallomer tubes. Membrane pellets were resuspended in 3 mL sterile deionized water using the same sonication program described above and adjusted to a uniform OD_{600}.

Absorbance spectra of membranes between 350 nm and 700 nm were measured in 10 mm pathlength plastic cuvettes using a DU 800 spectrophotometer (Beckman). Membrane preparations from the same *E. coli* strain without the photosystem were used to provide a blank measurement, adjusting for the effects of scatter and allowing the absorbance spectrum of the retinal-bound proteorhodopsin to be isolated.

Verification of Proton Pumping Behavior

Strains of Epi300 containing the vectors pMCL-PRPS, pMCL200, pFOS-PRPS, and pCC1FOS, HF10_19P19 were streaked on LB-agar plates with 12.5 ug/mL chloramphenicol and grown overnight at 37°C. An entire colony was picked from each plate using an inoculating loop and spread evenly over a 150 mm diameter bactoagar (BD Biosciences) plates with LB, 12.5 ug/mL apramycin plate containing 12.5 ug/mL chloramphenicol and the appropriate inducer (0.2 mM IPTG for pMCL200 based vectors and 0.001% L-arabinose for pCC1FOS based vectors). Induction plates were grown for 48 hours at 37°C. Cells were suspended from the plate in 5 mL of a sterile non-buffer salt mixture containing 10 mM $MgSO_4$, 100 uM $CaCl_2$, and 10 mM NaCl by gentle scraping with a glass rod. The cell suspensions were pelleted at 6,000 rpm in Sorvall Legend RT (Heraeus #3046 Rotor) for 5 minutes, followed by a wash step of resuspension in 5 mL of the non-buffering salt solution and an additional centrifugation step. The washed pellets were resuspended in 5 mL of the non-buffering salt solution and diluted to an OD_{600} between 0.5 and 0.8. Resuspensions were maintained in the dark at room temperature until assayed.

Induction of UT5600 pBAD31A8 strain for the positive control of proteorhodopsin proton pumping behavior was performed by the following protocol adapted from (Maresca et al., 2007). An overnight culture inoculated from cryogenically frozen stock was grown on LB with 100 ug/mL ampicillin. The starter culture was diluted 1:100 into 25 mL LB with ampicillin and grown at 37°C with shaking at 250 rpm for 3 hours in a 250 mL Erlenmeyer flask. L-arabinose and all-trans retinal were added to the culture to final concentrations of 0.2%, and 10 uM, respectively, and the culture was grown for another 3 hours at the same conditions. The culture was pelleted, washed twice, resuspended in 5 mL non-buffering salt solution, and maintained in the dark until assayed.

The proton pumping assay was performed in a respiration chamber (Hansatech Oxygraph Plus). The water jacket surrounding the chamber was constantly recirculated to a water bath maintained at 40°C which resulted in a steady chamber temperature of approximately 31°C. The stirring setting was set to a

speed of 100. Light was provided to the chamber from Hanstech LS2H lamp through attenuating filters (Edmund Optics 46217 and 46218). Ambient light from the room was blocked from the chamber using a Styrofoam box. 2 mL of sample was introduced into the chamber which was enclosed by a modified plunger (part) which allows the introduction of a pH probe (AMANI-1000-L, Innovative Instruments) into the sample chamber. The pH probe was connected to the auxiliary channel of the respiration chamber via a pH amplifier (Hansatech PHA). The pH probe slope and offset were manually calibrated to pH 4.01, 7.01, and 10.01 standards prior to starting the proton pumping assay. After the introduction of samples into the chamber, a dark equilibration period of 2-3 minutes was allowed for the pH signal to stabilize. After the signal stabilized, the sample was subjected to repeated cycles of a 2-minute light exposure interval followed by a 2-minute dark interval.

Photophosphorylation with the Photosystem

Strains of Epi300 with the plasmids pMCL200, pMCL-PRPS, and pFOS-PRPS were used to test photophosphorylation of the *E. coli* containing the photosystem. Starter cultures were inoculated from frozen stock into 3 mL LB with 12.5 ug/mL chloramphenicol and grown overnight at 37°C with shaking at 250 rpm. The starter cultures were used at 1:1000 dilution to inoculate 25 mL cultures in LB with chloramphenicol. Induction for increased photosystem production with the pMCL200-based vectors was achieved using 0.5 mM IPTG included in the growth media at the time of inoculation; pFOS-PRPS copy-up induction was performed by addition of L-arabinose (0.001% final concentration) 3 hours after inoculation. All cultures were grown at 37°C, shaking at 250 rpm in 250 mL Erlenmeyer flasks for a total of 24 hours after dilution. Cultures were pelleted for 5 minutes at 5,000 rpm in Sorvall Legend RT (Heraeus #3046), washed twice with 5 mL non-buffering salt solution (described above for proton pumping assay) with centrifugation steps in between and resuspended in 10 mL of the non-buffering salt solution. Cultures were stored at 4°C for 72 hours and diluted to an OD_{600} of 0.55 to 0.60 prior to assaying for photophosphorylation.

3 mL of the resuspended culture was placed in two 5 mL glass vials with a magnetic stir bar. One of the two vials was covered with aluminum foil. Both vials were equilibrated in the dark for 60 minutes prior to the initial time measurement. Both vials were placed on a magnetic stir plate (Corning PC-420) operating on setting 4 to provide mixing. Illumination was provided by a desk lamp utilizing a halogen bulb (120V/50WGY8.0). To reduce excess heating effects from the lamp, a 500 mL glass bottle filled with deionized water was placed between the lamp and the samples. Irradiation at the samples was between 80-120 $\mu E/m^2/s$. Sample ATP content was measured again after 30 minutes of illumination.

For the measurement of culture ATP, 20 uL of sample was added to wells of a white opaque-bottom 96 well plate (Corning Costar 3917); five replicate measurements were taken for each condition. Dark (with foil) and light (without foil) conditions for any given strain were assayed in the same row of the plate. Columns 1 and 12 were reserved for blank samples, and samples were not measured in Row A to avoid edge effects of the plate. ATP standards ranging from 0.1 to 1000 nM were located in Row H. 100 uL of Promega Bac-titer-glo ATP reagent was added to each well of a row simultaneously using a 12-channel pipette, immediately after the addition of all samples to the wells. 5 minutes after addition of the ATP reagent, luminescence was read on a BioTek Synergy 2 plate reader without emission filter using a 1.0 second integration time, top optic position with 1mm probe vertical offset, and using an autosensitivity set to scale the 1000 nM ATP standard reading to 4,000,000 RLU.

Results

Subcloning the Proteorhodopsin Photosystem

For the purpose of demonstrating the sufficiency of the PRPS for light driven proton pumping and ATP synthesis and utilization for engineering applications, the PRPS was isolated from the neighboring genes on the environmental shotgun library fosmid HF10_19P19 previously characterized by Martinez et al (2007). We set about subcloning the PRPS from the fully sequenced HF10_19P19 fosmid by PCR amplification. The PCR protocol required several iterations of varying thermocycling conditions to produce a product of correct length and to obtain amplification efficiencies suitable to generate sufficient amounts of the 7.6 kb PCR product. After a suitable PCR protocol was established, the PCR product was confirmed using a HindIII endonuclease digestion which was predicted from the target sequence to yield a restriction pattern with bands at 1000, 2650, and 4000 nucleotides in length. Successful PCR product and the correct banding pattern are demonstrated in Figure 2-2.

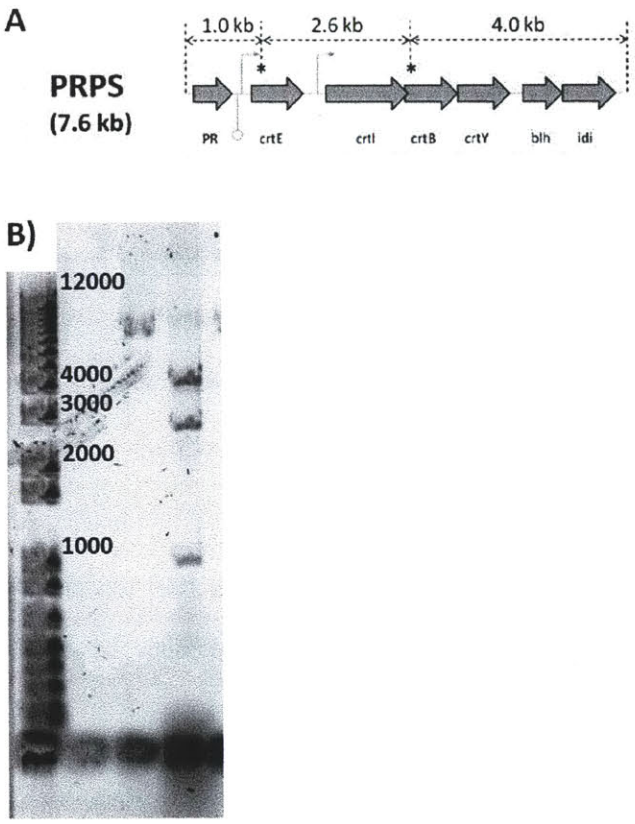

Figure 2-2: Hind III Restriction Verification of PCR Product. A) Linear map indicating the arrangement of the amplified PRPS. Asterisks indicate the location of Hind III cleavage. B) Agarose gel electrophoresis of PCR product and Hind III digestion band pattern. DNA ladder shown on left in lane 1 is the 1 kb plus ladder (Invitrogen). PCR product is shown in lane 3 (7650 bp). Hind III digest of the PCR product is shown in lane 4 (1000, 2650, and 4000 bp).

As a result of initial difficulties encountered in attempts to clone the PCR product into a pBAD33 vector, the strategy was changed in three critical ways. First, a high fidelity polymerase was used to reduce the possibility of errors in the PCR process to reduce the risk of mutations, which would cause loss of functionality in cloning products with the correct length and restriction pattern. Second, the screening process was modified to select colonies for further analysis on the basis of color, as was done for the discovery of the PRPS on the HF10_19P19 fosmid (Beja et al., 2000b). Finally, cloning vectors designed to accommodate large inserts were employed. The copy-control fosmid, pCC1FOS (Epicentre) was an obvious choice because of the established success with HF10_19P19. The 8139 nucleotide pCC1FOS vector contains two origins of replication which can be utilized by the Epi300 strain of *E.* coli. The first origin (*ori2*) is based on the F factor and provides for single copy maintenance and partitioning during replication; the second origin (*oriV*) allows high copy reproduction in the presence of the gene product from a mutant *trfA* gene which is under L-arabinose inducible control in Epi300. The low copy allows for stable maintenance of the fosmid, and the inducible increase in copy numbers allows for increased production of DNA which results in an increase expression of genes encoded on the fosmid.

These changes in the cloning strategy yielded a successful result. One pigment producing clone was identified in well B6 of plate two of two 96-well plates screened (Figure 2-3, left), one successful clone of 192 picked. The color produced by the clone was compared to the color produced by HF10_19P19 and contrasted to the unsuccessful clones SBG-B3 and SBG-A8 (Figure 2-3, right) to select a correctly pigmented photosystem.

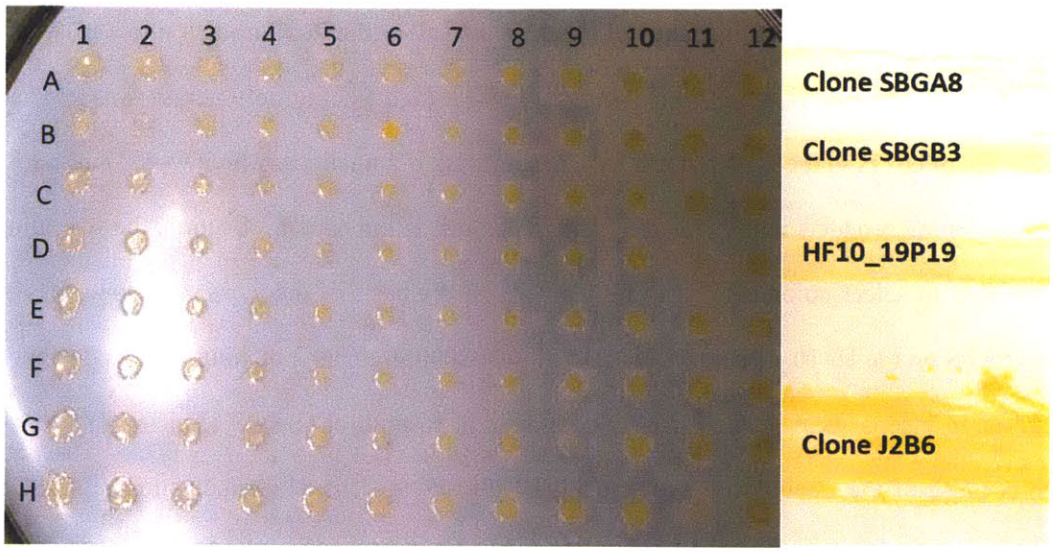

Figure 2-3: Color Screening of PRPS Subcloning Colonies. Left: 96-well plate #2 showing the color of selected clones from which the clone in well B6 was selected for its bright orange color. Right: streak of both functional (J2B6) and non-functional (SBGA8 and SBGB3) clones of the PRPS for color comparison to the parental PRPS-containing fosmid HF10_19P19.

The Hind III restriction pattern of the clone indicates the orientation of the PRPS in cloning site based on the location of the restriction site; a single Hind III restriction site (location 395) exists in the pCC1FOS vector downstream of the cloning site (location 361). Bands of approximately 1000, 2650 (internal to PRPS), and 12000 nucleotides indicates a reverse orientation (with respect to the vector nucleotide numbering system); bands of approximately 2650 (internal to PRPS), 4000, and 9000 nucleotides indicate a forward orientation (Figure 2-4A). Using this characteristic pattern, the PRPS was found to be in the reverse orientation in the fosmid (Figure 2-4B). The reverse orientation was confirmed by PCR using the pCC1FOS vector forward and reverse sequencing primers and the 3'-end primer for the amplification of the PR gene; only the reverse sequencing primer resulted in the amplification of the PR gene when used in combination with the 3'-end primer (Figure 2-4C). The PRPS is also in the reverse orientation in HF10_19P19 (Martinez et al., 2007). This configuration is also in the same orientation as the Lac promoter and chloramphenicol resistance gene (*cat*, chloramphenicol acetyltransferase) which is downstream of the cloning site suggesting the possibility that expression of the photosystem genes is due in part to read-through from these promoters.

To provide an alternative expression system to the pBAD-based arabinose induced copy-up fosmid, the subcloned PRPS was transferred to pMCL200 (Joint Genome Institute), a medium-copy number (P15A *ori*) vector with chlorampenicol antibiotic selection marker (*cat* gene) utilizing the Lac operator for IPTG-inducible expression of the genes located in the cloning site (Martinez et al., 2007). The PRPS was removed from the pFOS-PRPS vector through digestion with BamH I which cleaves at restriction sites (locations 353 and 365) immediately adjacent to the cloning site (location 361) and does not cleave at any restriction sites within the PRPS. These properties, along with the common use of BamH I as a restriction sequence in the multi-cloning site in vectors, make this approach attractive for moving the PRPS to other expression systems. Clones resulting from moving the BamH I restricted PRPS into the cloning site of pMCL200 were screened for color production. As with the pCC1FOS vector, a characteristic Hind III restriction pattern indicates the orientation in the cloning site (Figure 2-4A); the

forward orientation yields bands 1000, 2650, and 6500 nucleotides; the reverse orientation produces bands at 2650, 3500, and 4000 nucleotides (Figure 2-4D). The screening resulted in several candidates which displayed the predicted pigmentation and contained the PRPS in the forward orientation (as defined by the vector nucleotide numbering system). End-sequencing of the PRPS from the forward and reverse pMCL200 sequencing primers confirmed the orientation in the vector (Figure 2-5) which is also consistent with inducible expression from the Lac operator on the vector which resulted in the observable color change. Results from end-sequencing with the forward and reverse primers confirm the PR gene at the beginning of the insert (forward primer) and *idi* gene at the end of the insert (reverse primer).

A)

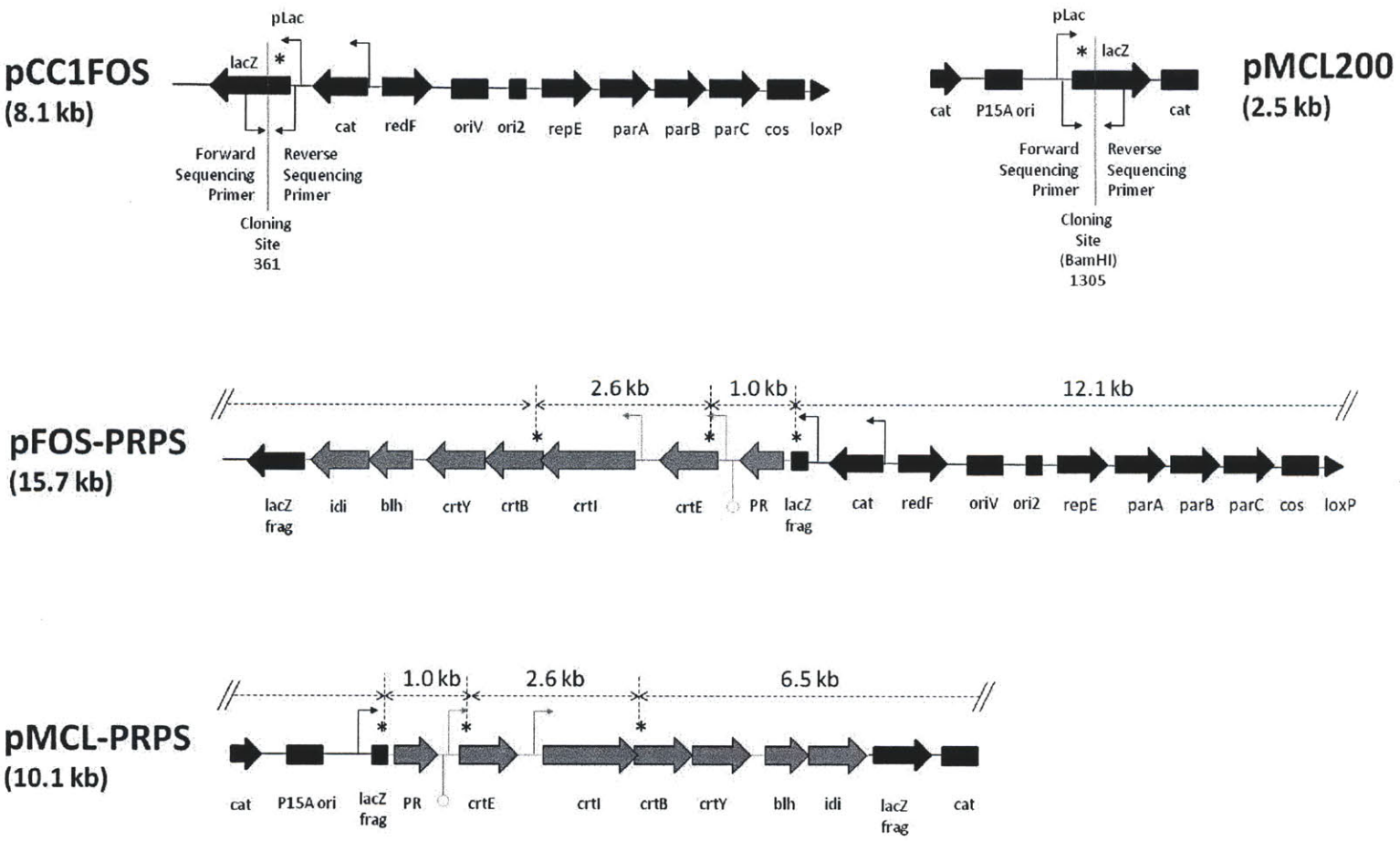

Figure 2-4: Results Confirming the Identity and Orientation of the PRPR Insert in pCC1FOS and pMCL200 Vectors. A) Linear vector maps indicating vector lengths, Hind III sites, and lengths of restriction fragments for vectors in the desired orientation.

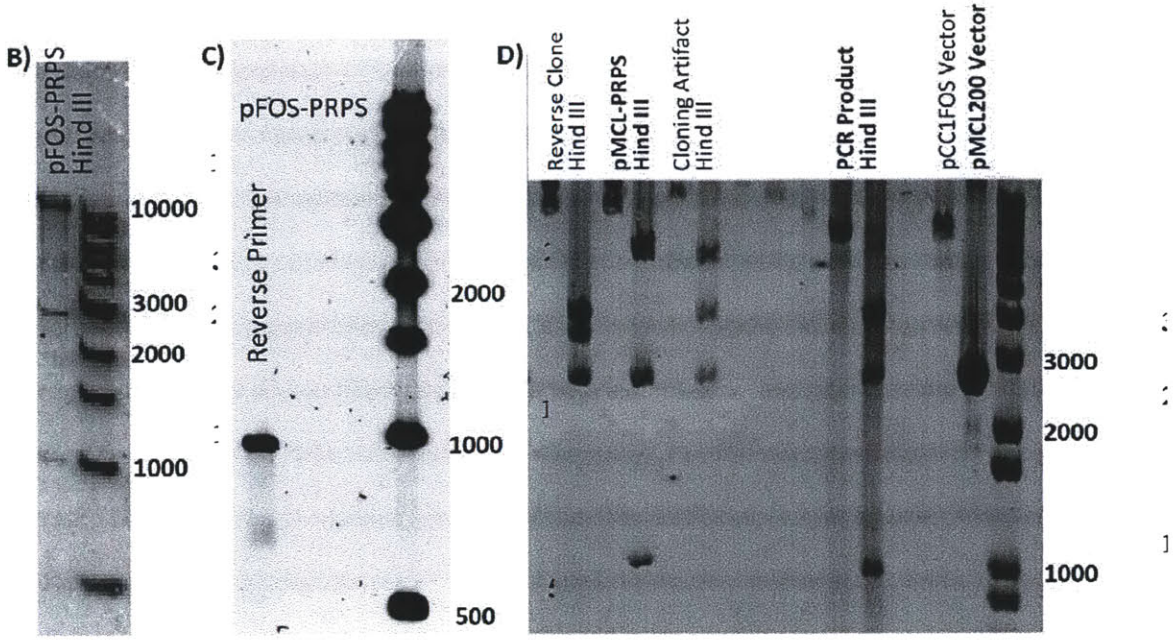

Continued from Figure 2-4. B) Clone J2B6 with the PRPS in vector pCC1FOS (pFOS-PRPS) Hind III Digested. Ladder at right is 1 Kb ladder (Invitrogen). Bands in the Hind III digest sample (approx. 1000, 2650, and 12000 bp) indicate the product identity and reverse orientation in the cloning site. B) PCR products of the PR gene using a primer located at the 3' region of the PR and reverse sequencing primer of the pCC1FOS vector. DNA ladder shown at right is the 1 kb ladder (Invitrogen). No product was present from the forward sequencing primer. C) pMCL-PRPS identification and orientation. DNA ladder shown at right is the 1 kb plus ladder (Invitrogen). From left: lanes 1 & 2 show a reverse orientation clone undigested and Hind III digested, respectively; lanes 3 & 4 show a pMCL-PRPS forward orientation clone undigested and Hind III digested, respectively; lanes 5 & 6 shows an unidentified cloning artifact; lanes 7,8, and 9 contain poorly detected traces of pFOS-PRPS DNA with various digestion states; lanes 10 and 11 contain undigested and Hind III digested PRPS PCR product for length standards; lane 12 is empty; lane 13 contains pCC1FOS vector linearized with Sca I; lane 14 contains pMCL200 vector linearized with Sca I; lane 15 contains 1 kb plus ladder.

A) pMCL-PRPS Forward Sequencing Primer Result

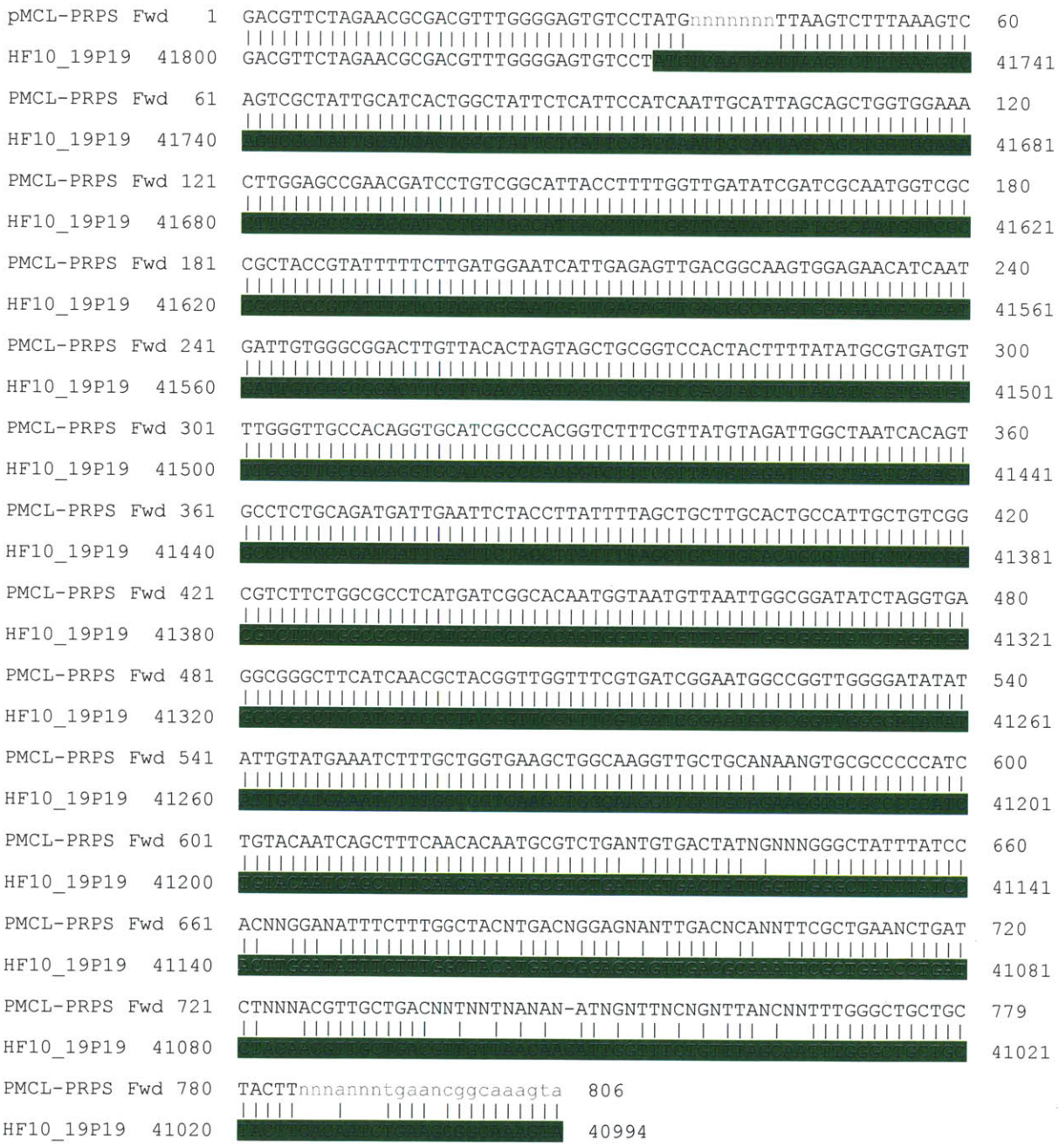

Figure 2-5: Sequence Data for pMCL-PRPS. A) Sequence data for forward sequencing primer aligned to HF10_19P19 using BLAST (NCBI)(Nakano et al., 1995). Coding region for the PR gene highlighted in green

B) pMCL-PRPS Reverse Sequencing Primer Result

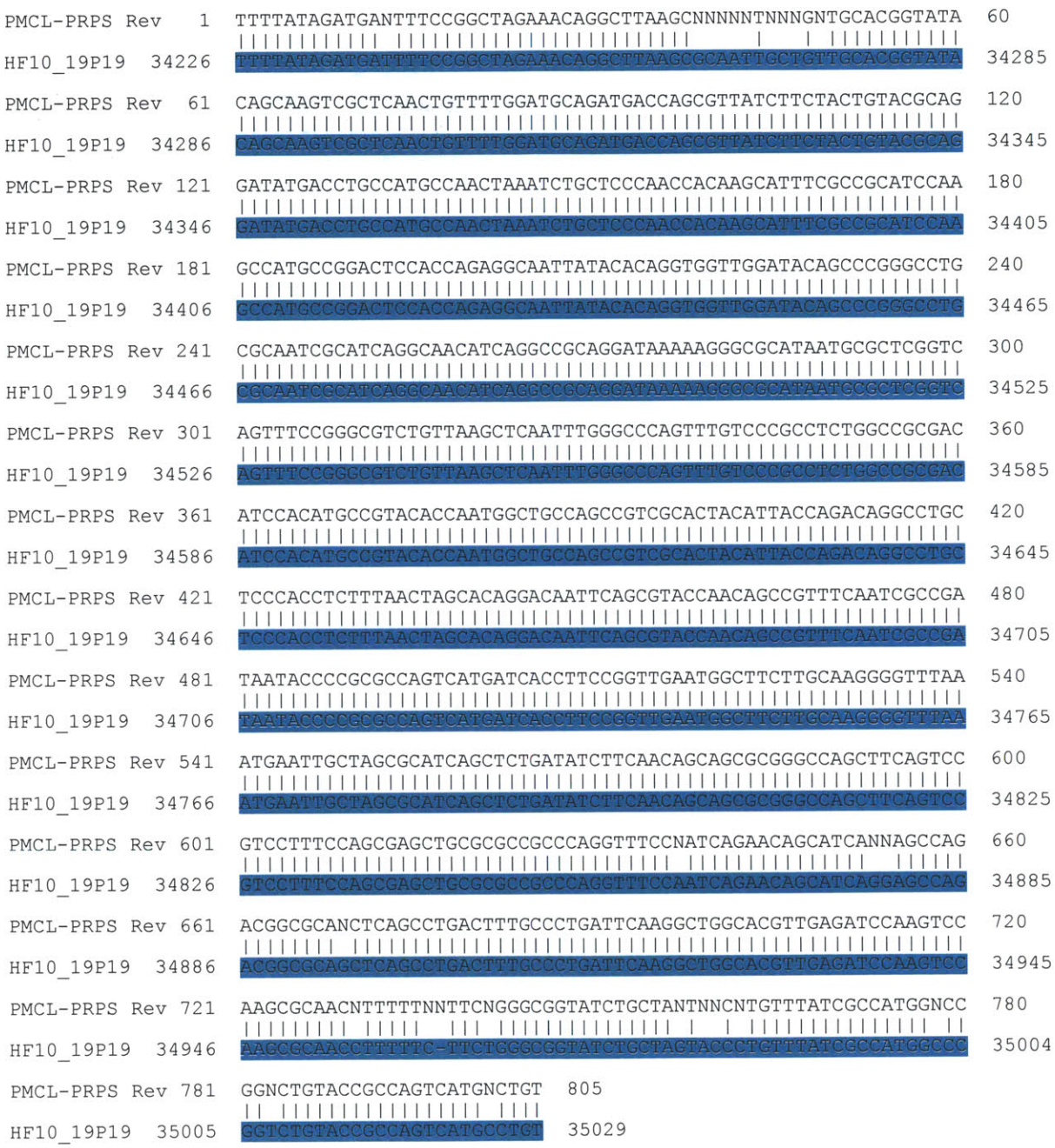

Continued from Figure 2-5: Sequence Data for pMCL-PRPS. B) Sequence data for reverse sequencing primer aligned to HF10_19P19 using BLAST (NCBI)(Altschul et al., 1990). Coding region for the *idi* gene highlighted in blue.

Production of Photosystem Components

While the change in color of the *E. coli* strain containing the photosystem is a strong indication that the components of the photosystem are being functionally expressed, it was important to verify both the production of retinal and the successful integration of retinal-bound proteorhodopsin in the plasma membrane of *E. coli* for the subcloned PRPS, confirming that this limited set of seven genes is sufficient for the production of the complete photosystem in *E. coli*.

The production of retinal is the end result of a metabolic pathway created by the enzyme products of six genes in the PRPS: *crtE*, *crtI*, *crtB*, *crtY*, *blh*, and *idi* (Altschul et al., 1990). Of these genes, five (*crtE*, *crtI*, *crtB*, *crtY*, and *blh*) are not found natively in *E. coli* and are required for production of retinal; disruption of any one of these five genes leads to the accumulation of an intermediate product in the retinal biosynthetic pathway as was demonstrated for the HF10_19P19 fosmid (Martinez et al., 2007). Verification that the PRPS contains a fully functional retinal biosynthetic pathway was achieved by HPLC analysis of extracted hydrophobic compounds produced by the Epi300 pFOS-PRPS strain following a period of copy-up induction. Results indicated the production of a compound with the same elution time as an authentic all-trans retinal standard (Figure 2-6A). Comparison of the absorbance spectrum at the period of peak elution confirmed that the absorption spectrum matched that of retinal (Figure 2-6C).

Inhibition of the retinal biosynthetic pathway provides a possible chemical option for the elimination or reduction in formation of the complete and functional photosystem. An inhibitor of lycopene cyclase (*crtY*), 2-(4-methylphenoxy)triethylamine (MPTA), has been shown to effectively block synthesis of β-carotene (Martinez et al., 2007) and resulted in elimination of a light-based growth effect in Dokdonia strain MED134 which has been attributed to a proteorhodopsin photosystem (Cunningham et al., 1994). In strain MED134, MPTA at concentrations as low as 10 uM was found to effectively eliminate the production of zeaxanthin, a carotenoid which shares β-carotene as a common precursor with

retinal (data not shown), as well abolish the light-enhanced growth in this strain (Kimura et al., 2011). To test the efficacy of such an approach in *E. coli*, MPTA was tested at various concentrations on Epi300 pFOS-PRPS induced for overexpression of the photosystem. HPLC results of cultures inhibited at 10, 40, and 160 uM MPTA show a reduction in the 8.5 minute elution product corresponding to retinal (Figure 2-6A, Figure 2-6C) with a concomitant accumulation of an elution product at 23 minutes corresponding to the elution (Figure 2-6B) and absorbance spectrum (Figure 2-6D) of lycopene. Comparison of the relative production of retinal across the concentrations of inhibitor tested demonstrates greater than 90% inhibition at 10 uM MPTA and greater than 100-fold reduction at higher MPTA concentrations (Figure 2-6E).

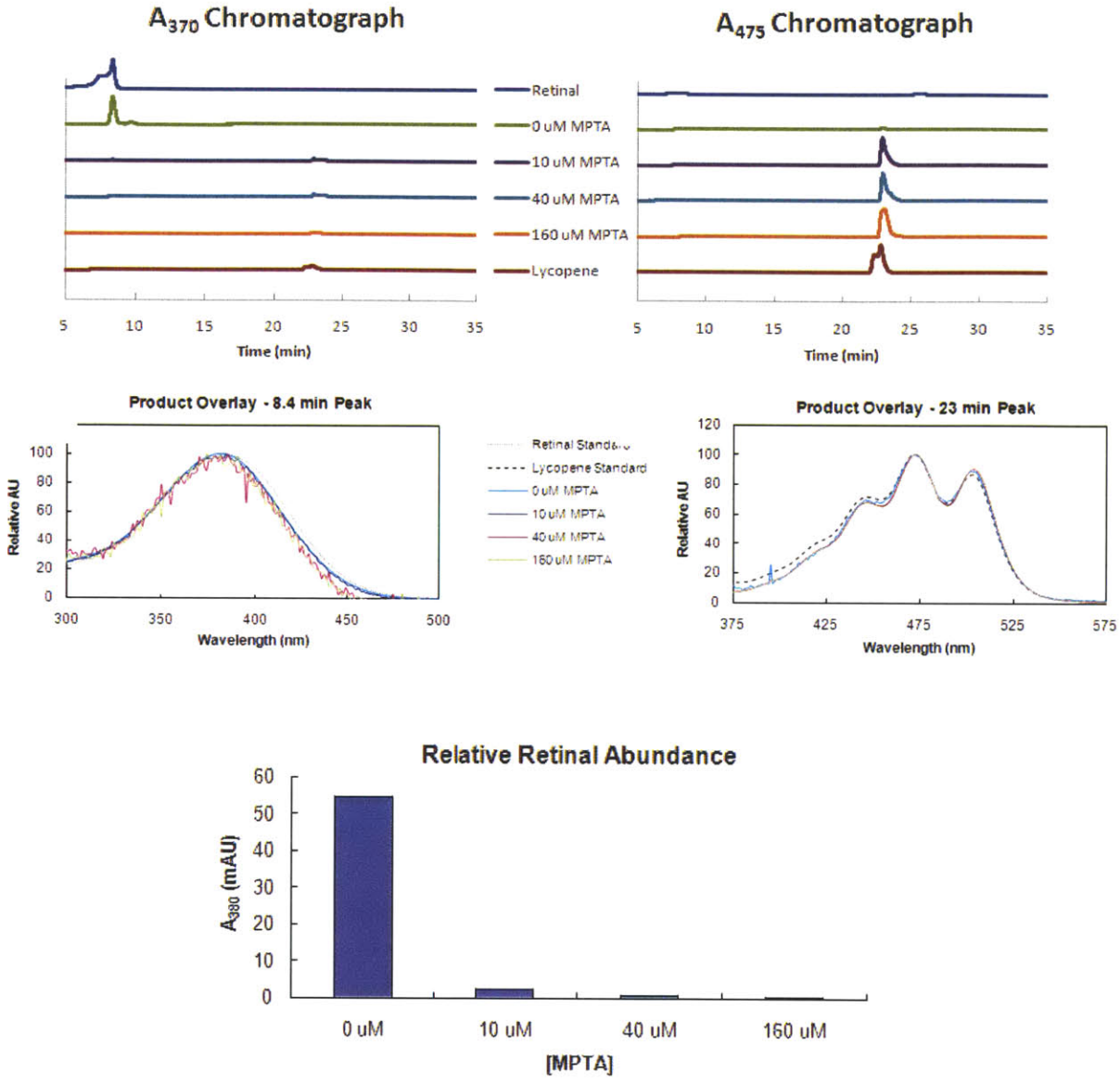

Figure 2-6: Production of Retinal in Epi300 pFOS-PRPS and Inhibition by MPTA. Chromatograph of absorbance at (A) 370 nm and (B) 475 nm throughout the 35 minute run time. Shown are samples of *E. coli* Epi300 pFOS-PRPS grown with 0, 10, 40, and 160 uM MPTA along with all-trans retinal and lycopene standards. Retinal with a peak absorbance near 370 nm elutes at 8.5 minutes, while lycopene with a peak absorbance near 475 nm elutes around 23 minutes. The culture without addition of MPTA shows a major product eluting at 8.5 minues; all cultures with MPTA show a major product eluting at 23 minutes. Comparison of the absorbance spectra for the products eluting at (C) 8.5 minutes and (D) 23 minutes confirms the identity of retinal and lycopene, respectively. (E) Comparison of the relative abundance of retinal as estimated by total absorbance at 370 nm shows the degree of inhibition in retinal synthesis achieved by various levels of MPTA.

With the biosynthetic production of retinal confirmed, the complete photosystem will be formed if the proteorhodopsin gene is expressed, correctly folded and inserted into the plasma membrane, and bound to the all-trans retinal. These conditions are confirmed simultaneously by the verification of the characteristic absorbance spectrum of the retinylidene protein in preparations of cellular membranes. Pellets of cultures of *E. coli* Epi300 pFOS-PRPS induced for copy-up expression show a bright orange color. Membranes prepared from *E. coli* Epi300 pFOS-PRPS pellets retain this pigmentation indicating that the chromophore is associated with the hydrophobic lipid bilayer and not the cytoplasmic fraction. Based on the HPLC results, this color is most likely attributed to proteorhodopsin as the absorbance spectrum of retinal is primarily in the ultraviolet spectrum (peak 374 nm) and the carotenoid intermediates, which produce orange and red colors (β-carotene and lycopene), do not accumulate in significant concentrations during retinal biosynthesis (Figure 2-6).

To observe the absorbance spectrum of the retinylidene protein in membranes isolated from *E. coli* Epi300 pFOS-PRPS overexpressing the PRPS, it was necessary to subtract background scatter associated with the membranes. To achieve this, membranes were prepared from *E. coli* Epi300 pCC1FOS and used at the same concentration to provide a blank spectrum. Matching the scatter from the two preparations is difficult as it depends on both the concentration of the membrane and the size distribution of the particles, which often results in small skews in the spectrum. These small flaws in the spectra do not detrimentally affect the qualitative interpretation and classification, however, they do lead to uncertainty in quantitative analysis. The spectrum in Figure 2-7 resulting from the baseline scatter subtraction matches the characteristic shape of a retinylidene protein, and the peak absorbance at 490 nm confirms that the proteorhodopsin is in fact a blue variant as was predicted from the glutamine residue at amino acid 105 and the sequence alignment with a proteorhodopsin variant exhibiting fast photocycle kinetics (Kimura et al., 2011).

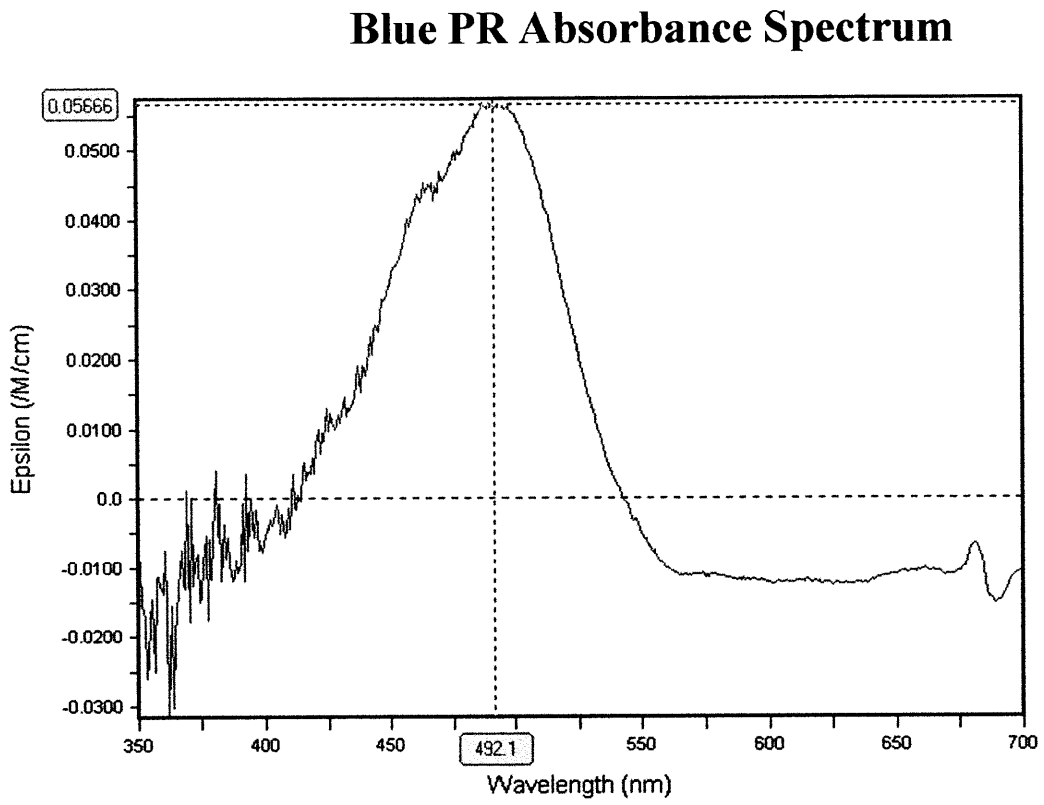

Figure 2-7: Absorbance Spectrum of Blue Proteorhodopsin from Subcloned PRPS. Membranes were prepared from *E. coli* Epi300 pFOS-PRPS induced for the expression of the photosystem. A blank spectrum was provided by Epi300 pCC1FOS not expression the PRPS. The absorption max at 490 nm and the shorter wavelength shoulder is indicative of a blue variant proteorhodopsin.

Functionality of the Photosystem

Following confirmation that the components of the photosystem are expressed in *E. coli*, the functionality of the photosystem was tested. The function of the proton pump can be observed directly by monitoring pH changes in the extracellular media. This method was pioneered by Stoeckenius and Oesterhelt in the characterization of the canonical proton pump bacteriorhodopsin (Martinez et al., 2007) found in the extremely halophilic archaea *Halobacterium salinarum and Halobacterium halobium* and has served as the standard method for validating potential proton pumps. A suspension of cells expressing a light-driven proton pump in a salt solution without appreciable buffering capacity will show a net acidification of the extracellular media in the light due to the translocation of protons from the cytoplasm into the periplasm and subsequent diffusion into the bulk media. In the dark, the acidification ceases, and a restoration of the media pH can be seen from the net transport of protons back to the cytoplasm.

Strains of *E. coli* Epi300 containing the vectors HF10_19P19, pFOS-PRPS, pCC1FOS, pMCL-PRPS, and pMCL200 were grown under induction conditions for the overexpression of the PRPS. The cultures were pelleted, washed, and resuspended in a non-buffering salt solution. The proton pumping capabilities of these systems were compared to the *E. coli* strain UT5600 pBAD31A08 containing the marine bacterial proteorhodopsin first discovered in EBAC31A08 (Oesterhelt and Stoeckenius, 1973), with induced expression and addition of exogenous all-trans retinal. *E coli* strains containing either pBAD31A08 or HF10_19P19 demonstrated clear proton pumping functionality as previously demonstrated (Beja et al., 2000b). Likewise, the strains containing pFOS-PRPS and pMCL-PRPS produced repeatable cycles of light-driven acidification followed by periods of pH increase in the dark (Figure 2-8). The control strains without the PRPS (pCC1FOS and pMCL200) did not demonstrate any light-dependent behavior. All strains exhibited a slight pH drift over the course of the experiment which is likely due to differences between the initial pH of the non-buffering salt solution and the internally buffered cytoplasm pH.

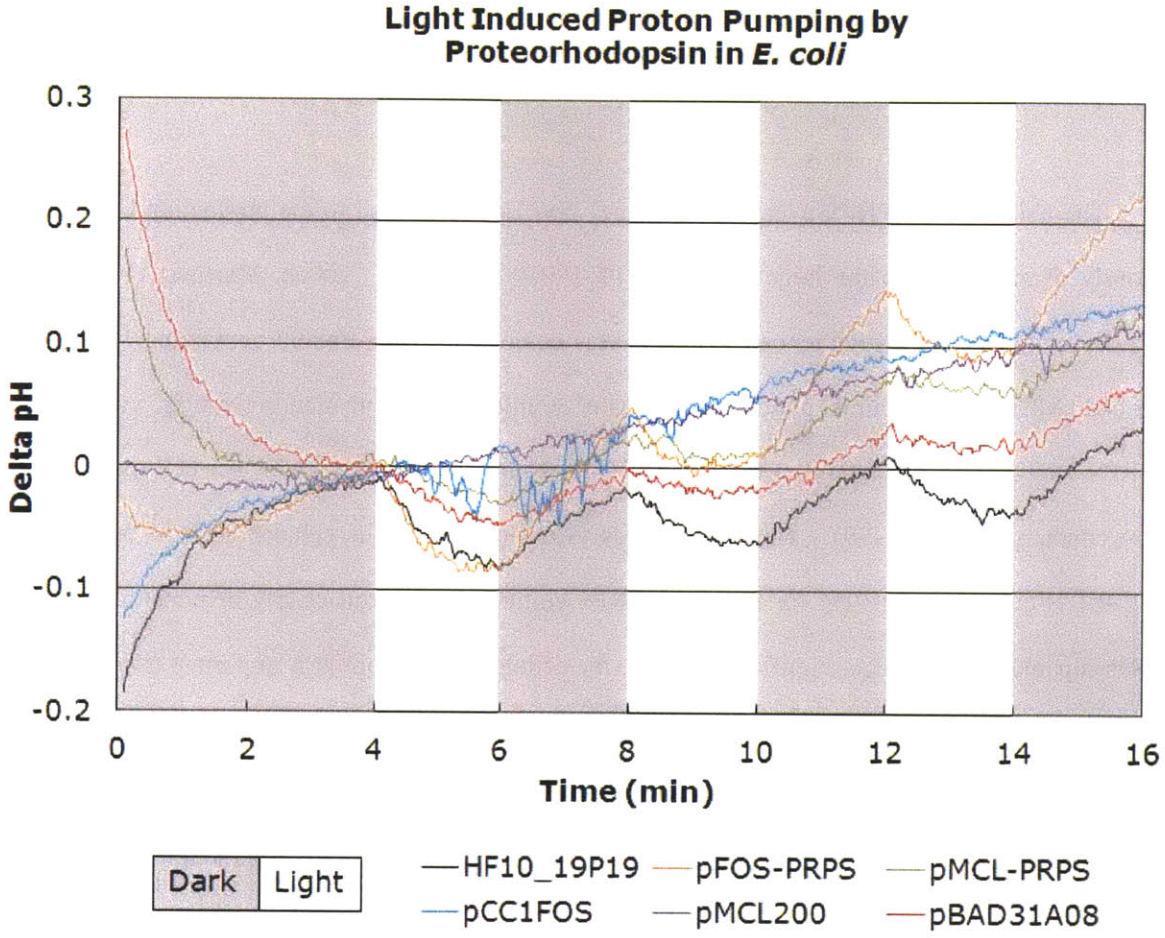

Figure 2-8: Light-Induced Proton Pumping Activity by Proteorhodopsin Photosystems in *E. coli*. Strains of *E. coli* Epi300 containing the PRPS photosystem (HF10_19P19, pFOS-PRPS, and pMCL-PRPS) were induced for overexpression with either L-arabinose or IPTG as appropriate. Cultures were pelleted, washed, and resuspended in non-buffering salt solution. Proton pumping behavior was verified after an initial three minute period of equilibration in the dark by repeated two minute cycles of light and dark. A drop in pH in the light and an increase in the dark is indicative of functional proton pumping. Results are compared to the extensively characterized PR of pBAD31A08 in *E. coli* UT5600 and negative controls of Epi300 containing empty expression vectors (pCC1FOS and pMCL200). A slight upward drift in pH through time can be seen in all samples resulting from endogenous metabolism and pH differences between the cell cytoplam and the salt solution.

The PMF produced by the proton pumping of the PRPS, analogous to that produced through the respiratory electron transport chain, can be used to drive energized membrane processes such as active transport, flagellar motility, and chemiosmotic ATP synthesis. Through these mechanisms, the light energy captured by the PRPS can power cellular functions and produce an effect on the physiology of the host.

The ability of the PRPS overexpressed in *E. coli* Epi300 to lead to the production of ATP was previously demonstrated in the large fosmid HF10_19P19 (Beja et al., 2000b; Martinez et al., 2007). Using the same approach, photophosphorylation was demonstrated for Epi300 containing both pFOS-PRPS and pMCL-PRPS minimal photosystems. After 30 minutes of incubation in the light, cultures with the PRPS were shown to contain on the order of 10,000 more molecules of ATP per cell than the dark culture counterpart Figure 2-9). This corresponds to an increase in the cellular ATP of 57% for the pMCL-PRPS cultures and 101% for the pFOS-PRPS cultures. This result clearly demonstrates that the PRPS is capable of providing a significant boost to the cellular energy pool. It is important to note that the light-driven differences in ATP are only observable for cultures after a period of starvation; cultures assayed for ATP immediately after removal from growth do not show substantial differences in ATP levels which is likely the result of ample respiratory activity overshadowing the effects of the PRPS.

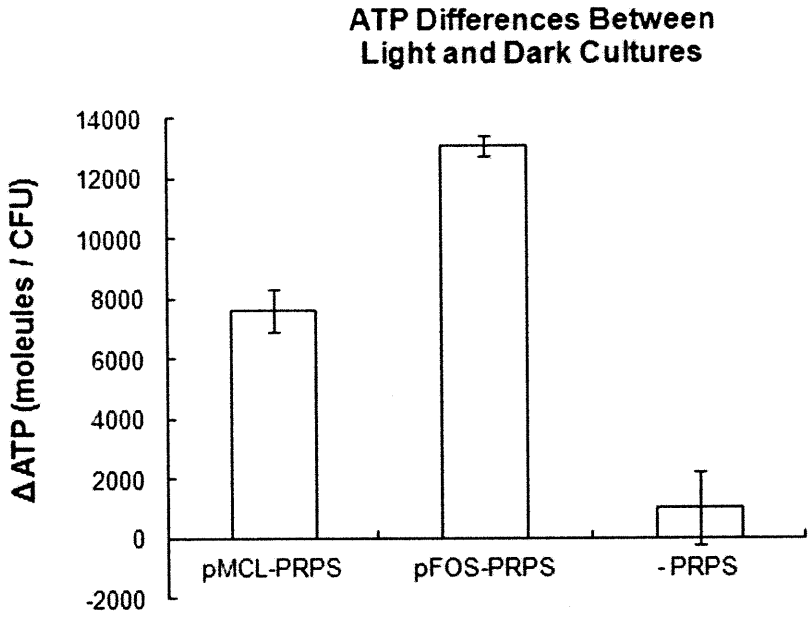

Figure 2-9: Photophosphorylation with the PRPS. Cultures of *E. coli* BW25113 were grown under induction conditions for the overexpression of the PRPS, pelleted, washed, and resuspended in a non-buffering salt solution and starved for 72 hours at 4°C to allow respiration of residual carbon sources. Viable cell counts (CFU) were tittered using serial dilutions on LB-agar plates with chloramphenicol. Samples were added to two vials, one was covered in foil, and both were equilibrated to the dark. ATP measurements were taken after 30 minutes of illumination. Data shown is the different in ATP between the light and dark cultures normalized to the CFU counts for each strain. Error bars indicate the standard deviation between five replicate ATP measurements.

Discussion & Conclusion

The work presented in this chapter has demonstrated that the seven subcloned genes of the PRPS derived from fosmid HF10_19P19 (Martinez et al, 2007) are sufficient for the production of a functional photosystem in *E. coli*. The photosystem genes resulted in the production of the cofactor chromophore retinal, as well as PR, which covalently bound retinal and properly folded as an integral membrane retinylidene protein in *E. coli* membranes *in vivo*. It was shown that overexpression of the photosystem conferred the ability to pump protons across the cytoplasmic membrane creating a PMF which is capable of generating ATP in the presence of light.

Overcoming the challenges in generating a functional cloning product of the 7.6 kb PRPS required the use of a high fidelity polymerase and a cloning vector suitable for medium to large target insert. The utility and the pitfalls of phenotypic color screening, described previously (Martinez et al., 2007), were demonstrated by this cloning process; while screening for visibly colored colonies was successful in identifying clone J2B6 with the functional PRPS, an earlier clone candidate appeared to have a suitably colored phenotype but was found incapable of light-driven proton pumping.

Here, the sufficiency of a minimal set of seven genes from HF10_19P19 to generate a functional photosystem was demonstrated by the overexpression of the PRPS in two vector systems with different mechanisms of expression control. The L-arabinose inducible copy-up system combining Epi300 and the pCC1FOS vector creates increased transcription resulting from additional copies of the fosmid DNA which leads to a higher overall activity of the promoters native to the vector and insert. A benefit of this system is that the basic mechanism of transcriptional control is unchanged between the single-copy and the multiple-copy states allowing any regulation native to the inserted PRPS to be maintained; promoter and terminator regions are predicted within the PRPS which were presumably optimized in the original host organism. The increased expression in this system comes at the additional cost of increased DNA replication, and another drawback of this system is the inability to transfer to a broader range of hosts and

maintain inducibility. On the other hand, the inducible transcription through the Lac operator located on the pMCL200 vector does not result in any increased DNA synthesis burden and is generically functional in hosts containing a compatible lactose regulon. The BamH I restriction fragment encompassing the PRPS allows the possibility to easily move the entire photosystem to other expression systems to cover the range of expression systems, replication origins (copy number), and selectable marker. This may prove useful not only for characterizing the performance of the photosystem, but also for integrating the mobile light powered system into other engineered systems for potential applications.

Induction is required for the increased expression levels that lead to the visual cue of color change, and color change generally correlates to the ability to observe proton pumping activity and ATP formation in the assays we employed [(Martinez et al., 2007), this work]. This raises the question of optimal physiological expression levels and the sensitivity of current assays for gauging functional activity of the photosystem, which may or may not be overlapping. It is clear that even at high levels of expression, the measurement of photosystem functionality is affected by the respiratory activity of the host; photophosphorylation and light-driven increases in flagellar rotation could only be clearly identified in cultures which have limited respiration due to starvation or the introduction of an inhibitor (Martinez et al., 2007). This is in agreement with the repeated observation that physiological effects of light on wild type bacterial strains containing proteorhodopsins are only observed in conditions of extremely low carbon, and presumably concomittant low respiratory rates (Martinez et al., 2007; Walter et al., 2007). Additional study is needed to determine what a suitable expression level is for evoking a physiological response, and to evaluate if this expression level is within the limits of detection of the assays for the functionality of the photosystem.

Chapter 3: Physiological Effects of a Proteorhodopsin Photosystem in *Pseudomonas putida*

Abstract

The mobility of the proteorhodopsin photosystem (PRPS) in the environment (Gomez-Consarnau et al., 2007; Gomez-Consarnau et al., 2010; Steindler et al., 2011) and the broad range of phylogenetic diversity of organisms harboring the photosytem genes (Frigaard et al., 2006; Sharma et al., 2006; McCarren and DeLong, 2007) indicates a degree of modularity and universality that warrants study of the PRPS in a variety of host organisms. In addition, studies of physiological behavior of strains with a native PRPS demonstrate a wide variety of responses (de la Torre et al., 2003; Sabehi et al., 2003; Venter et al., 2004; Slamovits et al., 2011) suggesting a range of physiological responses in heterologous hosts. The utility of a multiple host approach for functional characterization of environmental gene clusters has been previously demonstrated (Gomez-Consarnau et al., 2007; Gonzalez et al., 2008; Gomez-Consarnau et al., 2010; Steindler et al., 2011). Following this approach, the sub-cloned PRPS (Chapter 2) from HF10_19P19 (Martinez et al., 2004) was modified to include a cassette that allows the fosmid to be conjugated into a broad range of hosts (Asuncion Martinez, unpublished data). The modified fosmid also facilitates the site-specific integration of the vector into strains containing the specific ϕC31 *attB* recombination site, including the engineered strain *Pseudomonas putida* MBD1 (Martinez et al., 2007).

In this work, conjugation-capable pCC1FOS modified vectors pSJ2B6 and pSCCFOS (with and without the PRPS, respectively) were conjugated into strain *P. putida* MBD1 (Martinez et al., 2004). This produced strains *P. putida* pSJ2B6 and *P. putida* pSCCFOS, in which the conjugated vectors are integrated into the *P. putida* chromosome at the *attB* site. The transcription of the PR gene in *P. putida* pSJ2B6 was verified through reverse transcriptase polymerase chain reaction. While direct evidence of retinal production and functional assembly of retinal-bound integral-membrane PR was not confirmed in this study, a light-dependent growth yield increase was observed for *P. putida* pSJ2B6. The lack of a similar phenomenon in *P. putida* pSCCFOS suggests the light-dependent growth effect was due to the

presence of a functional PRPS. The observed PRPS-based light-dependent increase in growth yield was found to be dependent on the concentration of glucose added to the media; a glucose concentration of 1.1 mM abolished the light-dependent growth effect that was seen at lower glucose concentrations. The exact mechanism underlying the observed phenotype remains to be elucidated, but this work demonstrates the first time in which a light-dependent increase in the yield of a heterotrophic host could be attributed to heterologously exrpressed PRPS.

Introduction & Background Information

The small size and modular nature of the proteorhodopsin photosystem makes it an attractive target for expression in a variety of host organisms (Martinez et al., 2004). The observations that the proteorhodopsin gene and the photosystem cluster are found across a wide range of phylogenetic diversity (Martinez et al., 2007) and that the photosystem appears to be transferred through horizontal gene transfer mechanisms in the marine environment (de la Torre et al., 2003; Sabehi et al., 2003; Venter et al., 2004; Frigaard et al., 2006; Sharma et al., 2006; McCarren and DeLong, 2007; Slamovits et al., 2011) support the rationale for experimenting with different host systems. Studies with isolated strains possessing proteorhodopsin have displayed a variety of phenotypes in response to light including: increased growth rate and yield (Frigaard et al., 2006; Sharma et al., 2006; McCarren and DeLong, 2007), increased survival (Gomez-Consarnau et al., 2007), CO_2 uptake (Gomez-Consarnau et al., 2010), and ATP synthesis and decreased respiration rate (Gonzalez et al., 2008). The differences in phenotypic responses may be an indication of alternate strategies for utilizing the energy captured by proteorhodopsin. In this context, it is a logical progression to evaluate the physiological effects of proteorhodopsin in an alternative host organism, particularly when previous attempts to elicit a physiological response in *E. coli* did not yield conclusive results (data not shown).

A Conjugative and Integrative Vector-Host System for Functional Screening of Large-Insert Environmental Libraries in Multiple Hosts

Screening the products of environmental DNA across a background of multiple hosts is not a new concept. Motivated by the discovery of natural products of pharmaceutical therapeutic value from DNA isolated from uncultured soil microorganisms (Steindler et al., 2011), Martinez et al. developed a conjugative vector system for integration into *Streptomyces lividans* and *Pseudomonas putida* to be used for screening large-insert libraries of environmental DNA (Seow et al., 1997; Rondon et al., 2000; Wang et al., 2000; MacNeil et al., 2001; Courtois et al., 2003).

The vector-host system previously developed is conjugative and integrative in *Streptomyces* (CIS) at the host chromosomal ϕC31 *attB* recognition site (Martinez et al., 2004). A previously constructed conjugative and integrative plasmid (Martinez et al., 2004) containing the ϕC31 *attP* recognition site, ϕC31 integrase gene, and acc(3)IV conferring $Apra^R$, (Bierman et al., 1992) along with an origin of transfer (oriT) from the RK2 plasmid for conjugation (Kuhstoss et al., 1991; Bierman et al., 1992) was used to create a CIS cassette flanked by loxP sites (Guiney and Yakobson, 1983). The CIS cassette is maintained on the donor plasmid pMBD12 which contains a selectable marker for ampicillin resistance (*bla*, Amp^R), a counter-selectable marker for sucrose sensitivity (*sacB*, Suc^S) (Martinez et al., 2004), and the oriC origin of replication (Reyrat et al., 1998).

The CIS cassette can be transferred from the pMBD12 plasmid into any desired host vector containing a *loxP* site (Martinez et al., 2004). This is accomplished using a Cre-mediated recombination (Martinez et al., 2004). The resulting plasmid can be transferred from a donor strain into any recipient capable of accepting a vector through the broad host range RK2-type conjugation. *E. coli* DH10B can be made into a suitable donor strain by the incorporation of pUB307, a helper plasmid to facilitate conjugation in *trans* from oriT (Sauer, 1994).

The constructed system is naturally compatible with *Streptomyces* recipient strains which contain the *attB* site which is the target of recombination for ϕC31 (Flett et al., 1997). To broaden the range of

host organisms for screening environmental DNA libraries contained in the CIS-retrofit BAC vectors, Martinez et al. engineered a strain of *Pseudomonas putida* to contain the ϕC31 *attB* recognition site complementary to the ϕC31 *attP* site and integrase found on the CIS vectors. The ϕC31 *attB* was introduced into the *P. putida* KT-2440 strain (Martinez et al., 2004) using the phage ϕCTX integration site found on the chromosome (Franklin et al., 1981). Briefly, this was accomplished by combining the amplified ϕC31 *attB* sequence from *S. lividans* TK24 (John Innes Centre) with a DNA fragment containing the ϕCTX *attP* [from a *P. aeruginosa* phage, (Martinez et al., 2004)] on a plasmid with kanamycin resistance (Kan^R) and the colE1 origin of replication (Wang et al., 1995). The plasmid was contransformed with a helper plasmid containing the ϕCTX integrase (Martinez et al., 2004) into electrocompetent *P. putida* KT-2440 (Wang et al., 1995) allowing integration of the plasmid DNA at the *P. putida* KT2440 ϕCTX *attB* site (Franklin et al., 1981). The resulting strain was named *P. putida* MBD1 (Martinez et al., 2004).

This vector-host system was used to demonstrate the utility of multi-host functional screening of environmental large-insert libraries for antibiotic production (Martinez et al., 2004). BAC vectors with the CIS cassette were introduced into three hosts *Escherichia coli*, *Streptomyces lividans*, and *Pseudomonas putida* (Martinez et al., 2004). The vectors successfully integrated into the chromosomes of *S. lividans* and *P. putida* MBD1 at the ϕC31 *attB* site (Martinez et al., 2004). In confirmation of the utility of the multi-host approach, each strain demonstrated unique abilities for the production of antibiotic compounds; screening in all three hosts enabled a greater diversity of antibiotic production than would be achieved by a single host (Martinez et al., 2004).

Psedumonas putida

Pseudomona putida is a rod-shaped gram-negative bacterial belonging to the Pseudomonadaceae family of the Pseudomonadales order of Gamma Proteobacteria (Martinez et al., 2004). *P. putida* is an obligately aerobic heterotrophic saprophytic soil bacterium, decomposing organic matter in the soil as a source of nutrients (Bergey and Holt, 1984). The bacterium is known to colonize plant roots in a

symbiotic fashion (Bergey and Holt, 1984). *P. putida* is non-spore-forming and non-pathogenic (Molina et al., 2000), however it is closely related to the opportunistic pathogen *Pseudmonas aeruginosa* (Bergey and Holt, 1984). The National Institute of Health has designated *P. putida* as a safety strain, indicating that it is authorized for the introduction of heterologous DNA for study (Nelson et al., 2002).

In particular, the parent strain of *P. putida* MBD1 (United States. Office of the Federal Register. and National Archives (U.S.), 1982), *P. putida* KT2440, is perhaps the best studied soil bacterium and as a result it has become a workhorse of soil bacterium gene cloning and expression (Martinez et al., 2004). *P. putida* KT2440 is host-specific restriction negative (Ramos et al., 1987; Timmis, 2002), and vector systems have been developed to allow expression of genes from maintained plasmids (Bagdasarian et al., 1981). The diverse metabolic capabilities of *P. putida* have garnered extensive interest for use in bioremediation (Bagdasarian et al., 1981; Lushnikov et al., 1985; Olekhnovich and Fomichev, 1994), biocatalysis (Dejonghe et al., 2001; Nwachukwu, 2001), and biopolymer production (Schmid et al., 2001).

P. putida KT2440 is derivative of *P. putida* mt-2 lacking the TOL plasmid pWWO (Olivera et al., 2001) (Bagdasarian et al., 1981), a 117-kb plasmid containing genes encoding a metabolic pathway for the biodegradation of toluene (Regenhardt et al., 2002). The entire genome of *P. putida* KT2440 is a found on a single 6.2 Mb circular chromosome with an average GC content of 61.6% (Franklin et al., 1981; Greated et al., 2002). The genome contains 5420 open reading frames, 3571 with assigned function, 1037 conserved hypothetic proteins, and 600 unique hypothetical proteins (Nelson et al., 2002). In comparison, *E. coli* K-12 has a 4.6 Mb genome with 4288 open reading frames (Nelson et al., 2002).

P. putida KT2440 is renowned for diversity in metabolic capabilities (Blattner et al., 1997). In particular, *P. putida* is well known for its ability to degrade aromatic compounds including lignin derived compounds (ferulate, vanillate, hydroxybenzoate, protocatechuate, and cournaryl/coniferyl alcohols, aldehydes, and acids) (Timmis, 2002), BTEX (benzene, toluene, ethyl benzene, and xylene) hydrocarbons (Dagley, 1971) and derivatives such as trinitrotoluene (TNT) (Franklin et al., 1981) and styrene

(Caballero et al., 2005). The breakdown of aromatic compounds is channeled through a common intermediate phenylacetyl-CoA which leads to the production of citric acid cycle intermediates (Weber et al., 1993). The ability to degrade hydrocarbons has spurred interest in *P. putida* for bioremediation applications (Luengo et al., 2001). *P. putida* possesses an array of transport genes for resistance to xenobiotics as well as heavy metals (Nwachukwu, 2001) enabling it to demonstrate significant tolerance to organic solvents (Nelson et al., 2002), TNT (Ramos et al., 1998) and heavy metals (Cd^{2+}, Pb^{2+}, Zn^{2+}, Ni^{2+}, Co^{2+}, Hg^{2+}) (Fernandez et al., 2009).

The general diversity in catabolic function in *P. putida* is reflected in the abundance of genes for the conversion and oxidation/reduction of subtrates; as an indication of the ability for *P. putida* to degrade a wide range of recalcitrant materials, the genome contains 18 dioxygenases and 15 monooxygenases many of which are of unknown substrate specificity (Leedjarv et al., 2008; Miller et al., 2009). *P. putida* KT2440 contains many predicted enzymes of unknown substrate specificity including 51 hydrolases, 62 transferases, 80 oxidoreductases, and 40 dehydrogenases (Nelson et al., 2002), indicating a wealth of uncharacterized metabolic biochemistry. The metabolic diversity of *P. putida* is supported by a broad range of cytoplasmic membrane transport systems (approximately 350), many of which are uncharacterized (Nelson et al., 2002). A large number of those mapping to known transport systems are involved in amino acid transport while very few are related to carbohydrate transport (Nelson et al., 2002). *P. putida* also contains a broad range of chemotactic components interacting with the motility system which includes both flagellated as well as twitching motility (Nelson et al., 2002).

P. putida metabolizes glucose through an Entner-Doudoroff (ED) pathway, it does not possess the gene for phophofructokinase required for the Embden-Meyerhof (EM) glycolytic pathway (Nelson et al., 2002). Cytoplasmic and periplasmic conversions of glucose to gluconate and 2-ketogluconate lead to the production of 6-phosphogluconate which enters the ED pathway (Vicente and Canovas, 1973b). The pentose phosphate pathway does not seem to be a significant source of oxidative catabolism of glucose in *P. putida* (del Castillo et al., 2007; Latrach Tlemcani et al., 2008). Catabolite repression in *P. putida*

occurs through a different mechanism than the *Enterobacteriaceae* cyclic AMP (cAMP) catabolite activator protein (CAP), involving a greater number of components (Vicente and Canovas, 1973a). *P. putida* KT2440 is reported to be lac$^-$ and gal$^-$ (Ramos, 2004; del Castillo and Ramos, 2007); engineering efforts have enabled efficient use of D-xylose and L-arabinose as a substrate for *P. putida* (Hansen et al., 1997).

A pathway search using the Kyoto Encyclopedia of Genes and Genomes (KEGG) database (Meijnen et al., 2008) website reveals that, similar to *E. coli*, synthesis of the terpenoid/isoprenoid/carotenoid precursor isopentenyl diphosphate (IPP) in *P. putida* KT2440 appears to be via the non-mevalone pathway. Genes are present for the synthesis of IPP and dimethylallyl diphosphate (DMAPP) along with *ispA* for the synthesis of farnesyl diphosphate (FPP), but *P. putida* does not appear to have the *idi* gene for isomerization between IPP and DMAPP (Kanehisa and Goto, 2000). In addition, *P. putida* appears to have an analog of the β-carotene hydroxylase gene CrtZ, leading to the possibility for zeaxanthin production from β-carotene (Kanehisa and Goto, 2000; Nelson et al., 2002). The production of zeaxanthin in a mutant *P. putida* KT2440 was demonstrated through the inclusion of *crtEBIYZ* from *Pantoea ananatis* and debottlenecking genes *idi*, *ispA*, and *dxs* (1-deoxy-D-xyulose-5-phosphate synthase) from *E. coli* (Nelson et al., 2002). The authors also noted a toxicity effect from accumulation of the carotenoids which was circumvented through the use a transposon-generated mutant with tolerance to carotenoids (Beuttler et al., 2011).

P. putida has the capability for the biosynthesis of several compounds of potential industrial interest. *Pseudomonads* have been demonstrated to produced a diversity of polyketides which serve as useful antibiotic agents including coronatine, mupirocin, DAPG, and pyoluteorin and hold the potential for engineering novel polyketide structures (Beuttler et al., 2011). *P. putida* also produces polyhydroxyalkanoate (PHA) (Bender et al., 1999). The production of PHA in *P. putida* serves as means of carbon and energy storage and occurs during conditions of limitations of nutrients such as nitrogen (Haywood et al., 1989). The biological production of PHA is a potentially useful as a source of plastics

with various material properties (Haywood et al., 1989). Accumulation of large quantities of PHA polymers and copolymers with varying monomer length and copolymer ratios was accomplished by disruption of β-oxidation pathways (Anderson and Dawes, 1990). Pilot-scale demonstration of biosynthetic production of PHA in *P. putida* validated the potential for an industrial scale process (Olivera et al., 2001). Recently, the production of PHA in *P. putida* using styrene as a feedstock presents an interesting option for the recovery and recycling of polystyrene foam (Gorenflo et al., 2001).

This chapter will focus on the conjugation and chromosomal insertion of the subcloned PRPS (Chapter 2) derived from HF10_19P19 (Ward et al., 2006) into *P. putida* MBD1 (Martinez et al., 2007), verification of exconjugant identity and PR transcription, and the discovery of a growth yield effect observed during growth on low dissolved organic carbon (DOC) media attributed to the PRPS. To our knowledge, this is the first time a light-dependent growth yield effect has been demonstrated for a heterologous host engineered with a proteorhodopsin photosystem. The chapter will conclude with discussion of potential underlying mechanisms of the effect and future research directions which may elucidate the mechanism and extend the application of the system.

Methods

Construction of retrofit fosmid vectors pSJ2B6 and pSCCFOS

All work resulting in the construction of pSCCFOS and pSJ2B6 was performed by Dr. Asuncion Martinez according the method previously described (Martinez et al., 2004). Fosmid pSJ2B6 was constructed from pFOS-PRPS clone J2B6 (Chapter 2), and fosmid pSCCFOS was constructed from a circularized pCC1FOS vector (EpiCentre) supplied by Jay McCarren (unpublished work). The fosmids were modified to incorporate the CIS mobilization and integration cassette found between *loxP* sites of the pMBD12 vector (Martinez et al., 2004) using Cre-mediated recombination (Clontech). Successful recombination products were selected based on resistance to chloramphenicol (EMD CAS No: 56-75-7) and apramycin (Sigma CAS No: 65710-07-8) and lack of sensitivity to sucrose (Mallinckrodt CAS No: 57-50-1) (Martinez et al., 2004). The retrofit vectors were transformed into DH10B (Invitrogen) containing pUB307 (Martinez et al., 2004) prepared for electrocompetence (Bennett et al., 1977; Flett et al., 1997). Transformants were selected for resistance to kanamycin (IBI Scientific CAS No: 25389-94-0) (from pUB307 vector) and apramycin/chloramphenicol (from fosmid backbone) (Sambrook et al., 1989).

Conjugation from E. coli DH10B/pUB307 to *Pseudomonas putida*

Conjugation of the retrofit fosmids from *E. coli* into *P. putida* was performed as previously described (Martinez et al., 2004) with minor modifications. A donor strain of *E. coli* DH10B pUB307 (Martinez et al., 2004) containing the retrofit vector (pSJ2B6 or pSCCFOS), was grown as a starter culture in Luria-Bertani (LB) Broth [5 g/L yeast extract, 10 g/L tryptone, 10 g/L sodium chloride, BD Biosciences, (Martinez et al., 2004)] with 50 ug/mL kanamycin, 25 ug/mL apramycin, and 12.5 ug/mL chloramphenicol. A starter culture of recipient strain *P. putida* MBD1 (Sambrook et al., 1989) was grown in LB with 50 ug/mL kanamycin. Growth was at 30°C with shaking at 250 rpm overnight (Barnstead LabLine MaxQ 4000). Donor and recipient starter cultures were diluted 1:100 into LB with the

appropriate antibiotic and grown for 4 hours at 30°C with shaking at 250 rpm (Barnstead LabLine MaxQ 4000). Following previous methods, the recipient strain was incubated at 42°C for 15 minutes to inactivate the native restriction system (Martinez et al., 2004). Donor and recipient cultures were mixed in various ratios to a final volume of 1 mL, pelleted at 5000 rcf (Eppendorf 5415D), resuspended (Vortex Genie 2 Fisher Scientific), spotted on non-selective agar (Bactoagar, BD Biosciences) plates with LB, and grown overnight at 30°C in a plate incubator (VWR). Cultures were suspended from the non-selective plate and plated onto selective media; M9 [6 g/L Na_2HPO4 (Mallinckrodt Chemicals CAS No: 7558-79-4), 3 g/L KH_2PO_4 (Sigma CAS No: 7778-77-0), 0.5 g/L NH_4Cl (Sigma CAS No: 12125-02-9), 3 mg/L $CaCl_2$ (Sigma CAS No: 10035-04-8), 1 mM $MgSO_4$ (EMD CAS No: 10034-99-8)] (Martinez et al., 2004) with 15 mM Benzoate (Sigma CAS No: 532-32-1) as described previously (Ausubel, 1987) was used with 30 ug/mL nalidixic acid (Sigma 3374-05-8) to select for the *P. putida* recipient strain and select against donor *E. coli* strain, with 30 ug/mL apramycin present to select for successful vector conjugation. Donor and recipient controls were carried through to evaluate background colony formation. Potential clones were restreaked onto the selective plates. Exconjugant clones were selected from the restreaked plates, grown in LB and stored as 15% glycerol (BDH/VWR CAS No: 56-81-5) cryogenic stocks at -80°C.

Verification of *P. putida* MBD1 pSJ2B6 exconjugant identity was performed by screening clones for the presence of the target proteorhodopsin gene by colony polymerase chain reaction (PCR) (Espinosa-Urgel et al., 2000; Martinez et al., 2004). The 50 uL PCR reactions were performed in 1X thermopol buffer (NEB) containing 500 nM HF10_19P19-PRPS_5' primer (GGACGTTCTAGAACGCGACGTTTGGGGAG, Invitrogen), 500 nM HF10_19P19-PR-3' primer (TTACTTTGCCGCTTCAGATTGTGA, Invitrogen), 200 uM each dNTP (NEB), and 2.5 units Taq (NEB). The thermocycle program consisted of a 2 minute initial denaturing step at 93°C, 25 cycles of 40 seconds at 93°C, 30 seconds at 62°C, and 8 minutes at 72°C, followed by a final polishing step of 10 minutes at 72°C and a hold step at 4°C in a GeneAmp PCR System 9700 (Applied Biosciences). The

donor strain (DH10B pUB307 pSJ2B6) served as a positive control reaction and length marker for the PR product; the negative control was the recipient strain (*P. putida* MBD1) (Sambrook et al., 1989). PCR products were characterized using gel electrophoresis (Martinez et al., 2004) in a 1% agarose (EMD CAS No: 9012-36-6), 0.5X TBE [5.4 g/L tris base (Calbiochem CAS No: 77-86-1), 2.75 g/L boric acid (Mallinckrodt Chemicals CAS No: 10043-35-3), 0.1 mM EDTA (Mallinckrodt Chemicals CAS No: 6381-92-6), pH 8.0] (Sambrook et al., 1989) gel run at 125 V for 1 hour and stained with SYBR safe (Invitrogen). The gel was imaged on Fugifilm FLA-5100 using the 473 nm excitation laser and LPB emission filter.

Verification of the *P. putida* MBD1 pSCCFOS exconjugant identity was also performed by screening with PCR. In this case, the PCR was performed with the vector sequencing primers on either side of the pCC1FOS (EpiCentre) cloning site, GGATGTGCTGCAAGGCGATTAAGTTGG (forward, Invitrogen) and CTCGTATGTTGTGTGGAATTGTGAGC (reverse,Invitrogen). The 50 uL PCR reactions were performed in 1X thermopol buffer containing 500 nM each primer, 200 uM each dNTP, and 2.5 units Taq (NEB). The thermocycle program consisted of a 2 minute initial denaturing step at 95°C, 25 cycles of 40 seconds at 95, 30 seconds at 61°C, and 1 minute at 72°C, followed by a final polishing step of 10 minutes at 72°C and a hold step at 4°C. The donor strain (DH10B pUB307 pSCCFOS) served as a positive control reaction and length marker for the PCR product; the negative control was the recipient strain (*P. putida* MBD1). PCR products were characterized using gel electrophoresis in a 1% agarose 0.5X TBE gel containing 1X SYBR Safe run at 125 V for 90 minutes. The gel was imaged on Fugifilm FLA-5100 with 473 nm excitation and LPB emission filter.

Transcription of the PR through RT-PCR

The transcription of the proteorhodopsin gene from the PRPS was confirmed by reverse-transcriptase polymerase chain reaction (RT-PCR) (Ausubel, 1987). *P. putida* MBD1 pSJ2B6 was grown overnight at 30°C shaking at 200 rpm (Barnstead LabLine MaxQ 4000) in a 3 mL LB with 50 ug/mL

kanamycin and 25 ug/mL apramycin as a starter culture. The starter culture was diluted 1:100 into identical media and grown for 6 hours at 30°C with shaking 200 rpm. A culture of *E. coli* Epi300 pFOS-PRPS was grown under the same conditions (using 12.5 ug/mL chloramphenicol for selection instead of kanamycin and apramycin) as a positive control for PR transcription; increased transcription for the pFOS-PRPS was induced by the addition of 0.2% L-arabinose (Sigma CAS No: 5328-37-0) for the final 2 hours of growth.

RNA was extracted using the mirVana RNA isolation kit (Ambion). 200 uL of the cell culture was pelleted in a 1.7 mL microcentrifuge tube (Ambion) at 5,000 rcf for 5 minutes (Eppendorf 5415D). The supernatant was discarded and the pellet was resuspended in 500 uL of Lysis/binding buffer (Ambion). 50 uL of the homogenate additive (Ambion) was added to the mixture, vortexed to mix (Vortex Genie 2 Fisher Scientific), and incubated on ice for 10 minutes. 500 uL of a 50% acid-phenol, 50% chloroform mixture (Ambion) was added, and the sample was vortexed for 1 minute to mix and centrifuged for 5 minutes at 10,000 rcf (Eppendorf 5415D). The aqueous phase (top) was removed with careful attention to avoid disturbing the interface and placed in a clean RNase-free microcentrifuge tube (Ambion). 625 uL of 100% ethanol (Sigma CAS No: 64-17-5) was mixed with the aqueous layer, loaded into a filter cartridge (Ambion), and centrifuged at 10,000 rcf for 15 seconds (Eppendorf 5415D). The cartridge was washed with 700 uL of wash solution 1 (Ambion) and twice with 500 uL of wash solution 2/3 (Ambion) with centrifuge steps of 10,000 rcf for 10 seconds (Eppendorf 5415D) in between each wash. All wash effluent was discarded and the cartridge was centrifuged for 1.5 minutes at 10,000 rcf (Eppendorf 5415D) in a clean tube (Ambion) to remove all residual liquids. The cartridge was placed in a clean collection tube (Ambion) and the RNA was eluted from the cartridge twice for 30 seconds at 10,000 rcf (Eppendorf 5415D) using 50 uL elution buffer (Ambion) pre-warmed to 95°C (Hybex Microsample Incubator, SciGene) (100 uL total volume).

The isolated RNA was treated with Turbo-DNA-Free DNase (Ambion) to removal any residual genomic DNA contamination. 11.3 uL 10X buffer (Ambion) was added to the 100 uL of eluted RNA

along with 2 uL of the DNase enzyme (Ambion). The digestion was incubated at 37°C for 30 minutes (Hybex Microsample Incubator, SciGene). A second digestion was performed on the RNA with an additional 2 uL of Turbo DNase (Ambion)at 37°C for 2 hours.

Following DNase treatment, the RNA was purified using an RNeasy Minelute Cleanup Kit (Qiagen). 350 uL of RLT buffer (Qiagen) was added to the sample and mixed by repeated drawing into a pipette. 250 uL of 100% ethanol (Qiagen) was added to the sample and again mixed with a pipette before adding to a centrifuge column and spinning at 10,000 rcf for 30 seconds (Eppendorf 5415D). The column was placed in a clean collection tube and washed with 500 uL RPE with ethanol and centrifuged at 10,000 rcf for 30 seconds (Eppendorf 5415D). The column was washed with 500 uL 80% ethanol and 2 minutes of centrifugation at 10,000 rcf (Eppendorf 5415D). The column was transferred to a clean collection tube and centrifuged for 5 minutes at 12,000 rcf (Eppendorf 5415D) with the column lid open to removal all residual liquid. The column was placed in a clean RNase-free 1.5 mL microcentrifuge tube (Qiagen), and 25 uL of nuclease-free water (Ambion) was added to the column and incubated for 2 minutes at room temperature before spinning at 12,000 rcf for 1 minute (Eppendorf 5415D). The eluted RNA was stored at -80°C.

Proteorhodopsin mRNA was amplified by reverse transcriptase polymerase chain reaction (RT-PCR) using the SuperScript III One-step RT-PCR with Platinum Taq kit (Invitrogen). All reactions were performed in 50 uL final volume using the 25 uL of the 2X master mix supplied with the kit, 200 nM HF10_19P19-PRPS_5' oligonucleotide (GGACGTTCTAGAACGCGACGTTTGGGGAG, Invitrogen), and 200 nM HF10_19P19-PR-3' oligonucleotide (TTACTTTGCCGCTTCAGATTGTGA, Invitrogen). RT-PCR reactions were catalyzed by 2 uL SuperScript III RT/Taq mix (Invitrogen) while control reactions testing for DNA carryover were performed using 2.5 uL Platinum Taq polymerase (Invitrogen). All reactions used the same thermocycling program including: reverse transcriptase step for 30 minutes at 55°C, hot-start for 2 minutes at 94°C, 40 cycles of: 15 seconds at 94°C, 30 seconds at 62°C and 1 minute at 68°C. The program was ended with 5 minutes at 68°C and a hold step at 4°C. RT-PCR products were

separated using gel electrophoresis in a 1% agarose 0.5X TBE gel containing 1X SYBR Safe run at 125 V for 45 minutes. The gel was imaged on Fugifilm FLA-5100 using the 473 nm excitation laser and LPB emission filter.

Growth effect in low carbon defined media

Culture conditions

Cultures of *P. putida* were grown in M9 minimal media [6 g/L Na_2HPO4 (Mallinckrodt Chemicals CAS No: 7558-79-4), 3 g/L KH_2PO_4 (Sigma CAS No: 7778-77-0), 0.5 g/L NH_4Cl (Sigma CAS No: 12125-02-9), 3 mg/L $CaCl_2$ (Sigma CAS No: 10035-04-8), 1 mM $MgSO_4$ (EMD CAS No: 10034-99-8)] (Ausubel, 1987) supplemented with a carbon source at the indicated concentration. Apramycin was used at 25 ug/mL as a selective pressure for strains resulting from conjugation. Experiments were performed with triplicate biological replicates for each condition. Cultures were grown in 50 mL flasks (VWR 89000-358). Flasks for the dark condition were wrapped in two layers of aluminum foil (Reynolds); flasks for the light condition were left unwrapped. Flasks were placed in a water bath to maintain greater uniformity in temperature. The water bath was contained in a clear Pyrex® dish (9"x13"DIMENSIONS). Flasks were weighted with 1-1/4" ring clamps (Home Depot) to avoid floating and tipping in the water bath. The level of deionized water (Millipore MilliQ Biocel System) in the bath was maintained just below the height of the ring clamp, well above the liquid level in the flask.

Cultures were incubated in a walk-in light room incubator (Chisholm Lab, MIT) described previously (Ausubel, 1987). The incubator is maintained at an air temperature of 21°C - 22°C. Illumination was provided constantly by fluorescent light banks containing four Ff30T12/CW/RS fluorescent bulbs (Sylvania). Primary illumination was from directly beneath the samples through a wire shelf and the clear bottom Pyrex® water bath; ambient light from surrounding lamps provided additional illumination. The irradiation at the samples was approximately 120 $uE/m^2/s$. Consistent and reliable growth curves required the introduction of a water bath to moderate the effects of temperature

fluctuations in the incubator and temperature inequalities between the light and dark conditions arising from the differences in energy flux from the sample to the surroundings.

Several precautions were taken to avoid DOC contamination in experimental cultures. First, acid washing all glassware used for the experiments was critical to ensure suitable low DOC conditions. "Low DOC Only" glassware was acid washed prior to use using 10 vol% HCl (Macron Chemicals CAS No: 7647-01-0) with an overnight contact time. Acid washed glassware was rinsed thoroughly (greater than 10x) with deionized water and autoclaved prior to use. "Low DOC Only" glassware was not permitted to come into contact with high concentration organic compounds, particularly rich media components (e.g. tryptone, peptone, yeast extract) and dishwashing detergents (e.g.Alconox). "Low DOC Only" glassware was used for culturing and the storage of all media components.

Second, antibiotic used in the culture media was apramycin dissolved in deionized water. Chloramphenicol was not used due the carbon carryover from the vehicle ethanol which significantly increased growth at the low carbon concentrations tested (data not shown). Third, carbon carryover from the frozen stock and inoculation cultures was minimized by using starter cultures in media with low glucose concentration (0.02%). Finally, handling of the culture flasks during sampling also required care to ensure carbon from airborne particles or ethanol used for sterilization of surfaces did not contaminate a culture leading to increased yield.

Sampling and colony forming unit (CFU) determination

Flasks were mixed vigorously by vortexing for 10 seconds prior to sampling to reduce variability from aggregate formation and ensure an even distribution throughout the liquid for a representative sample (VWR Mini Vortex Setting 10). Sampling was performed by removing 200-650 uL (depending on the dilution and volume to be plated) from each flask aseptically in a laminar flow hood (Envirco Corporation) with a P1000 LTS pipette (Rainin). Samples were taken for all cultures consecutively and maintained on ice until use; flasks were returned to incubation immediately after sampling. Cultures were

serial diluted to the proper 10-fold increment using a solution of M9 media without carbon source or antibiotic with thorough mixing exceeding 15 seconds of vortexing (VWR Mini Vortex Setting 10) at each dilution. The proper dilution was plated at a volume ranging from 10-100 uL. All replicate cultures of the same condition were handled identically, and when possible cultures of different conditions were plated with the same dilution and/or volume. Samples were plated in triplicate on plates of LB with 15 g/L bactoagar (BD Biosciences) with 25 ug/mL apramycin. CFUs were counted following incubation at 30°C and multiplied by the proper dilution factor to determine culture density. Negative control plates were used to verify the absence of contamination in the dilution media.

Direct cell counts & microscopy

Direct cell counts were performed following methods described previously (Kimura et al., 2011). The appropriate volume of culture containing approximately 10^6 CFU was diluted up to 3 mL using M9 media and stained with 100 uL of 100X SYBR Green (Molecular Probes/Invitrogen) for 5 minutes. The solution was vacuum filtered with a 25 mm diameter, 15-mL funnel filter apparatus (VWR) onto a black 0.22 um isopore membrane (Millipore type GTBP) mounted onto glass slide (Gold Seal Microslides #3010) with immersion oil (Zeiss Immersol 518) and coverslip (Thermoscientific mSeries Lifterslip 22x25I-2-4816), and viewed under a 100X magnification objective (Zeiss Plan-NEOFLUAR) on a Zeiss Axioskop 2 microscope. Counting was performed with the aid of a 10x10 counting grid (10 um square, 100 um total length, 0.01 mm^2 total area) using 20 separate fields of view across the filter. The number of squares in the grid counted depended on cell density and was typically 9 or 18. Total cell levels in the filtered samples were calculated using the size of the used filter area (201.06 mm^2, based on cross-sectional area of the filter apparatus) and the average count from the area of the grid counted. Cell densities were calculated using the calculated total cell numbers and the volume of culture stained and filtered. Representative images of the fields of view counted were taken with a Nikon D90 camera with Nikon Remote Capture 4 software.

Baseline low DOC growth experiments

Starter cultures for the baseline low DOC experiments were grown in acid-washed borosilicate glass culture tubes (25 x 150 mm, VWR), with 15 mL of M9 media supplemented with 25 ug/mL apramycin and 0.02% glucose (D-Glucose, Sigma CAS No: 50-99-7) (1.1 mM). The starter culture was inoculated from a colony grown on an M9-agar plate with 0.02% glucose streaked from frozen stock and grown in a 30°C incubator (VWR) until colonies were clearly visible (approximately 3 days). The starter culture was covered in aluminum foil (Reynolds) and grown in the light incubator room at 21°C - 22°C. OD_{600} of the starter culture was tracked during growth on a Spectronic 20 spectrophotometer. The late exponential phase starter culture was used to inoculate the low DOC experiment culture when an OD_{600} between 0.08 and 0.16 was reached. The starter culture was mixed well by vortexing (VWR Mini Vortex Setting 10) followed by 100-fold dilution into M9 without glucose addition. The diluted starter culture was mixed thoroughly by vortexing and used to inoculate the growth experiments at a dilution ranging between 1:250 and 1:1000, depending on the starter culture OD_{600}, to reach an inoculation between 100 - 1000 CFU/mL. For the baseline low DOC experiments, the M9 media was supplemented with 25 ug/mL apramycin and 0.0002% (11 uM) glucose. A common culture was mixed for all replicates of light and dark conditions and divided into replicate 50 mL flasks (VWR 89000-358) at the beginning of the experiment. Results were confirmed with multiple independent experiments originating from separate starter cultures.

Glucose concentration dependence experiments

Experiments for determining the effect of glucose concentration on light-dependent physiological effect of the PRPS were inoculated from a stationary phase culture grown on 11 uM glucose (grown as described above in Baseline low DOC growth experiments) in a dark condition. Inoculation was taken from this stationary phase culture after 150-200 hours of growth. The culture density was followed (CFU/mL) up to the time of inoculation and was used to determine the dilution of the starter culture into

the glucose concentration experiment cultures. The final density of the 11 uM glucose dark starter culture was typically around 10^5 CFU/mL and the resulting dilution into the glucose concentration experiment was approximately 1:100 to achieve a seed density of 1000 CFU/mL. A common culture was inoculated for all experimental conditions (glucose concentrations and light conditions) in M9 with 25 ug/mL apramycin without glucose addition. Aliquots were removed from the stock culture using a sterile serological pipette (VWR) for the light and dark replicates at a given glucose concentration before subsequent addition of a higher glucose concentration. Thorough mixing was provided at each step through rigorous vortexing. Concentrations of glucose in the M9 media tested were: 0 uM, 1.1uM, 11 uM, 110 uM, and 1.1 mM. Each concentration utilized triplicate cultures for both light and dark conditions. The experiment was repeated for result validation using an independent starter culture.

Results

Conjugation of Modified Fosmid (pCC1FOS) Vectors pSJ2B6 and pSCCFOS into *P. putida* MBD1

The fosmid vector originally used to identify (Gomez-Consarnau et al., 2007; Kimura et al., 2011) and subclone the proteorhodopsin photosystem (Chapter 2) is a suitable vector for working in *Escherichia coli*, but is not necessarily compatible in other strains. To extend the host range of cloned PRPS from a variety of sources, the pFOS-PRPS vector and a negative control pCC1FOS vector were modified for use in a broad range of host organisms (Asuncion Martinez, unpublished). This modification was performed using constructs and methods previously found to be successful in transferring fosmids between *E. coli* and *Streptomyces lividans* (Martinez et al., 2007). Briefly, this technique involves the incorporation of a CIS cassette (containing the origin of transfer, ϕC31 integrase and *attP* site, and apramycin resistance marker) flanked by *loxP* sites from a donor vector (pMBD12) into the *loxP* site of the target vector using Cre-mediated recombination (Figure 3-1). The successfully modified vectors were resistant to both chloramphenicol (from the target fosmid) and apramycin (from the CIS cassette).

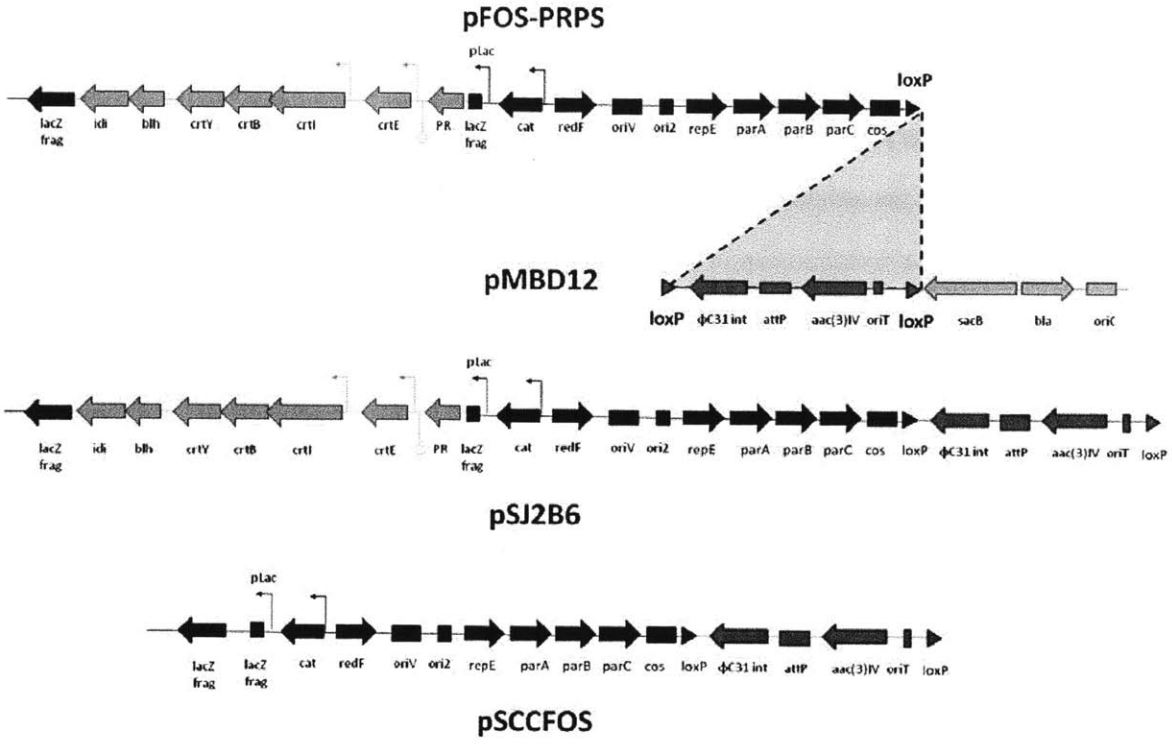

Figure 3-1: Vector modification for use in *P. putida* MBD1. Two fosmids, pFOS-PRPS (contain the seven gene PRPS described in Chapter 2) and pCC1FOS (identical vector without the PRPS), were modified to include the conjugative and integrative (CIS) cassette (Asuncion Martinez, unpublished) allowing their use in *P. putida* MDB1 (Martinez et al., 2004). The CIS cassette was transferred from the donor plasmid pMBD12 to the loxP site of the fosmids using Cre-mediated recombination. The vectors resulting from the integration are shown at bottom, pSJ2B6 and pSCCFOS.

Using the modified vectors (Asuncion Martinez, unpublished) and the engineered strain of *P. putida* MBD1 (Martinez et al., 2004), in this thesis work I constructed and characterized strains of *P. putida* with integrated DNA from the pSJ2B6 vector (*P. putida* pSJ2B6) and the pSCCFOS vector (*P. putida* pSCCFOS) (Figure 3-2). The strains were constructed through the conjugation of recipient *P. putida* MBD1 and donor strain DH10B pUB307 carrying the modified fosmids (either pSJ2B6 or pSCCFOS). Colonies resulting from the conjugation which were capable of growing on M9-Benzoate plates with apramycin ensured selection of only *P. putida* strains successfully receiving the modified vector. Four transconjugants of each strain were clonally purified and preserved cryogenically. The presence of recombinant DNA in these strains was verified through PCR using primers specific to the modified vectors. For *P. putida* pSJ2B6, the PCR verified the presence of the proteorhodopsin gene (Figure 3-3A); for *P. putida* pSCCFOS, the PCR verified the amplification of the DNA fragment located between the forward and reverse sequencing primers on the pCC1FOS vector which corresponds to same fragment from the pSCCFOS vector (Figure 3-3B).

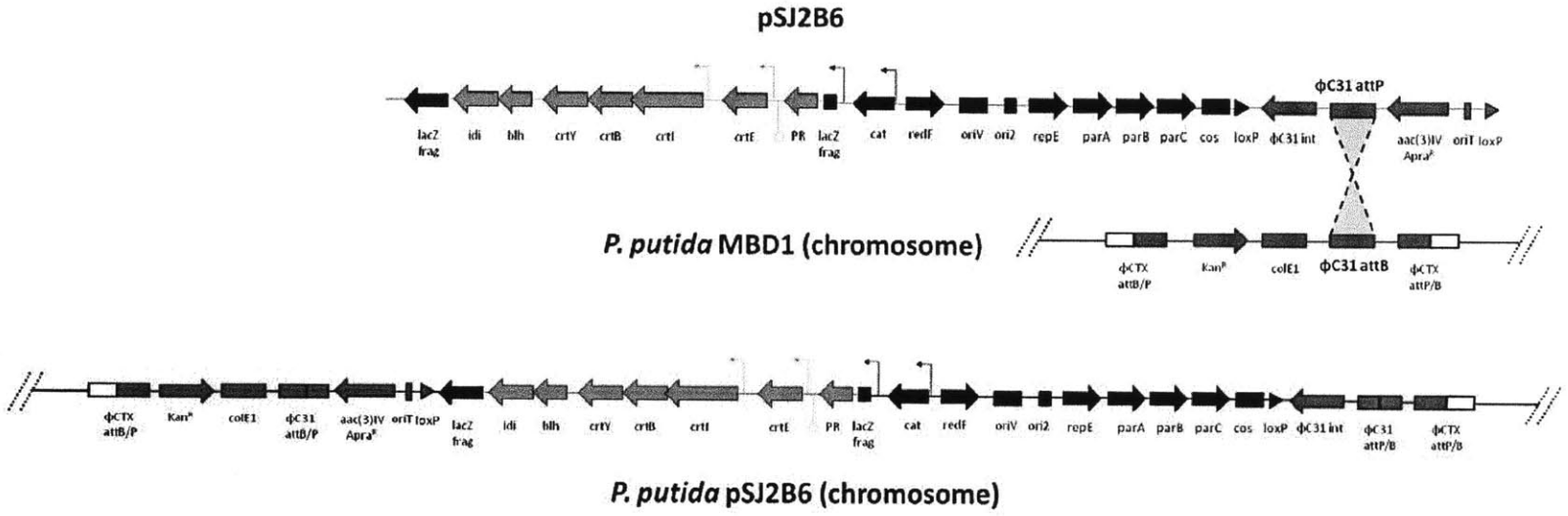

Figure 3-2: Chromosomal Integration of Modified Vectors into *P. putida* MBD1. Strain *P. putida* MBD1 is engineered to contain a ϕC31 *attB* site on the chromosome to allow integration of vectors contain the CIS cassette (Martinez et al., 2004). The modified vectors pSJ2B6 and pSCCFOS were conjugated into host strain *P. putida* MBD1 with the expected integration into the chromosome as depicted.

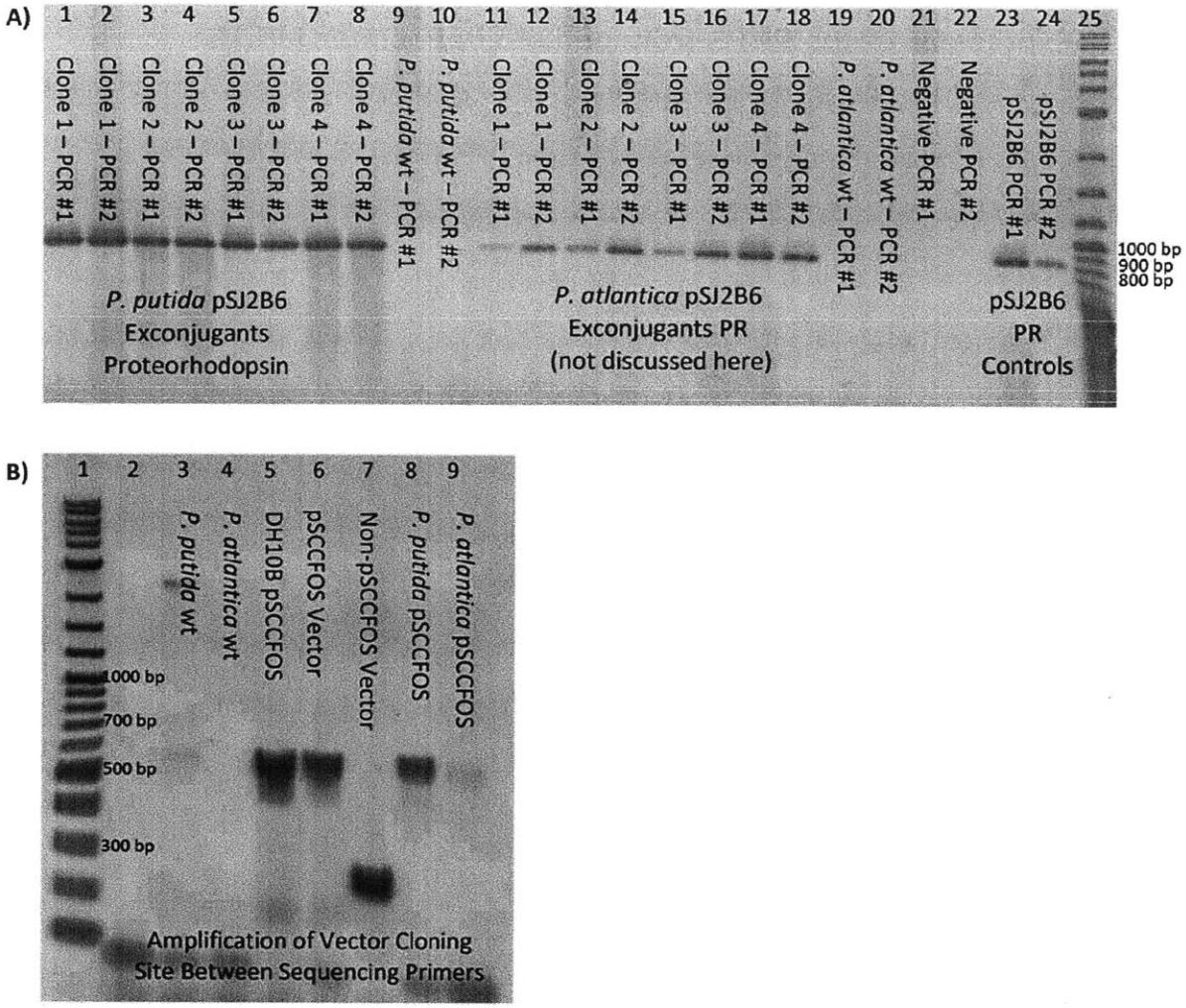

Figure 3-3: Verification of Exconjugants. A) Verification of pSJ2B6 clones was performed by two PCR reactions of the PR gene on the clone J2B6 PR. Four exconjugants selected for *P. putida* pSJ2B6 demonstrate the expected length of the PR PCR product (lanes 1-8). *P. putida* MBD1 (wt) does not display any PCR product (lanes 9-10). Lanes 11-20 pertain to *P. atlantica* pSJ2B6 exconjugants (Chapter 4). Lanes 21-22 are PCR negative control reactions. Lanes 23-24 are pSJ2B6 PCR positive control reactions to confirm product length. Lane 25 is 2-log ladder (NEB). B) Verification of pSCCFOS clones was performed by PCR of the cloning site using the pCC1FOS sequencing primers (EpiCentre). Lane 1, 2-log ladder (NEB); Lane 2, PCR negative control; Lane 3, *P. putida* MBD1 (wt); Lane 4, *P. atlantica* wt (not described here, see Chapter 4); Lane 5, DH10B pSCCFOS positive control; Lane 6, pSCCFOS PCR positive control length marker; Lane 7, alternative pCC1FOS-based vector; Lane 8, *P. putida* pSCCFOS; Lane 9, *P. atlantica* pSCCFOS clone (not described here, see Chapter 4).

Expression of the PRPS from pSJ2B6 in *P. putida* MBD1

With verification that the selected *P. putida* clones contain the correct DNA integrations, we sought evidence of transcription of the foreign DNA in the new host. This effort was focused on demonstrating transcription of the proteorhodopsin gene from the pSJ2B6 photosystem as a preliminary step to establishing functional expression of the PRPS. RNA was extracted from cultures of *P. putida* pSJ2B6 and *P. putida* pSCCFOS grown in LB media to mid-late exponential phase. Reverse transcriptase polymerase chain reaction (RT-PCR) of RNA samples, which were thoroughly digested with DNase to remove all traces of genomic DNA contamination, verified the transcription of the PR gene in *P. putida* pSJ2B6 (Figure 3-4).

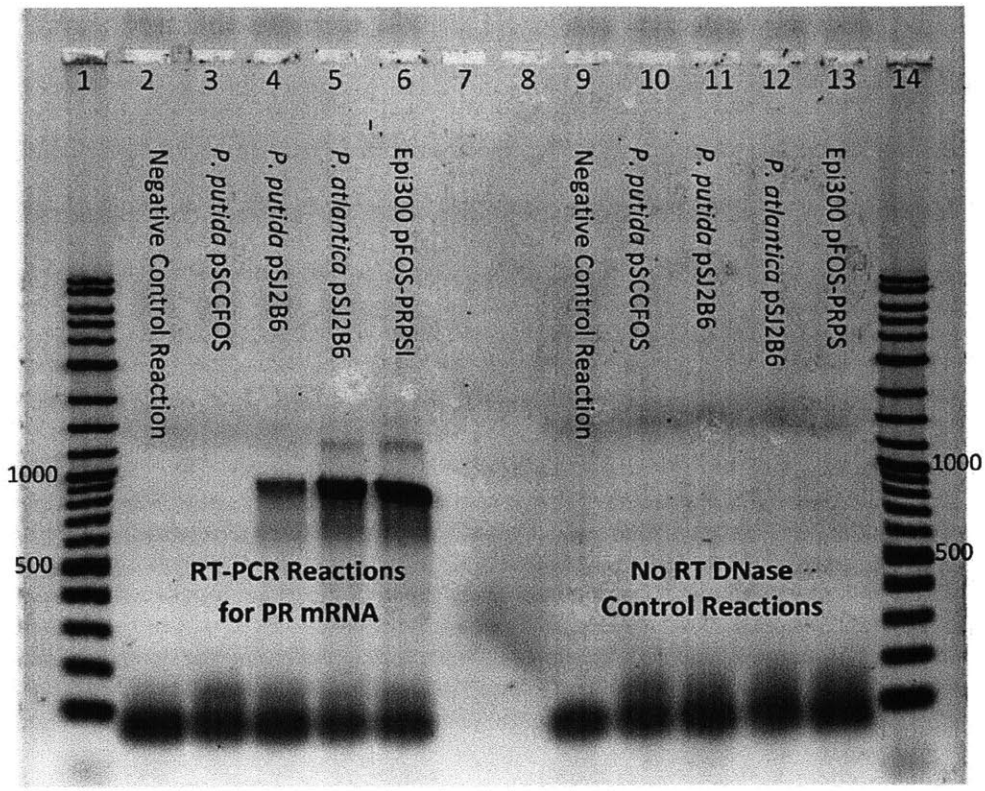

Figure 3-4: RT-PCR results for transcription of the pSJ2B6 proteorhodopsin. DNA ladder is 2-log ladder (NEB), lanes 1 and 14. RT-PCR results (lanes 2-6) shown for amplification of PR mRNA; No-RT control PCR reactions of the same samples demonstrate sufficient DNase treatment (lanes 9-13). Lanes 7-8 are empty. Lanes 2 & 9, Negative control reactions; Lanes 3 & 10 *P. putida* pSCCFOS (no PRPS); Lanes 4 & 11, *P. putida* pSJ2B6; Lanes 5 & 12, *P. atlantica* pSJ2B6 (see Chapter 4); Lanes 6 & 13, *E. coli* Epi300 pFOS-PRPS positive control induced for overexpression.

Following evidence for the transcription of the PR, attempts were made to verify expression of the photosystem using several other methods. Membrane preparations from *P. putida* pJS2B6 were used in an attempt to isolate the absorbance spectrum of PR, but without success. It is possible that the expression levels resulting from the single copy PRPS were too low to observe the PR spectrum above the background scatter of the membrane preparations. Efforts were made to measure retinal production in the recombinant *P. putida* strains containing the PRPS. In attempts to increase the sensitivity of retinal detection, cultures of *P. putida* pSJ2B6 in excess of 1 liter were extracted to provide a single sample for HPLC analysis. The results of this analysis were inconclusive; a small peak/shoulder occurred at the elution time corresponding to retinal, but large quantities of other compounds more hydrophilic than retinal with strong absorbance in the UV range continued to elute at same time, distorting the spectrum and confounding the results (data not shown). Once again it was expected that the low level of retinal production resulting from the lower expression levels was difficult to detect in the noise from other cellular products. Additional attempts to provide better HPLC purification and separation of products were not undertaken, but might improve the chances of detecting retinal production.

Attempts to directly observe the function of proteorhodopsin in *P. putida* pSJ2B6 through measurement of proton pumping or photophosphorylation were also unsuccessful. This may be attributable to low levels of expression and the limits of detection of these functional assays in the context of the background physiology of the host. It is worth noting that direct retinal detection, detection of PR in membranes, or measurement of proton pumping, has not be performed in any isolate containing native PR [incuding *Dokdonia* MED134 (Martinez et al., 2004), *Vibrio* AND4 (Gomez-Consarnau et al., 2007), *Pelagibacter ubique* (Gomez-Consarnau et al., 2010)), in part due to these signal to noise problems.

Growth Effects at Low Dissolved Organic Carbon Imparted by the PRPS

Systems with established growth effects have not necessarily displayed direct demonstration of PR function through proton pumping and photophosphorylation (Steindler et al., 2011), so the lack of these indicators in *P. putida* was not a deterrent to testing for light-based growth effects from the PRPS. Since a common attribute of successful demonstrations of light dependent proteorhodopsin function is a condition of carbon limitation (Gomez-Consarnau et al., 2007; Gomez-Consarnau et al., 2010), we evaluated the growth of *P. putida* pSJ2B6 and *P. putida* pSCCFOS under conditions of extremely low dissolved organic carbon (DOC) to determine if an effect of proteorhodopsin activity on growth could be observed. For experiments with low DOC, care must be taken not to contaminate the experiments with organic carbon which could rapidly exceed the low levels of substrate added to the experiment.

Figure 3-5 shows characteristic growth curves for *P. putida* pSJ2B6 and *P. putida* pSCCFOS grown on M9 minimal media with 11 uM glucose and 25 ug/mL apramycin. While the growth curves for the cultures grown in the light and dark coincide for the negative control *P. putida* pSCCFOS without the PRPS, a clear difference between the cultures grown in the light and those in the dark can be seen for *P. putida* pSJ2B6 with the PRPS. The primary effect observed is an increase in the yield (CFU on LB-agar plates with 25 ug/mL apramycin) beginning at the end of exponential phase and the entry to stationary phase. Direct cell counts performed under the microscope with SYBR Green (Applied Biosystems) staining support the yield difference represented by CFU counts; cultures grown in the light and the dark resulted in cells of similar size and shape and clustering of cells was not the cause of differences in the CFU counts (Figure 3-6).

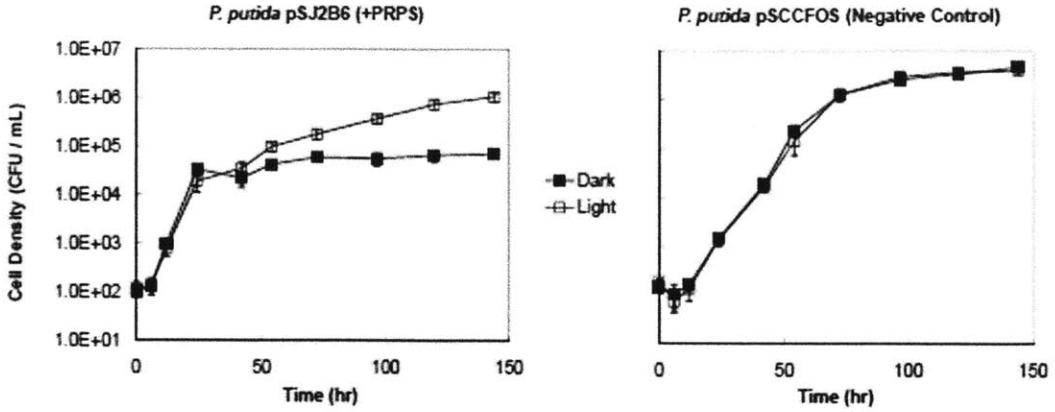

Figure 3-5: Growth of P. putida Strains in M9 with 11 uM Glucose. Growth of *P. putida* pSJ2B6 (shown on left) demonstrates an increased yield when grown in the light (open squares) compared to growth in the dark (filled squares). The negative control strain *P. putida* pSCCFOS lacking the PRPS (shown on right) demonstrates equivalent growth in the light and the dark. Yield of the *P. putida* pSCCFOS strain is higher than that of *P. putida* pSJ2B6 as seen by comparing the two figures with identical axes. Growth curves presented are representative of multiple experiments. All data points shown are the mean of three technical replicates and error bars indicate the standard deviation between all measurements of the same condition.

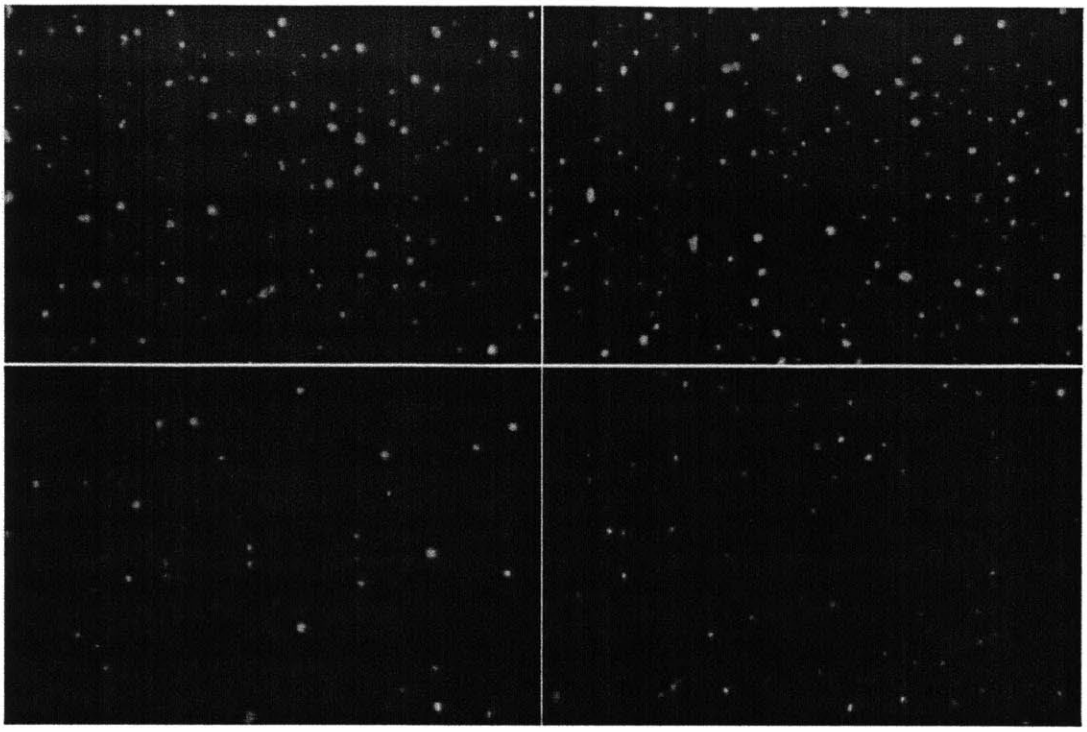

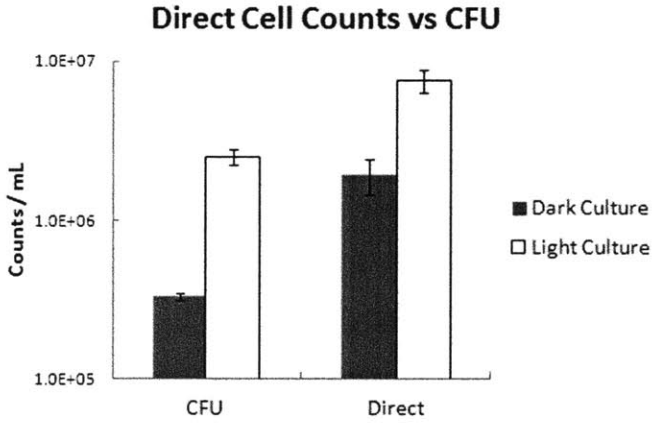

Figure 3-6: Direct Counts and Cell Morphology of *P. putida* pSJ2B6 Grown in Light and Dark. Two representative fields of view for SYBR Green stained cultures of *P. putida* pSJ2B6 grown in the light (Top Row) and dark (Middle Row) illustrate differences in total cell counts between the two cultures. Comparison of the cell morphology of two growth conditions does not indicate substantial differences in average cell size or degree of aggregation which would skew CFU results. Comparison of CFU results to direct counts (Bottom Row) demonstrates the same trends for light and dark cultures with a difference between CFU and direct count attributed to differences in cell viability and aggregation. Error bars for CFU measurements indicate standard deviation of triplicate measurements for cultures for each condition; error bars for direct counts are the standard deviation of counts from 20 fields of view for each culture. Cultures for direct count and CFU comparison were grown on a glucose concentration of 1.1 uM as described in the methods section for "Glucose concentration dependence experiments" and counts were performed at the end of the growth curve, 250 hours after inoculation.

The increase in CFU and direct counts indicate an advantage in the *P. putida* pSJ2B6 strain for growth in the light compared to growth in the dark, a result which is not observed for the negative control *P. putida* PSCCFOS strain. When comparing the growth in the dark of *P. putida* pSJ2B6 to *P. putida* pSCCFOS, a decrease in yield is observed. Because the difference between the two strains is the presence of the seven genes of the PRPS, it is likely that the differences in phenotypic responses are a result of the photosystem genes. It is hypothesized that metabolic burden associated with the expression of the photosystem and the biosynthesis of retinal may contribute to the decreased overall yield of *P. putida* pSJ2B6 compared to *P. putida* pSCCFOS. However, once the cost of this burden is factored out, the PRPS imparts a light-driven benefit to the host.

Effect of Glucose Concentration on PRPS-Associated Light-Related Yield Increase

The requirement for limiting carbon for observable effects from proteorhodopsin has been reported in several species and systems (Gomez-Consarnau et al., 2007; Martinez et al., 2007; Gomez-Consarnau et al., 2010; Steindler et al., 2011). To determine the sensitivity of the observed PR-dependent light-based increase in yield of *P. putida* pSJ2B6, the concentration of glucose in the culture media was varied. To minimize potential issues from endogenous carbon or carryover from the starter culture which would potentially interfere extremely low levels of DOC, experiments for determining the effect of glucose concentration were inoculated from a stationary phase culture grown on 11 uM glucose in dark.

The growth of *P. putida* pSJ2B6 in the light and dark on various concentrations of glucose demonstrates a diminishing advantage for growth in the light over the dark as the glucose concentration increases (Figure 3-7). This result is similar to results of experiments on the effect of carbon concentration on the light-dependent increase in growth yield observed in the PR-containing flavobacterium strain MED134 (Gomez-Consarnau et al., 2007; Martinez et al., 2007; Gomez-Consarnau et al., 2010; Steindler et al., 2011). For glucose concentrations below 1.1 mM, a significant difference ($p < 0.001$) in the maximum growth yield observed over the course of the experiment exists between the cultures grown in the light and those in the dark (Figure 3-7B). At a glucose level of 1.1 mM, the difference between the light and dark cultures is not statistically significant ($p \approx 0.32$). The yield ratio between light and dark shows a decreasing trend with increasing glucose concentration (Figure 3-7C) which indicates the advantage imparted by the PRPS only exists at low glucose concentrations.

The cultures grown in M9 without glucose addition show a nearly 100-fold increase in CFU over the inoculation level when grown in the dark. Given that these cultures were inoculated

from a stationary phase culture grown on 11 uM glucose, it seems unlikely that carbon carryover or reductive doubling can explain this increase in CFUs. It would then appear likely that DOC capable of supporting growth of *P. putida* is present at a background level in the M9 media. Furthermore, the observation that the cultures grown without glucose addition in the light show a 10-fold increase in yield over the cultures grown in the dark implies that the DOC responsible for the growth under this condition is amenable to increased yield associated with the PRPS. The yield of cultures grown on M9 with 1.1 uM glucose is equivalent to the yield of those grown without glucose addition, and the yield of cultures grown on 11 uM glucose is approximately double the yield grown without glucose. Using these numbers, a rough estimate is that the background DOC in these experiments is approximately equivalent to the addition of 10 uM glucose or 60 uM DOC. This estimate is in fair agreement with DOC values measured for artificial seawater produced from commercially available salts in related literature [50 uM (Gomez-Consarnau et al., 2007) and 60 uM (Kimura et al., 2011)] leaving this as the likely explanation for the growth on media without a supplemented carbon source.

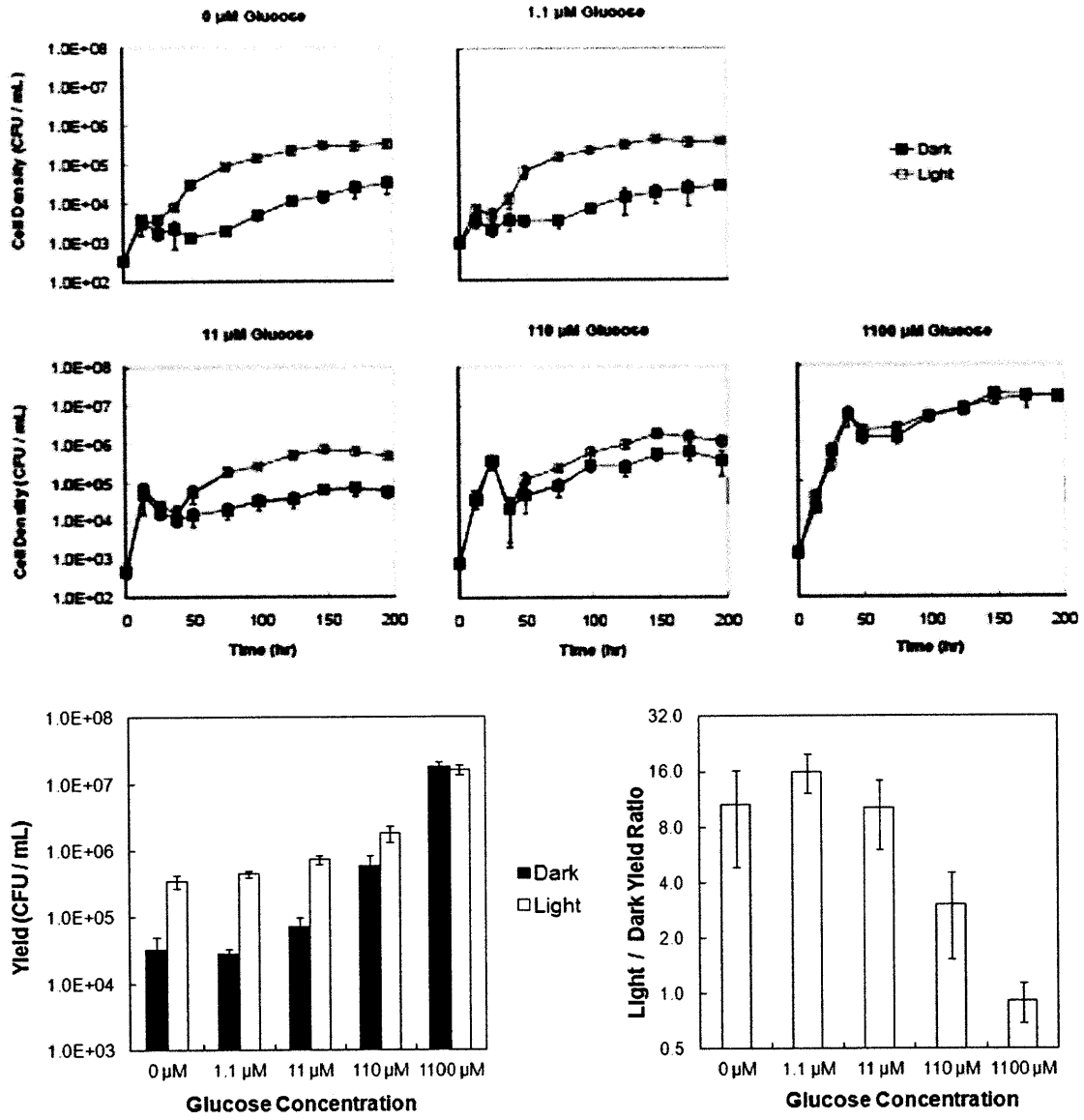

Figure 3-7: Effect of glucose concentration on PRPS-dependent growth effect. Cultures were grown on M9 media with the indicated amount of glucose. Inoculation was provided from a stationary phase culture grown on 11 uM glucose in the dark. A) Growth curves for light and dark cultures at various glucose concentrations tested. Points represent the mean of 3 technical replicates and error bars indicate the standard deviation. B) Maximum observed CFU yield (average of triplicate cultures) for each glucose and light condition is shown. Error bars are the same as above. C) Ratios of the yield of cultures grown in the light to cultures grown in the dark for each glucose concentration tested. Error bars represent the propagation of uncertainty associated with standard deviations of the yield values used to calculate the ratio.

Discussion

With *P. putida* pSJ2B6, for the first time in a heterologous host, a light-dependent growth response was demonstrated for a strain containing a proteorhodopsin. The negative control strain *P. putida* pSCCFOS, identical except for the lack of the photosystem genes, did not demonstrate a light-dependent increase in growth yield, indicating that the growth benefit is a result of the photosystem. In comparison to the control, the overall yield in the PRPS-containing strain was significantly lower, so the PRPS-associated light-dependent response in effect alleviates the lower yields observed in the PRPS-containing strain which may occur as a result of burden associated with the PRPS. The exact source and cause of the light-dependent benefit remains to be conclusively verified. Several possibilities exist for cause of the effect, and further investigation is required to determine the underlying mechanisms.

The light-dependent increase in CFU (Figure 3-5) and the similarity of cell size for light and dark cultures (Figure 3-6) of *P. putida* pSJ2B6 suggest an increased efficiency in carbon assimilation into biomass, which could be confirmed using a metabolic flux analysis of the substrate carbon during growth in light and dark conditions. A light-derived supplement to the PMF from the PR could reduce the need for respiratory energy production and thus result in a decrease in the amount of organic carbon catabolized through the citric acid cycle, making the excess carbon available for anabolic cellular processes and growth. Light has been shown to decrease rates of aerobic respiration in several microbial strains possessing proton-pumping rhodopsins (Gomez-Consarnau et al., 2007), and in the case of bacteriorhodopsin-containing *Halobacterium halobium*, growth in light results in an increased yield of biomass (Oesterhelt and Krippahl, 1973; Boichenko et al., 2006; Steindler et al., 2011).

The mechanism by which the PMF produced by the PR would lead to the decrease in respiration is unknown. One idea postulated in literature involves "backpressure" of PMF interacting directly between the respiratory proteins and proteorhodopsin allowing PR proton

pumping to be exchanged for respiration, resulting in an inability of the electron transport chain components to translocate protons and shuttle electrons to a terminal electron acceptor (Rogers and Morris, 1978). Another possibility would be regulation of metabolic pathways to decrease the formation of reduced electron donors of the respiratory chain, mainly NADH and the $FADH_2$ of the tricarboxylic acid (TCA) cycle. Regulation of these processes could be from the level of availability of ATP, known to be global regulator of glycolysis and other metabolic pathways (Oesterhelt and Krippahl, 1973; Litvin et al., 1977; Balashov et al., 2005; Boichenko et al., 2006; Walter et al., 2007). Alternatively, a decrease in respiratory flux could be caused by competition for metabolites from anabolic pathways. One possibility of this could be the action of a membreane-bound transhydrogenase which interconverts NADH and NADPH in a PMF-dependent fashion, thus shifting the availability of NADH and NADPH available for respiration and growth (Voet and Voet, 2004).

The translation of PR function to a growth phenotype may occur by mechanisms other than ATP and interaction with respiration. As seen in other hosts, the PMF generated by PR could lead to a physiological response by affecting systems directly interacting with the PMF such as membrane transport systems (Sauer et al., 2004) and flagellar motility (Johnson et al., 2010). Although, without changing the distribution of metabolic flux of the carbon through various intracellular pathways, it is difficult to explain how these processes would produce a yield effect rather than a kinetic effect. While it seems that these factors are not relevant for pure culture experiments as performed in this work, the ecological relevance of increased kinetics of transport or motility may play a significant role in providing a fitness advantage in a competitive environment (Walter et al., 2007).

An interesting feature of the shape of the growth curves of PRPS-containing *P. putida* pSJ2B6 on glucose is the lack of kinetic effect on growth during the exponential growth phase, in which the PRPS-containing strain resembles the control strain. For all carbon concentrations

tested, the effect caused by light first appeared after an initial period in which light and dark growth is equivalent. The reason for the timing of the effect onset is unknown, and additional information about the substrate utilization rate is needed to understand if differences are occurring in the exponential phase which result in the increased yield observed at the end of the growth curve.

The importance of the PRPS expression level on the observed physiological effects has not been evaluated, and no attempt was made in this study to determine the levels of expression of the PR at different phases of growth. The balance between PMF generated by respiration and PR will depend both on the expression level of functional PR and the rate of respiration. A proteorhodopsin exhibiting fast photocycle kinetics of approximately 20 ms (Kelly et al., 1988; Hibbing et al., 2010) can translocate 50 H^+/s in saturating light conditions and at 100% efficiency. The efficiency of proton translocation in aerobic respiration varies depending on the type of NADH dehydrogenase and ubiquinol oxidase utilized and can range from 2-4 H^+/e^- transported corresponding to 8-16 H^+/O_2 reduced (Beja et al., 2000b). Taking the conservative number of 8 H^+/O_2 we can determine the relative performance of PR to aerobic respiration; the action of one PR corresponds to 6.25 molecules of O_2 respired per second. In high concentrations of glucose, the oxygen uptake rate of *P. putida* was measured in the range of 1 to 10 uL / min / 10^9 cell (Ingledew and Poole, 1984; Unden and Bongaerts, 1997). This corresponds to 4.1e5 to 4.1e6 molecules of O_2 per second per cell. Using the ratio of 6.25 molecules O_2/second/PR, this indicates that approximately 65,000 to 650,000 PR per cell would be required to produce the same flux of protons as respiration of oxygen under these conditions. PR expression levels have been estimated at 24,000 PR per cell (Gosmann and Rehm, 1986) and it is clear that this level of expression is not capable of producing a flux of hydrogen ions on the same order of magnitude as high rates of aerobic respiration. As noted previously (Beja et al., 2001), it would seem that the

PR contribution to PMF is only significant at low levels of respiration; when ample supplies of carbon and oxygen are present, respiratory energy production likely dominates.

Expression of the PRPS from *P. putida* pSJ2B6 is assumed to occur from a combination of regulatory regions native to the PRPS and on the pSJ2B6 vector backbone as with HF10_19P19 (Gomez-Consarnau et al., 2007; Martinez et al., 2007; Walter et al., 2007; Gomez-Consarnau et al., 2010; Johnson et al., 2010; Steindler et al., 2011). The gene conferring chloramphenicol resistance is located upstream of the PRPS and is successfully expressed in *P. putida* (determined by observed resistance to chloramphenicol). There is also a region on the vector upstream of the PRPS which matches the *lac* promoter and operator in *E. coli*. While *P. putida* does not utilize the same type of cAMP-CAP catabolite repression system (Martinez et al., 2007), it is possible that differences in global gene regulation affect levels of expression from any of the promoters in the foreign system, thus possibly effecting expression of the PRPS in different growth phases and with various substrates.

The expression level of proteorhodopsin may depend on the growth rate. As the mechanisms regulating PR expression are unknown, it is not possible to predict if there is any dependence on the growth rate or the availability of DOC on the transcription and translation rate of PR. In the case of constitutive expression and first order degradation of the PR, the number of PR in the cell membrane will decrease as the growth rate increases due to the effects of dilution from cell division. As a result, at high DOC concentrations and higher growth rates, there may be less PR present in each cell resulting in a decreased contribution to PMF.

The observation that the light-based growth effect in *P. putida* pSJ2B6 only occurs at low substrate concentration is reminiscent of findings in the flavobacterium *Dokdonia* MED134 (Phillips and Mulfinger, 1981), although for that strain both growth rate and yield were increased in the light. This result reinforces many observations documenting the requirement for limiting carbon conditions to produce a light-dependent effect associated with PR (Gomez-Consarnau et

al., 2007). The mechanism by which increased carbon concentration diminishes the light-effect is not known at this time, but the interaction of PMF generated respiration with the PR has been suggested (Gomez-Consarnau et al., 2007; Martinez et al., 2007; Gomez-Consarnau et al., 2010; Steindler et al., 2011).

The light-dependent growth effect in *P. putida* pSJ2B6 has been seen during growth on minimal media with low concentrations of glucose added. However, as the metabolic fate of the glucose has not been determined, the increased CFU yield cannot be definitively attributed to an increased yield of the glucose substrate; substrates endogenous to the cells (such as PHA) or residual carbon in the M9 may be responsible for the increased growth yield. In addition to metabolic flux analysis to understand the carbon flow within the cell, future experiments might include changing the growth substrate to examine whether specific metabolic pathways influence the shape of the growth curve and the observed PRPS-associated light response. Performing growth experiments with a range of substrates would allow the evaluation of different metabolic profiles within the same host to determine if the substrate affects the type of physiological response to light. The relative balance of carbon, reducing potential, and ATP yield for a given substrate could determine if the PRPS provides a valuable addition or not. Utilizing different carbon sources is also a means of generating different rates of respiration and growth which may provide useful insight about the mechanism of light-based growth differences contributed from the PRPS.

The experiments in this work with the PRPS-containing *P. putida* pSJ2B6 demonstrated a light-dependent effect at 21°C in minimal media with excess nitrogen and phosphorous and limited carbon availability. The optimal temperature for growth of *P. putida* is around 30°C and additional studies are needed to determine if temperature and the associated changes in growth rate, respiration rate, and transcriptional profile play a role in the observed light-dependent

growth yield effect. Likewise, growth experiments with other limiting nutrients may help to uncover the underlying mechanism of the PRPS-associated light-based increase in yield.

The *P. putida* pSCCFOS strain without the entire photosystem severed as the negative control construct in these experiments. The observation of a higher yield in strain *P. putida* pSCCFOS than *P. putida* pSJ2B6 during growth in the dark suggests a burden associated with the seven genes of the photosystem. A control strain with the retinal synthesis pathway, but lacking the PR would allow comparison of yields to determine if the decreased growth of *P. putida* pSJ2B6 is associated with toxicity or metabolic burden from retinal production. This strain would also enable definitive attribution of the light-based growth effect to the PR, which could be complemented in *trans* to the retinal biosynthesis genes, allowing a range of expression levels and evaluation of different PR sequence variants. Similarly, the use of other genetic constructs with modifications to the PRPS or *P. putida* genome will enable elucidation of the underlying mechanism of the increased growth yield and the systems directly and indirectly affected by the function of PR.

Preliminary attempts to produce a growth response in *E. coli* have so far been unsuccessful (data not shown). Comparing and contrasting the results in *P. putida* to other host systems, such as *E. coli*, would be a useful means for testing theories about the mechanism of the growth effect and understanding the various strategies for utilizing PR phototrophy. For instance, if the metabolic flux distribution in *E. coli* could be made to generally match that of *P. putida* the same effect may be observed in the light with the PRPS. One way in which this might be approached is to coax *E. coli* into using the ED pathway instead of the EM pathway for glycolysis, which could be achieved through a deletion of the phosphfructokinase gene of the EM pathway or using gluconate as a substrate (Gomez-Consarnau et al., 2007; Martinez et al., 2007; Walter et al., 2007; Gomez-Consarnau et al., 2010; Steindler et al., 2011).

Extending beyond the effect of the PRPS to the growth physiology of *P. putida,* this system may be used to study the production of PHA. PHA is typically formed under conditions of excess carbon and nutrient limitation as a means of storing carbon and energy (Eisenberg and Dobrogosz, 1967), which is a different system for study than the low DOC growth conditions evaluated in this work. Even though the production of PHA is maximized during times of minimal growth and nutrient limitation (Anderson and Dawes, 1990), the excess carbon present may result in a high respiration rate which may prevent contribution from the PR. This problem could potentially be circumvented through the use of limiting oxygen conditions or through genetic engineering efforts to minimize the respiratory activity.

Conclusion

The PRPS-associated light-dependent growth effect of *P. putida* pSJ2B6 represents the first time an increase in growth has been attributed to a PRPS in a heterologous host. The increased growth manifested as a light-dependent increase in yield at the transition between exponential and stationary phase. In confirmation that the observed effect was attributable to the PRPS, a negative control strain (identical except for the PRPS) did not demonstrate a differential response in the presence or absence of light. The negative control strain did achieve higher yields than the PRPS-containing strain, but growth in the light alleviated the much of the growth yield differences between the strains. Increasing concentrations of glucose in the culture media diminished the relative effect of the PRPS until no difference between light and dark cultures was observed at glucose concentrations of 1.1 mM, providing further evidence for the beneficial role of PR in carbon and respiration limited conditions.

Chapter 4: Survey of Heterologous Expression of Various PRPS-Containing Constructs

Abstract

Following the discovery of proteorhodopsin on the large insert BAC library clone EBAC_31A08 (Anderson and Dawes, 1990), extensive surveys of PR diversity uncovered a wealth of sequence variants (Beja et al., 2000b) with phenotypic variation in absorbance spectrum and photocycle rate (Beja et al., 2001; de la Torre et al., 2003; Sabehi et al., 2003; Sabehi et al., 2004; Venter et al., 2004; Sabehi et al., 2005; McCarren and DeLong, 2007) which correspond to environmental conditions of light availability (Beja et al., 2001; Man et al., 2003; Man-Aharonovich et al., 2004). The discovery of biosynthetic pathways in marine picoplankton large insert DNA libraries for the production of the proteorhodopsin cofactor, retinal, indicated a modular photosystem capable of mobilization between hosts by horizontal gene transfer (Beja et al., 2001). These findings (Sabehi et al., 2005; Sharma et al., 2006; Martinez et al., 2007; McCarren and DeLong, 2007) as well as the whole-genome sequences of marine isolates (de la Torre et al., 2003; Sabehi et al., 2005; McCarren and DeLong, 2007) also revealed a wide taxonomic distribution of organisms harboring proteorhodopsin photosystems.

The large-insert environmental libraries offer an opportunity to survey the diverse space of proteorhodopsin photosystem variants observed in nature. While the phylogenetic diversity of species possessing PRPS is vast (Giovannoni et al., 2005a; Gomez-Consarnau et al., 2007; Stingl et al., 2007; Giovannoni et al., 2008; Gonzalez et al., 2008; Lami et al., 2009; Gomez-Consarnau et al., 2010; Oh et al., 2010; Riedel et al., 2010), the reasons for the observed differences in phenotypic responses to light with various host organisms are unclear (de la Torre et al., 2003; Sabehi et al., 2005; Sharma et al., 2006; McCarren and DeLong, 2007). Current evidence suggests that the PRPS provides a benefit only under specific nutritional conditions (Gomez-Consarnau et al., 2007; Stingl et al., 2007; Giovannoni et al., 2008; Gonzalez et al., 2008; Lami et

al., 2009; Gomez-Consarnau et al., 2010; Riedel et al., 2010; Steindler et al., 2011). Subtle differences in PRPS properties including amino acid sequence, protein structure, codon utilization, and transcriptional and translational regulation are also likely to be of profound importance to its function.

This work provides a preliminary survey of six proteorhodopsin-containing vectors derived from large-insert BACs and fosmids and expressed in two organisms, *Pseudomonas putida* and *Pseudoalteromonas atlantica* as a starting point for understanding differences in heterologous expression of proteorhodopsin photosystems and the resulting effect on host physiology. Strains were produced successfully for all photosystem-host combinations with the exception of one, *P. atlantica* with the large BAC pS31A08, derived from EBAC_31A08. For all strains produced, evidence of proteorhodopsin transcription was demonstrated through RT-PCR. *P. putida* strains containing three unique photosystems were tested for the light-based increased growth yield at low dissolved organic carbon (DOC) concentrations. *P. putida* strains possessing pSHF10_19P19 (derived from fosmid HF10_19P19, the parent fosmid of pSJ2B6 described in Chapter 3) and pS41B09 (derived from BAC EB0_41B09) demonstrated an increase in growth yield at low carbon concentrations as was observed for pSJ2B6 (Chapter 3, this thesis), while pS55B11 (derived from EB0_55B11) demonstrated a decreased growth in the light. The increased yield observed for *P. putida* pS41B09 indicates that the *idi* gene is not required for the response in *P. putida,* this function likely being supplied by host metabolic pathways. The similarity in phenotype of strains *P. putida* pSHF10_19P19 and pS41B09 suggests that the light-driven growth phenotype can be supplied by photosystems having different sequences and origins.

Introduction & Background

Extensive diversity in proteorhdopsin variants and marine microbial hosts has been uncovered in the past decade (Gomez-Consarnau et al., 2007; Martinez et al., 2007; Walter et al.,

2007; Gomez-Consarnau et al., 2010; Johnson et al., 2010; Steindler et al., 2011). PR has been found extensively both without and with the gene clusters for retinal biosynthesis (Beja et al., 2001; de la Torre et al., 2003; Sabehi et al., 2003; Sabehi et al., 2004; Venter et al., 2004; Sabehi et al., 2005; Frigaard et al., 2006; Sharma et al., 2006; McCarren and DeLong, 2007; Slamovits et al., 2011), forming fully functional photosystems with as few as six required genes (Sabehi et al., 2005; McCarren and DeLong, 2007). Variants of the complete photosystem have been found with and without the *idi* gene encoding isopentenyl diphosphate isomerase (Martinez et al., 2007). Proteorhodopsin are distributed among a wide range of taxonomic lineages (Sabehi et al., 2005; McCarren and DeLong, 2007). Within the context of the PRPS, there appears to be significant ability to fine tune the system to optimize the utility for the environmental conditions (de la Torre et al., 2003; Sabehi et al., 2005; Frigaard et al., 2006; McCarren and DeLong, 2007; Slamovits et al., 2011) and host physiology.

Proteorhodopsin Diversity

The diversity of proton-pumping rhodopsin sequences spans a range from the archetypical bacteriorhodopsin (Beja et al., 2001; Bielawski et al., 2004) and well established proteorhodopsin groups (Oesterhelt and Stoeckenius, 1973), to other proton pumping rhodopsins such as xanthorhodopsin (Venter et al., 2004; Sabehi et al., 2005) and actinorhodopsin (Balashov et al., 2005). Following the discovery of proteorhodopsin on large insert BAC EBAC_31A08 (Sharma et al., 2009), a wide range of amino acid sequence variants of PR have been discovered (Beja et al., 2000b).

Based on the absorbance spectrum, PR fall into one of two primary categories which are designated by the color of light at the peak of absorbance: green (525 nm) and blue (490 nm)(Beja et al., 2001; de la Torre et al., 2003; Sabehi et al., 2003; Sabehi et al., 2004; Venter et al., 2004; Sabehi et al., 2005; Frigaard et al., 2006; McCarren and DeLong, 2007). Blue variants frequently display slow photocycle kinetics typical of sensory rhodopsins (Beja et al., 2001),

however blue variants with fast photocycle kinetics have also been discovered indicating that spectral tuning is not always related to the speed of the photocycle (Spudich et al., 2000). Aside from the phenotypic green and blue groupings, sequence variation throughout the PR allows clustering of proteins which share sequence homology (Sabehi et al., 2005). Many groups from sequence alignments contain both green and blue variants, indicating that the color tuning is independent of the divergence seen in the other regions of protein (Sabehi et al., 2003).

Interestingly, a rhodopsin aligning closely with the proton-pumping xanthorhodopsin of the halophilic *Salinibacter ruber* was discovered in the large insert BAC clone EB0_41B09 (Sabehi et al., 2003; Sabehi et al., 2005; McCarren and DeLong, 2007). Xanthorhodopsin is known to have an associated antenna pigment, salinixanthin, which broadens the action spectrum of the retinylidene protein (McCarren and DeLong, 2007); the discovery of a similar protein structure and associated carotenoid synthesis genes in a large-insert library opens the possibility of similar antenna systems in marine microbes (Balashov et al., 2006). However, the functionality of the xanthorhodopsin in this construct is yet to be verified, and the lack of the conserved Schiff-base-forming lysine residue raises questions about its ability to covalently bind retinal (McCarren and DeLong, 2007).

Variants in Photosystem Composition

The suspected biosynthetic pathways for retinal were discovered on large insert BAC libraries, frequently at locations adjacent to the proteorhodopsin gene (McCarren and DeLong, 2007). These retinal synthesis gene clusters were found to encompass subsets of the carotenoid synthesis genes cluster *crtEIBY* (Sabehi et al., 2005). Additionally, the *idi* gene, which has been shown to increase the production of carotenoids in *E. coli* (Sabehi et al., 2005), is found with the carotenoid synthesis genes. The discovery of *blh* [Bacteriorhodopsin-related-protein(*brp*)-like homolog] on the large insert DNA along with the retinal synthesis genes marked the first observation of the 15,15'-beta-carotene dioxygenase in bacteria (Kajiwara et al., 1997).

Experiments in *E. coli* producing beta-carotene and expressing proteorhodopsin confirmed that the *blh* gene is responsible for the production of retinal from beta-carotene (Sabehi et al., 2005). Additional BACs and fosmids possessing both the retinal synthesis genes and PR in a contiguous gene cluster were identified using high-throughput phenotypic screening in *E. coli (Sabehi et al., 2005)*. It was verified that the genes *crtEIBY, blh*, and PR were the only components on the environmental fosmid necessary for the formation of a functional photosystem capable of translocating protons and generating ATP via photophosphorylation in *E. coli* (Martinez et al., 2007). Further sequencing of large-insert BAC and fosmid libraries revealed a number of constructs that harbor PRs adjacent to various components of the photosystem (Martinez et al., 2007).

Host Diversity from Large-Insert Environmental Libraries

Compared to other cultivation independent methods, large-insert environmental libraries provide useful information about the organism from which the proteorhodopsin is derived (McCarren and DeLong, 2007) and the opportunity to identify adjacent associated genes such as the retinal biosynthetic pathways (Beja et al., 2000b; de la Torre et al., 2003). Proteorhdopsin was originally discovered in a marine gamma proteobacterium of the SAR86 group (Sabehi et al., 2005). Screening of microbial libraries produced from environmental DNA concentration from the seawater in the Antarctic (Beja et al., 2000b), Hawaii Ocean Time series (HOT)(Beja et al., 2002), and Monterey Bay (Karl and Lukas, 1996; DeLong et al., 2006), revealed PR sequences from not only gamma but also alpha proteobacteria hosts (Beja et al., 2000a). Following upon this discovery, proteorhodopsin has been found in a wide range of microbial species. Large-insert libraries revealed a proteorhodopsin photosystem from a beta proteobactrium (de la Torre et al., 2003). In addition to proteobacteria, proteorhodopsin photosystem components have been discovered in clones with DNA derived from *Planctomycetales* (McCarren and DeLong, 2007), *Euryarchaea* (McCarren and DeLong, 2007), and eukaryotic dinoflagellates (Frigaard et al.,

2006; McCarren and DeLong, 2007). Table 4-1 lists fully-sequenced large-insert BACs and fosmids from environmental metagenomic libraries which contain PR and/or genes for carotenoid biosynthesis.

Table 4-1: Fully Sequenced Large-Insert BACs and Fosmids Containing Proteorhodopsin and/or Carotenoid Biosynthetic Genes from Environmental Sources

BAC / Fosmid	Genbank Accession #	DNA Source Water [A]	Putative Genetic Origin [B]	PR [C]	Retinal Biosynthetic Genes [D]	Insert Size	Reference
EBAC31A08	AF279106	Monterey Bay, Station M2, surface	Gammaproteobacterium, SAR86-II	G-PR	None	129 kb	Beja (2000)
EB000_60D04	AE008921	Monterey Bay, Station M2, surface	Alphaproteobacteria, Roseobacter	None	crtAIBCDEF, idi	103 kb	Beja (2002)
EB0_35D03	EF089397	Monterey Bay, Station M2, surface	Proteobacterium	G-PR*	None	48 kb	McCarren (2007)
EB0_39F01	EF089398	Monterey Bay, Station M2, surface	Alphaproteobacterium	G-PR*	crtEIBY, blh	36 kb	McCarren (2007)
EB0_39H12	EF089399	Monterey Bay, Station M2, surface	Proteobacterium	G-PR*	None	110 kb	McCarren (2007)
EB0_41B09	EF089400	Monterey Bay, Station M2, surface	Betaproteobacterium	B-PR* XR °	crtEIBY, blh	44 kb	McCarren (2007)
EB0_49D07	EF107099	Monterey Bay, Station M2, surface	Proteobacterium	B-PR*	None	82 kb	McCarren (2007)
EB0_50A10	EF107100	Monterey Bay, Station M2, surface	Gammaproteobacterium	G-PR*	None	43 kb	McCarren (2007)
EB0_55B11	EU221239	Monterey Bay, Station M2, surface	Alphaproteobacteria, Rhodobacter	G-PR*	crtEIBY, blh	72 kb	Rich (2008) McCarren (2007)
EB80_02D08	EF107104	Monterey Bay, Station M2, 80m depth	Gammaproteobacterium SAR-86	G-PR*	None	54 kb	McCarren (2007)
EB80_69G07	EF107105	Monterey Bay, Station M2, 80m depth	Alphaproteobacterium	B-PR*	None	34 kb	McCarren (2007)
HF10_3D09	DQ257435	Hawaii Station ALOHA, 10m depth	Unassigned	B-PR*	None	40 kb	Frigaard (2006)
HF10_05C07	EF107101	Hawaii Station ALOHA, 10m depth	Proteobacterium	B-PR*	None	18 kb	McCarren (2007)
HF10_12C08	EF107102	Hawaii Station ALOHA, 10m depth	Alphaproteobacterium	B-PR*	None	36 kb	McCarren (2007)
HF10_19P19	EF100190	Hawaii Station ALOHA, 10m depth	Alphaproteobacterium	B-PR	crtEIBY, blh, idi	42 kb	McCarren (2007) Martinez (2007)
HF10_25F10	EF100191	Hawaii Station ALOHA, 10m depth	Alphaproteobacterium	B-PR	crtEIBY, blh, idi	40 kb	McCarren (2007) Martinez (2007)
HF10_29C11	EF089401	Hawaii Station ALOHA, 10m depth	Euryarchaea	None	crtI, crtBY, blh	37 kb	McCarren (2007)
HF10_45G01	EF107103	Hawaii Station ALOHA, 10m depth	Proteobacterium	B-PR*	None	34 kb	McCarren (2007)
HF10_49E08	EF089402	Hawaii Station ALOHA, 10m depth	Planctomycete	B-PR*	crtEIBY, blh	39 kb	McCarren (2007)
HF70_19B12	DQ257434	Hawaii Station ALOHA, 70m depth	Unassigned	B-PR*	None	37 kb	Frigaard (2006)
HF70_39H11	DQ156349	Hawaii Station ALOHA, 70m depth	Marine Euryarchaea Group II	B-PR*	None	36 kb	Frigaard (2006)
HF70_59C08	DQ156348	Hawaii Station ALOHA, 70m depth	Marine Euryarchaea Group	B-PR*	None	37 kb	Frigaard (2006)

BAC / Fosmid	Genbank Accession #	DNA Source Water [A]	Putative Genetic Origin [B]	PR [C]	Retinal Biosynthetic Genes [D]	Insert Size	Reference
			II				
HF130_81H07	EF107106	Hawaii Station ALOHA, 130m depth	Gamma proteobacteria	B-PR*	None	37 kb	McCarren (2007)
HOT2C01	AY372455	Hawaii Station ALOHA, Surface	Alpha proteobacterium	B-PR*	None	42 kb	de la Torre (2003)
HOT4E07	AY619685	Hawaii Station ALOHA, Surface	Gamma proteobacterium SAR86-I	B-PR*	crtR	71 kb	Sabehi (2004)
MED13K09	DQ068067	Mediterranean Sea, 12m depth	Unassigned	B-PR	crtE, crtIBY, blh	100 kb	Sabehi (2005)
MED18B02	DQ088853-DQ088855	Mediterranean Sea, 12m depth	Alpha proteobacteria	B-PR	None	21+ kb	Sabehi (2005)
MED35C06	DQ077553	Mediterranean Sea, 12m depth	Gamma proteobacteria	G-PR*	None	39 kb	Sabehi (2005)
MED42A11	DQ088869-DQ066676	Mediterranean Sea, 12m depth	Alpha proteobacteria SAR11	B-PR*	None	2+ kb	Sabehi (2005)
MED46A06	DQ088847	Mediterranean Sea, 12m depth	Alpha proteobacteria	G-PR	crtEIBY, blh, idi	69 kb	Sabehi (2005)
MED49C08	DQ077554	Mediterranean Sea, 12m depth	Gamma proteobacteria SAR-86	B-PR	None	68 kb	Sabehi (2005)
MED66A03	DQ065755	Mediterranean Sea, 12m depth	Alpha proteobacteria	G-PR	crtEIBY, blh, idi	45 kb	Sabehi (2005)
MED82F10	DQ073796	Mediterranean Sea, 12m depth	Unassigned	G-PR*	crtE, crtIBY, blh	24 kb	Sabehi (2005)
MED86H08	DQ088848-DQ088852	Mediterranean Sea, 12m depth	Alpha proteobacteria SAR11	B-PR*	crtE	3+ kb	Sabehi (2005)
RED17H08	DQ068068	Red Sea, 12m depth	Alpha proteobacteria	B-PR*	crtEIBY, blh, idi	135 kb	Sabehi (2005)
RED20E09	AY552545	Red Sea, 7m depth	Gamma proteobacterium SAR86-I	B-PR*	crtE	144 kb	Sabehi (2004)
RED22E04	DQ088856-DQ088868	Red Sea, 12m depth	Unassigned	B-PR*	crtI	2+ kb	Sabehi (2005)
ANT32C12	AY372453	Antactica, Palmer Station, surface	Gamma proteobacterium	B-PR*	None	39 kb	de la Torre (2003)
ARCTIC37_F_02	EU795235	Arctic Sea †	Not Evaluated	G-PR*	crtEIBY, blh	37 kb	Henn (2008)
ARCTIC22_G_02	EU795243	Arctic Sea †	Not Evaluated	G-PR*	crtEIBY, blh	25 kb	Henn (2008)
ARCTIC07_E_02	EU795232	Arctic Sea †	Not Evaluated	G-PR*	crtEIBY [#]	35 kb	Henn (2008)
ARCTIC42_C_05	EU795236	Arctic Sea †	Not Evaluated	G-PR*	crtEIBY, blh	39 kb	Henn (2008)
ARCTIC20_C_09	EU795107	Arctic Sea †	Not Evaluated	G-PR*	crtEIBY, blh	24 kb	Henn (2008)
ACRTIC32_A_02	EU795088	Arctic Sea †	Not Evaluated	B-PR* XR°	crtEIBY, brp/blh[&]	33 kb	Henn (2008)

BAC / Fosmid	Genbank Accession #	DNA Source Water [A]	Putative Genetic Origin [B]	PR [C]	Retinal Biosynthetic Genes [D]	Insert Size	Reference
ARCTIC14_B_11	EU795105	Arctic Sea †	Not Evaluated	B-PR*	crtEIBY, brp/blh[&]	34 kb	Henn (2008)
ARCTIC10_A_01	EU795233	Arctic Sea †	Not Evaluated	G-PR*	crtE [#]	27 kb	Henn (2008)
STA2_11_A_06	EU795108	Sargasso Sea ‡	Not Evaluated	G-PR[•]	crtY, brp/blh[&]	32 kb	Henn (2008)

[A] Library DNA sampling source as described by cited reference

† Fosmid from the Kirchman Envinormental Fosmid Library, Broad Institute, as part of NCBI Project 29035 (Artic Environmental Sampling Metagenome), unannotated sequence (Slamovits et al., 2011). PR and retinal biosynthesis pathway components for this fosmid identified in this work through tBLASTn (Henn et al., 2008) using the components of the HF10_19P19 PRPS as the query sequence.

‡ Fosmid from the Kirchman Envinormental Fosmid Library, Broad Institute, as part of NCBI Project 29043 (Sargasso Sea Environmental Sampling Metagenome), unannotated sequence (Gertz et al., 2006). PR and retinal biosynthesis pathway components for this fosmid identified in this work through tBLASTn (Henn et al., 2008) using the components of the HF10_19P19 PRPS as the query sequence

[B] Source DNA phylogengy as reported by cited reference, determined using various methods

[C] G-PR, green variant PR; B-PR, blue variant PR; XR, xanthorhodopsin

* PR color predicted based on amino acid identity at the tuning residue (Gertz et al., 2006)

° Rhodopsin aligns most closely with the cluster containing xanthorhodopsin (Man et al., 2003)

• Rhodopsin aligns with rhodopsins of the Bacteroidetes group which are characterized by a methionine at the tuning residue and exhibit a green absorption maximum when expressed in *E. coli* (McCarren and DeLong, 2007)

[D] Gene clusters located on vector insert are grouped by spatial arrangement (e.g. crtE, crtIBY indicates that crtE is separate from crtIBY which contains crtI, crtB, and crtY arranged in the indicated order

[#] Retinal gene cluster is located at the fosmid end, additional genes may exist adjacent to those discovered

[&] The gene in cluster does not have significant similarity to the *blh* of the PRPS from HF10_19P19, but BLASTx (Gomez-Consarnau et al., 2007) to nr protein database has hits to both *brp* and *blh* type oxygenases (e-values < 1e-3; top hit e-value < 1e-45)

Diversity of Isolated Strains Containing Proteorhodopsin

In support of the diversity of PR hosts discovered in large-insert BAC libraries, proteorhodopsin genes have recently been discovered in a number of cultured isolates with diverse backgrounds ranging from proteobacteria (Altschul et al., 1990) to bacteriodes (Giovannoni et al., 2005a; Stingl et al., 2007; Giovannoni et al., 2008; Gomez-Consarnau et al., 2010; Oh et al., 2010) to marine eukaryotes (Gomez-Consarnau et al., 2007; Lami et al., 2009; Riedel et al., 2010).

Proteorhodopsins have been found in several cultured isolates of alpha-proteobacteria (Slamovits et al., 2011). *Pelagibacter ubique* was the first cultured isolated identified with PR and is among the most abundant and well-studied marine microorganisms (Giovannoni et al., 2005a; Giovannoni et al., 2006b; Rappe et al., 2009; Oh et al., 2010). In addition to the alpha-proteobacteria, PRs have been discovered in a beta-proteobacterium (Morris et al., 2002; Steindler et al., 2011), gamma-proteobacteria (Giovannoni et al., 2008), *Vibrionaceae* (Giovannoni et al., 2006a; Stingl et al., 2007; Amann et al., 2008), and Photobacteria (Bassler et al., 2007; Gomez-Consarnau et al., 2010). Of all instances of PR in proteobacteria, the only two reports of light-depenedent physiological function have been reported; a light-dependent decrease in respiration and increase in ATP was attributed to PR in *Pelagibacter ubique* (Hagstrom et al., 2006; Lauro et al., 2009), and PR has been directly attributed to the light-based increase in survival during starvation of *Vibrio* sp. AND4 (Steindler et al., 2011).

Several cultured species of bacteroides contain proteorhodopsin (Gomez-Consarnau et al., 2010). Of these cultured isolates, *Dokdonia donghaensis* MED134 remarkably demonstrates a light-dependent increase in growth-rate and yield which is presumably attributed to the PR due to the agreement of the growth effect the absorbance spectrum of proteorhodopsin (Bowman et al., 2006; Gomez-Consarnau et al., 2007; Hagstrom et al., 2007; Gonzalez et al., 2008; Lail et al.,

2010; Riedel et al., 2010; Klippel et al., 2011; Lucas et al., 2011) and the elimination of the effect in the presence of an inhibitor of the carotenoid biosynthesis prior to the formation of retinal (Gomez-Consarnau et al., 2007). *Polaribacter* sp. MED152 does not demonstrate a light-dependent increase in growth; however rates of carbon dioxide uptake were shown to be elevated in the light, which may demonstrate a shift in metabolic profile for carbon utilization (Kimura et al., 2011).

Heterologous Hosts for Proteorhodopsin

Reported experimentation with proteorhodopsin in heterologous hosts has been limited to date to gamma proteobacteria (Gonzalez et al., 2008). The most extensive characterization of proteorhodopsin function in heterologous hosts has been in *Escherichia coli*. In *E. coli*, PR has been demonstrated to pump protons (Martinez et al., 2007; Walter et al., 2007; Johnson et al., 2010) leading to utilization for both phosphorylation (Beja et al., 2000b) and flagellar rotation (Martinez et al., 2007). No reports have yet shown increased growth rate, yield, or survival of *E. coli* associated with the light and the function of PR. Heterologous expression of PR in *Shewanella oneidensis* demonstrated an increased survival in stationary phase and increased current production in a microbial fuel cell (Walter et al., 2007). The increased electrical current is associated with an increased respiration rate which was attributed to faster transport and consumption of lactate due the proton motive force supplied by the PR (Johnson et al., 2010). The work described in Chapter 3 of this work widens the range of heterologous host systems to include *Pseudomonas putida*, also a gamma proteobacterium.

Pseudoaltermonas atlantica: A potential marine host bacterium for studying function and physiological effects of PR

Pseudoalteromonas atlantica, formally known as *Pseudomonas atlantica* (Johnson et al., 2010) and *Alteromonas atlantica* (Yaphe, 1957), is a marine gamma-proteobacterium (Akagawamatsushita et al., 1992). *P. atlantica* is a polar flagellated, rod-shaped, heterotrophic,

non-fermentative aerobe (Gauthier et al., 1995). *P. atlantica* was originally found associated with marine eukaryotic species such as algae (Akagawamatsushita et al., 1992) and *Cancer pagurus* (edible crabs) to which the bacterium is known to be a pathogen responsible for shell disease (Yaphe, 1957). *P. atlantica* has also been found unassociated in the water column and has been shown to multiply rapidly in bottle incubation overtaking other populations (Costa-Ramos and Rowley, 2004).

P. atlantica is well-known for the ability to degrade agarose (Eilers et al., 2000) and other polysaccharides (Yaphe, 1957) with the use of a pathway involving beta-agarase and beta-neoagarotetraose hydrolase enzymes (Yaphe and Morgan, 1959). The species is also well known for its ability to produce extracellular polysaccharides for the formation of biofilms (Groleau and Yaphe, 1977; Morrice et al., 1983a; Morrice et al., 1983b).

The genetic tools available make *P. atlantica* DB27 an attractive target for studies with heterologous PRPS. Strain *P. atlantica* DB27 is an *hsd-1* Rif^R derivative of *P.atlantica* T6C (Uhlinger and White, 1983; Bartlett et al., 1988); the antibiotic marker is advantageous for the use of this strain in the laboratory. Strain T6C has been fully sequenced and is not known to contain any rhodopsin proteins (Bartlett et al., 1988). *P. atlantica* T6C can be made competent and genome modifications affected via homologous recombination (Copeland et al., 2006). *P. atlantica* DB27 has been shown to accept via conjugation and maintain the conjugative-and-integrative-in-*Streptomyces* (CIS) vectors (Dr. Asuncion Martinez, unpublished observation) developed previously (Belas et al., 1988).

In this work, a preliminary survey of six constructs containing proteorhodopsin photosystems from five large-insert environmental BAC and fosmid clones are tested within two host organisms, *Pseudomonas putida* and *Pseudoalteromonas atlantica*. This work confirms that both hosts retain the exogenous PR constructs and demonstrates transcription of the PR gene during late exponential phase for each of the photosystems in both hosts grown using rich media

(LB or marine broth). Furthermore, three of the photosystem constructs, pSHF10_19P19, pS41B09, and pS55B11, were tested for the ability to confer a light-based growth yield effect in M9 minimal media supplemented with glucose as described in Chapter 3 for *P. putida* pSJ2B6.

Methods

Construction of retrofit vectors

Select vectors containing PRPS from environmental shotgun libraries (Martinez et al., 2004) were modified with the conjugative-and-integrative-in-*Streptomyces* (CIS) cassette following the original procedure described (Beja et al., 2000a; Beja et al., 2002; DeLong et al., 2006) according to the methods detailed in Chapter 3. The vectors were constructed by Dr. Asuncion Martinez, from clones previously identified through metagenomic library screens (Martinez et al., 2004), several of which were used previously in the creation of a Genome-Proxy Microarray (Beja et al., 2000b; Beja et al., 2002; Martinez et al., 2007; McCarren and DeLong, 2007). Several of these clones utilize the pCC1FOS Fosmid vector (Epicentre) detailed in Chapters 2 and 3 of this work; the other clones were created using the BAC pIndigoBAC536 (Rich et al., 2008).

Conjugation from E. coli DH10B/pUB307 to Pseudomonas putida and Pseudoalteromonas atlantica

Conjugation retrofit vectors into *P. putida* was performed as described in Chapter 3 following previous methods (Stein et al., 1996). Conjugation of the retrofit vectors into *P. atlantica* followed a similar method adapted for growth conditions suitable for *P. atlantica*. Development of this method occurred with assistance from Dr. Martinez. The donor strain for *P. atlantica* conjugations, *E. coli* DH10B pUB307 (Martinez et al., 2004) containing the retrofit vector (pSJ2B6 or pSCCFOS), was the same as for *P. putida*. The donor strain containing the appropriate vector was grown as a starter culture in Luria-Bertani (LB) Broth [5 g/L yeast extract, 10 g/L tryptone, 10 g/L sodium chloride, BD Biosciences, (Martinez et al., 2004)] with 50 ug/mL kanamycin, 25 ug/mL apramycin, and 12.5 ug/mL chloramphenicol. A starter culture of recipient strain *P. atlantica* DB27 (a generous gift from Douglas Bartlett, Scripps Institution of Oceanography) (Sambrook et al., 1989) was grown in marine broth (BD Difco 2216, 28 g/L) with

50 ug/mL rifampicin (Sigma CAS No: 13292-46-1) at 30°C with shaking at 250 rpm overnight (Barnstead LabLine MaxQ 4000). Donor and recipient starter cultures were diluted 1:100 into the same media formulation used for the starter culture and grown for 4 hours at 30°C with shaking at 250 rpm (Barnstead LabLine MaxQ 4000). Donor and recipient cultures were mixed in various ratios to a final volume of 1 mL, pelleted at 5000 rcf (Eppendorf 5415D), resuspended (Vortex Genie 2 Fisher Scientific), spotted on non-selective agar (Bactoagar, BD Biosciences) plates with 28 g/L marine broth, and grown overnight at 30°C in a plate incubator (VWR). Cultures were suspended from the non-selective plate and plated onto selective media; marine broth (28 g/L) with rifampicin (50 ug/mL) was used to select for the *P. atlantica* recipient strain and select against donor *E. coli* strain, with 30 ug/mL apramycin present to select for successful vector conjugation. As with *P. putida* conjugations, donor and recipient controls were carried through to evaluate background colony formation. Potential clones were restreaked onto the selective plates and monoclonal stocks were prepared from colonies grown in marine broth (28 g/L) with cryopreservation at -80°C (Revco Legaci) in 15% glycerol (BDH/VWR CAS No: 56-81-5).

Verification of the *P. putida* and *P. atlantica* exconjugants was performed by polymerase chain reaction of the PR gene as described in Chapter 3. Primers specific to the PR and thermocycling conditions for the pS55B11, pS41B09, and pSHF10_25F10 vectors were designed previously by Dr. Martinez (unpublished work); the primer sequences and the thermocycling conditions used for pSHF10_19P19 were the same as for pSJ2B6 (Chapter 3); primers and thermocyclings conditions for pS31A08 were from (Reference Beja, 2000). The primers and thermocycling programs for each vector are listed in Table 4-2 and Table 4-3.

Table 4-2: Primers for Verification of PR in Exconjugants

Vector	Primer 1	Primer 2
pSHF10_19P19	GGACGTTCTAGAACGCGACGTTTGGGGAG	TTACTTTGCCGCTTCAGATTGTGA
pSHF10_25F10	ATGAAACTCTCAATGGGTAAGGTG	CATTTAGGCTTTCGCGGC
pS41B09 PR#1	TTAGGCTCCAATATCCGACT	ATGCAAGTAGCTGACTACAA
pS41B09 PR#2	TTACTTGGCTTTTGCACCTG	ATGTTAAATCCATCAGATTA
pS55B11	GAGGAATAATAAATGACGATTTTATCAAAAAAAGGC	TTATTTAGATTCTGATTCAGTTAC
pS31A08 (Bartlett et al., 1988)	ACCATGGGTAAATTATTACTGATATTAGG	AGCATTAGAAGATTCTTTAACAGC

Table 4-3: Thermocycling Conditions for PR Amplification

Vector	Denaturing	Melting	Annealing	Elongation	Polishing/Hold	Cycles
pSHF10_19P19	2 minutes @ 93°C	40 seconds @93°C	30 seconds @62°C	1 minute @72°C	10 minutes @72°C ∞ @4°C	25
pSHF10_25F10	2 minutes @ 95°C	40 seconds @95°C	30 seconds @56°C	1 minute @72°C	10 minutes @72°C ∞ @4°C	25
pS41B09 PR#1	2 minutes @ 94°C	15 seconds @94°C	30 seconds @45°C	1 minutes @68°C	5 minutes @68°C ∞ @4°C	25
pS41B09 PR#2	5 minutes @ 94°C	1 minute @94°C	1 minute @45°C	1 minute @74°C	10 minutes @74°C ∞ @4°C	25
pS55B11	5 minutes @ 94°C	1 minute @94°C	1 minute @45°C	1 minute @74°C	10 minutes @74°C ∞ @4°C	30
pS31A08	2 minutes @ 95°C	40 seconds @95°C	30 seconds @52°C	1 minute @72°C	10 minutes @72°C ∞ @4°C	30

Transcription of the PR through RT-PCR

Transcription of the PR gene from the PRPS of the various vectors was confirmed by reverse-transcriptase polymerase chain reaction (RT-PCR) (Beja et al., 2000b) as described for *P. putida* pSJ2B6 (Chapter 3). *P. putida* exconjugant cultures were grown according to the method in Chapter 3 for the transcription of PR. Cultures of *P. atlantica* were grown overnight at 30°C shaking at 200 rpm (Barnstead LabLine MaxQ 4000) in 3 mL marine broth (28 g/L) with 50 ug/mL rifampicin and 30 ug/mL apramycin as a starter culture. The starter culture was diluted 1:100 into identical media and grown for 6 hours at 30°C with shaking 200 rpm. RNA extraction, DNase treatment, RNA purification, and RT-PCR were performed according the methods described in Chapter 3. Primers used for the RT-PCR were the same as for the exconjugant verification, and the thermocycling program was the same as the exconjugant verification except the number of cycles was increased to 40 and a preliminary RT step of 30 minutes at 55°C was added as described in Chapter 3.

Low Dissolved Organic Carbon (DOC) Growth Experiments

The culture conditions for *P. putida* exconjugant growth experiments were identical to those described in Chapter 3: including incubator temperature, light conditions, water bath, and culture vessel. M9 media with 25 ug/mL apramycin was used for all experiments as described earlier (Chapter 3). Cultures of *P. putida* exconjugants were grown as described in Chapter 3 for 11 uM glucose "Baseline low DOC growth experiments", including starter culture conditions. Following 11 uM glucose concentration experiments, growth experiments in 1.1 uM glucose were performed according the methods described in Chapter 3 for the "Glucose concentration dependence experiments". All sampling procedures and colony forming unit (CFU) measurements were performed as described in Chapter 3.

Results

A select group of the vectors containing proteorhodopsin photosystem components listed in Table 4-1 were retrofit by Dr. Asuncion Martinez to include a mobilization cassette to allow conjugation into a broad range of hosts and integration at the ϕC31 *attB* site found in *Streptomyces* strains as well as the engineered *P. putida* MBD1 strain (Ausubel, 1987). The vector constructs differ in several ways including the vector backbone, protorhodopsin color variant, retinal synthesis gene cluster composition, and the size and makeup of the non-photosystem insert DNA (Table 4-4). Linearized vector maps for these constructs are depicted in Figure 4-1 to demonstrate the relative position and orientation of the photosystem within the insert DNA. In addition to the differences in the PRPS location, orientation, and gene composition, the slight differences which exist in the arrangement of the photosystem components, primarily in the location and extent of overlapping reading frames of retinal biosynthetic genes, are also depicted Figure 4-1.

Table 4-4: Vectors Retrofit with CIS Cassette

Retrofit CIS Vector	Fosmid / BAC Source	Vector Backbone	Rhodopsin	Carotenoid Synthesis Genes
pS55B11	EB000_55B11	pIndigoBAC536	Green PR*	crtEIBY, blh
pS41B09	EB0_41B09	pIndigoBAC536	PR1= Blue PR* PR2 = Xanthorhodopsin †	crtEIBY, blh
pS31A08	EBAC31A08	pIndigoBAC536	Green PR	None
pS60D04	EB000_60D04	pIndigoBAC536	None	crtAIBCDEF, idi
pSHF10_19P19	HF10_19P19	pCC1FOS (Epicentre)	Blue PR	crtEIBY, blh, idi
pSJ2B6	pFOS-PRPS Clone J2B6‡	pCC1FOS (Epicentre)	Blue PR	crtEIBY, blh, idi
pSHF10_25F10	HF10_25F10	pCC1FOS (Epicentre)	Blue PR	crtEIBY, blh, idi
pSCCFOS	pCC1FOS	pCC1FOS (Epicentre)	None	None

* Proteorhodopsin color predicted based on expected amino acid sequence, no experimental verification (Martinez et al., 2007)

† The second rhodopsin in the pS41B09 gene cluster aligns most closely with the xanthorhodopsin from *Salinibacter ruber* (McCarren and DeLong, 2007; Rich et al., 2008)

‡ Subcloned photosystem derived from HF10_19P19, described in Chapter 2 of this work

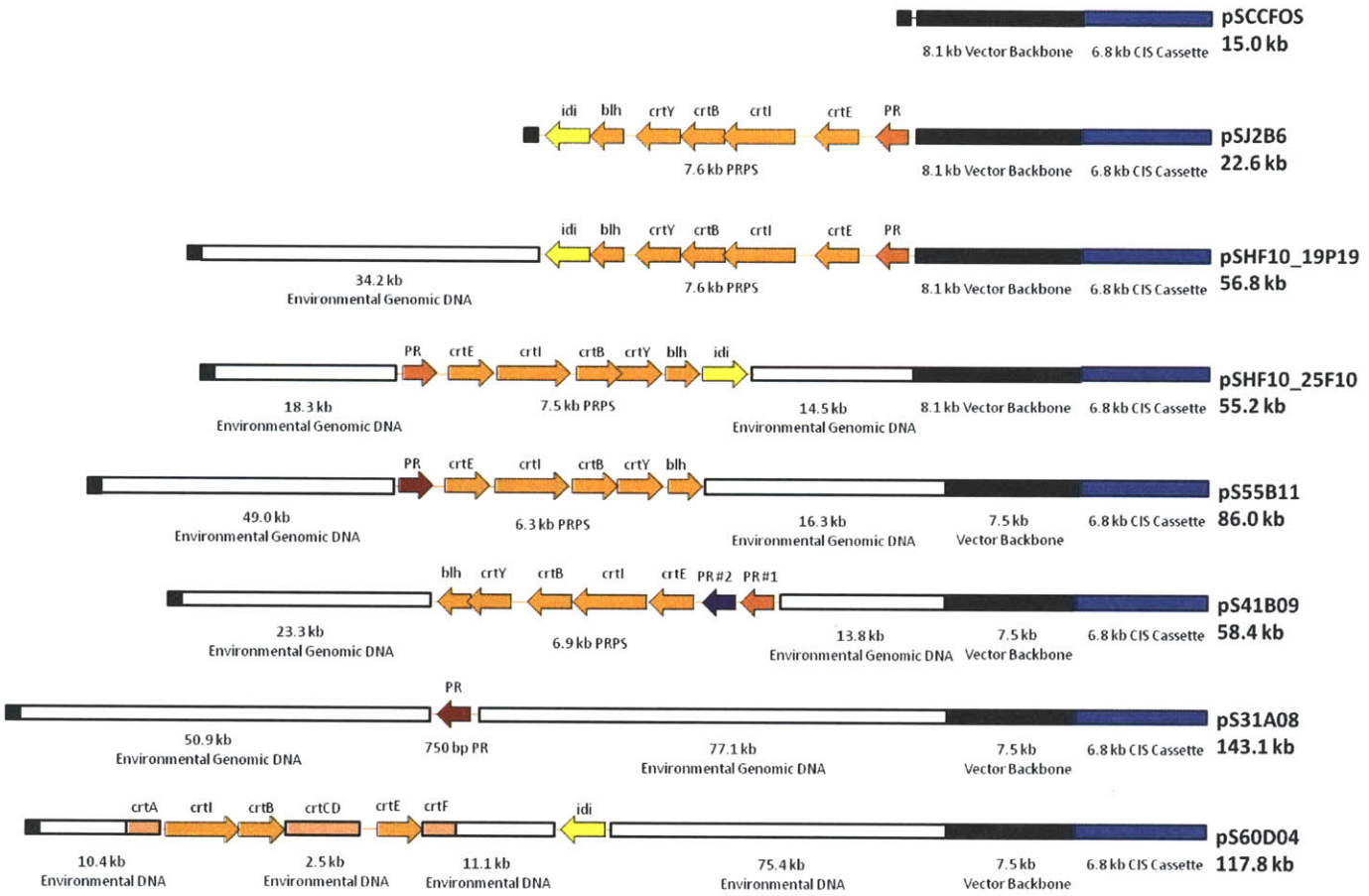

Figure 4-1: Linearized Vector Maps of CIS Retrofit Vectors. Vector numbering starting with 0 at left and increasing to the right. Sizes not to scale. Vectors backbone shown in black; pIndigoBAC536, 7.5 kb; pCC1FOS, 8.1 kb due to the inclusion of OriV. CIS Cassette shown in blue. PRPS gene ORF orientation indicated by arrow direction. Rhodopsins are shown in red (G-PR), salmon (B-PR), or purple (XR). Retinal synthesis pathway (*crtEIBY*) in orange, *idi* in yellow, other *crtA,CD,F* in pink on chromosome. Non-PRPS genomic DNA is shown in white at locations relative to the PRPS components.

The retrofit vectors, pSHF10_19P19, pSHF10_25F10, pS41B09, pS55B11, pS31A08, and pS60D04 were conjugated into *P. putida* MBD1 (McCarren and DeLong, 2007), complementing the *P. putida* pSJ2B6 and *P. putida* pSCCFOS strains discussed earlier (Chapter 3 this work). All eight vectors were also conjugated into the host *Pseudoalteromonas atlantica* DB27 (Martinez et al., 2007) which, despite not having a ϕC31 *attB* integration site, appears to maintain the vector as a plasmid (not integrated into the genome) via an unknown mechanism (Dr. Asuncion Martinez unpublished observation).

The results of the conjugations were verified with gel electrophoresis of the PCR product of the PR gene on the insert (if applicable) for each of the exconjugants selected. The results of the exconjugant verification are shown in Figure 4-2. All vectors were successfully conjugated into both hosts with the exception of the pS31A08 vector in *P. atlantica*, which failed in numerous attempts at conjugation. The reason for the failed conjugation of pS31A08 into *P. atlantica* is unknown, but the large size of the BAC (143 kb compared to the 22.6 kb of the complete photosystem vector pSJ2B6) is a potential factor as well as potential toxicity to *P. altantica* of the gene products found in the environmental DNA; several attempts were required to successfully produce exconjugants for *P. putida* pS31A08 demonstrating poor efficiency of transfer and integration into this host as well. A single successful exconjugant was selected for each construct for further evaluation. While exconjugants for *P. putida* pS60D04 and *P. atlantica* pS60D04 were selected and cryogenically preserved, no verification of the identity of these strains was performed as the construct contains carotenoid and chlorophyll biosynthesis genes but lacks a PR gene. No additional studies were performed with these strains in the course of this work.

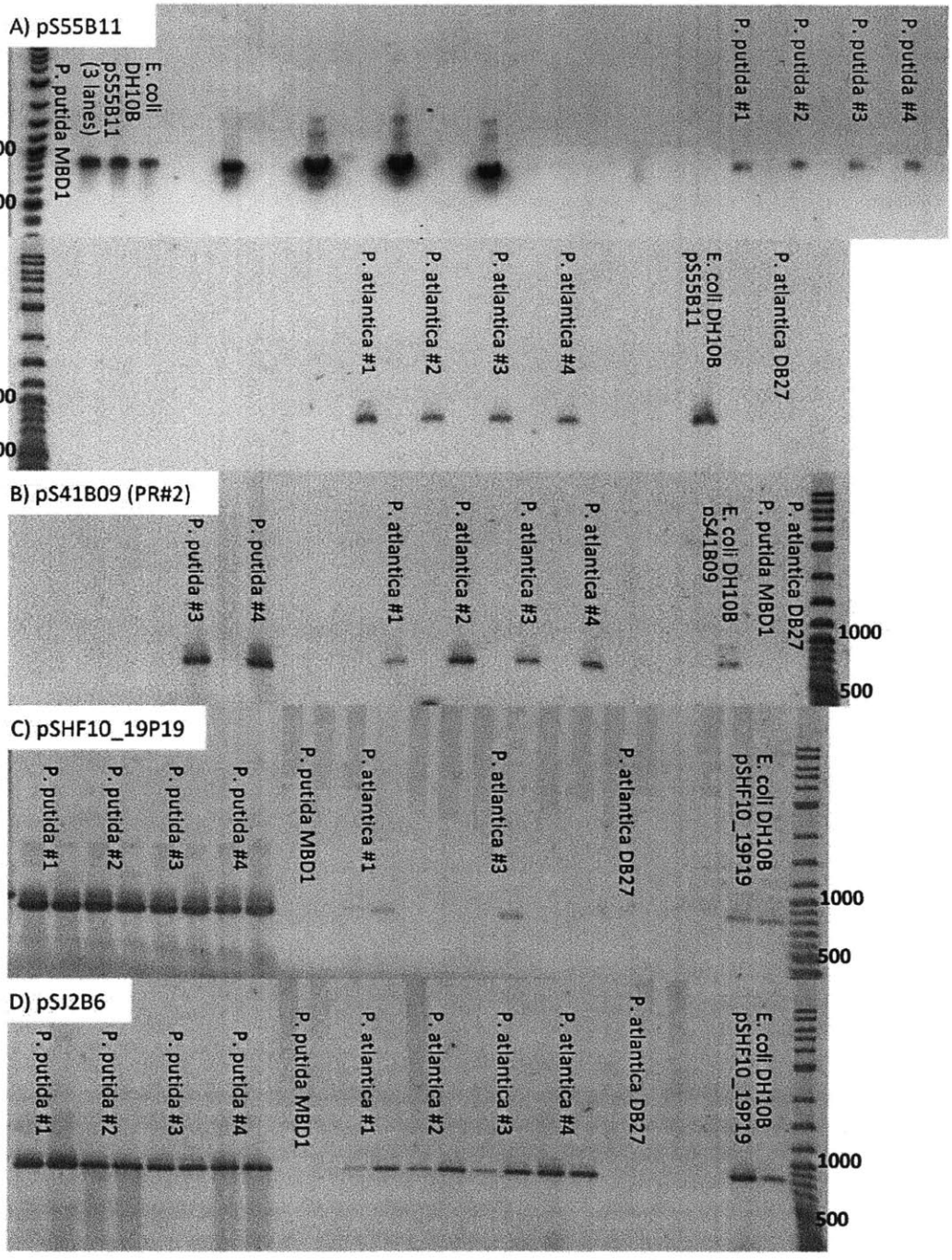
A) pS55B11
P. putida #4
P. putida #3
P. putida #2
P. putida #1
E. coli DH10B pS55B11 (3 lanes)
P. putida MBD1
P. atlantica DB27
E. coli DH10B pS55B11
P. atlantica #4
P. atlantica #3
P. atlantica #2
P. atlantica #1
1000
500
B) pS41B09 (PR#2)
P. atlantica DB27
P. putida MBD1
E. coli DH10B pS41B09
P. putida #3
P. putida #4
C) pSHF10_19P19
E. coli DH10B pSHF10_19P19
D) pSJ2B6

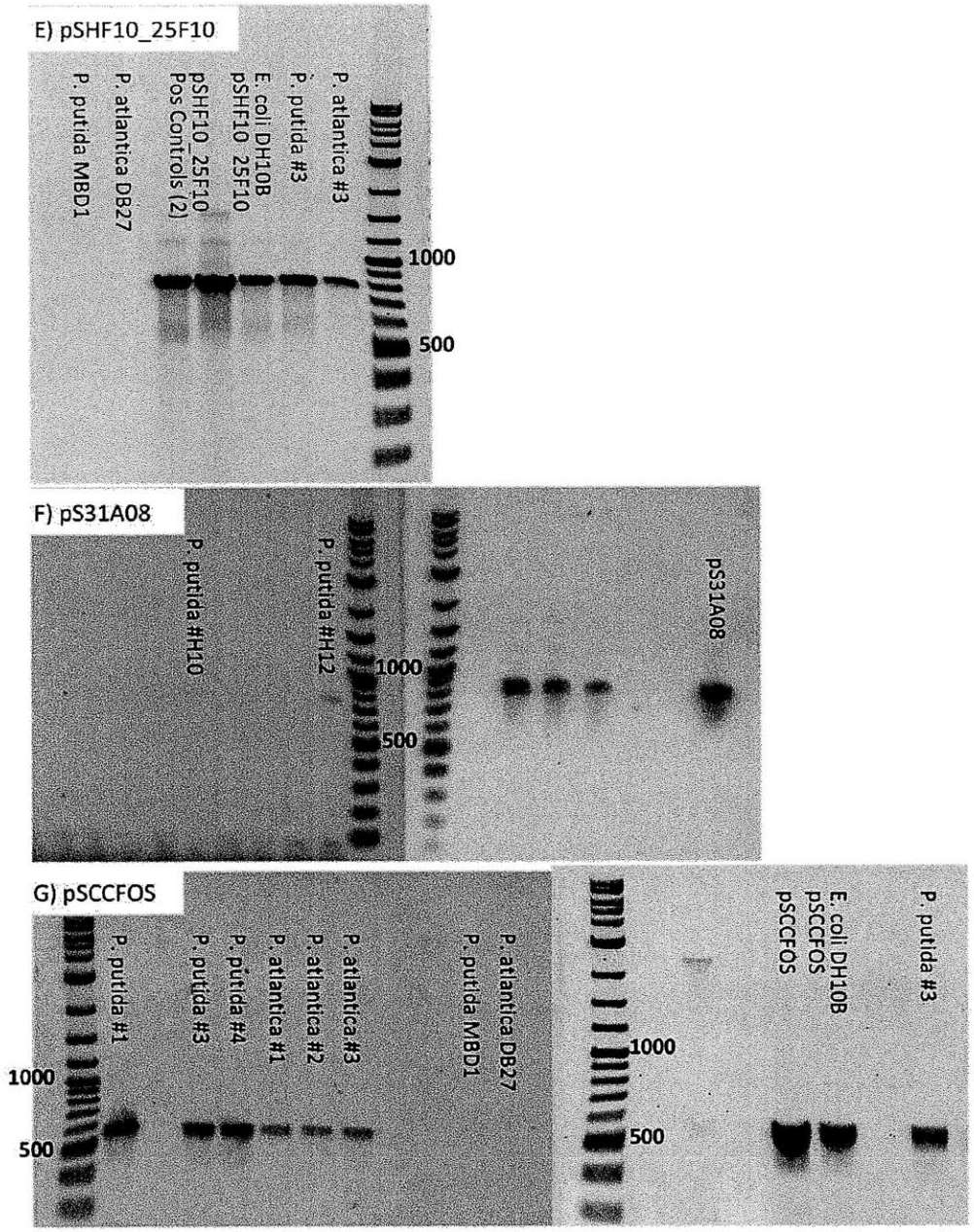

Figure 4-2: PCR Verification of Exconjugants. Colony PCR was performed on each of the *P. putida* and *P. atlantica* exconjugants possessing a PR: A) pS55B11, B) pS41B09, C) pSHF10_19P19, D) pSJ2B6, E) pSHF10_25F10, F) pS31A08. Colony PCR was also used to confirm the control strain by amplification of the region between the vector sequencing primers: G) pSCCFOS. From the four (minimum) replicate clones selected, at least one demonstrated amplification of the PR gene. For each result, the target vector is given for a length standard. Ladder shown is 2-log ladder (NEB), with markers every 100 bp between 500 and 1000 bp. One successful clone was selected for additional study.

Transcription of the PR gene for each of the relevant constructs was verified through RT-PCR of RNA extracted from cultures grown in rich media (LB for *P. putida*, marine broth for *P. atlantica*) to late exponential phase. Results of the gel electrophoresis of RT-PCR products are shown in Figure 4-3. Issues of background DNA contamination in the RT-PCR master mix exist for several of the vectors. In these cases (pSHF10_19P19 and pS41B09), the quantitative results clearly show a very strong signal for the presence of RNA compared to the weak band across all controls. As such, there was a reasonable belief that transcription of the PR gene was occurring for all hosts and vector combinations, and the source of the contamination was not tracked down and eliminated for the purpose of this study. Regulation of the PR transcription is unknown, and two possibilities exist. First, transcription may be from the regulatory elements on the vector or in the host organism in the case of *P. putida* strains. While this is quite feasible for the pSJ2B6 and pSHF10_19P19 vectors due to the locations near the vector junctions, it is not likely for any of the other constructs due the low probability of transcriptional read through in excess of 10 kb (Figure 4-1). Alternatively, transcription may be initiated at native promoters within the environmental DNA fragment intended for the PRPS itself. Quantitative analysis of PR transcription was not performed during growth experiments with glucose in M9 minimal media, and transcription of the remaining photosystem components was not verified for this study, so the regulation of the photosystem expression remains unknown.

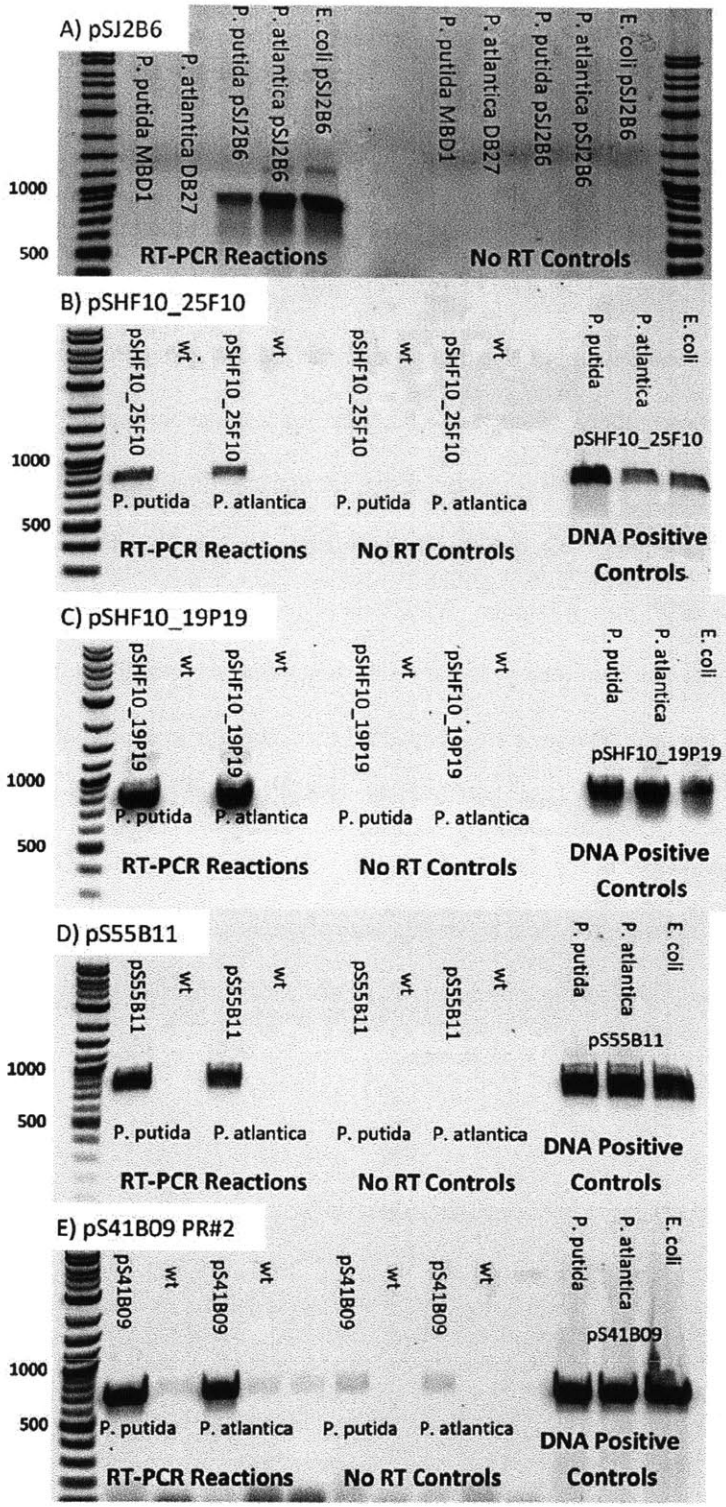

Figure 4-3: RT-PCR Evidence of PR Transcription in Exconjugants for *P. putida* and *P. atlantica* strains of A) pSJ2B6, B) pSHF25F10, C) pSHF10_19P19, D) pS55B11, and E) pS41B09 (PR#2). Control PCR reactions without the reverse transcriptase treatment verify that the signal is from mRNA and not DNA carried over from. DNA positive controls are presented for a length standard. Ladder is 2-log ladder (NEB), with dark bands at 500 and 1000 bp and bands every 100 bp.

Following the results of low DOC growth for *P. putida* pSJ2B6 presented in Chapter 3, growth experiments were performed with several of the *P. putida* exconjugant strains. The first strain tested was *P. putida* pSHF10_19P19. This vector contains an identical PRPS in the analagous orientation and position within the same vector backbone as pSJ2B6. This gives the best possibility for similarities in expression and function of the PR and retinal synthesis genes for any of the alternative photosystems which could be tested; the primary difference between the two constructs is the presence of non-PRPS genes in pSHF10_19P19.

Growth of *P. putida* pSHF10_19P19 was tested on 11 uM glucose as previously described in the "baseline low DOC growth experiment" of Chapter 3. Unlike *P. putida* pSJ2B6, the results of *P. putida* pSHF10_19P19 yielded no difference between growth in the light and dark under these conditions Figure 4-4A. Following up on this observation, the strain was tested at a lower concentration of glucose (1.1 uM) to determine if a light-dependent growth effect would emerge. This condition resulted in a significant difference between light and dark growth curves Figure 4-4B. For comparison purposes, the growth curves for the PRPS-negative control strain *P. putida* pSCCFOS which demonstrates no light-dependent growth effects under these same conditions are shown adjacent to the *P. putida* pSHF10_19P19 results (Figure 4-4C & D). The results of the 1.1 uM glucose experiment demonstrate the same trend as was observed for *P. putida* pSJ2B6.

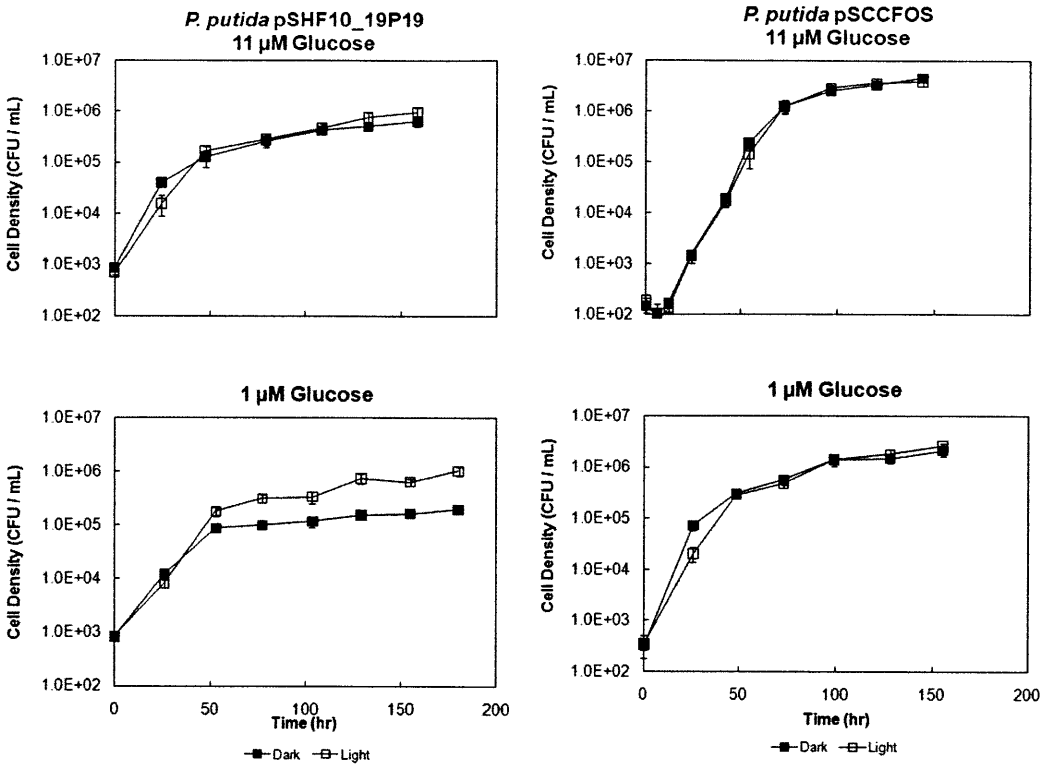

Figure 4-4: Low DOC Growth Results of *P. putida* pSHF10_19P19. Growth of *P. putida* pSHF10_19P19 in M9 media with A) 11 uM glucose and B) 1 uM glucose was as described in the methods section. Growth curve for the negative control strain *P. putida* pSCCFOS are shown under identical conditions of C) 11 uM glucose and D) 1 uM glucose.

The *P. putida* pS41B09 strain was selected next for low DOC growth experimentation. The pS41B09 vector contains two rhodopsin sequences; PR1 contains a glutamine at the tuning residue suggesting a blue variant (Bartlett et al., 1988), and PR2 aligns most closely with the xanthorhodopsin from *Salinibacter ruber* (McCarren and DeLong, 2007). The differences in the source host organism as well as the origins of the retinal synthesis genes (McCarren and DeLong, 2007) makes this vector interesting for examining the effect of a relatively divergent PRPS from that of pSJ2B6/pSHF10_19P19. As with *P. putida* pSHF10_19P19, *P. putida* pS41B09 was grown first in 11 uM glucose inoculated from a late stationary phase culture with 1 mM glucose, followed by growth at 1.1 uM glucose inoculated from the stationary phase of the 11 uM glucose culture. As with the *P. putida* pSHF10_19P19 strain, little to no light-dependent response was observed at 11 uM glucose Figure 4-5A, but when moved to the 1.1 uM glucose concentration a drastic difference between cultures grown in the light and those grown in the dark emerged Figure 4-5B. At the 1.1 uM glucose concentration, *P. putida* strains containing pSJ2B6, pSHF10_19P19, and pS41B09 exhibit similar trends for light-dependent increase in growth yield.

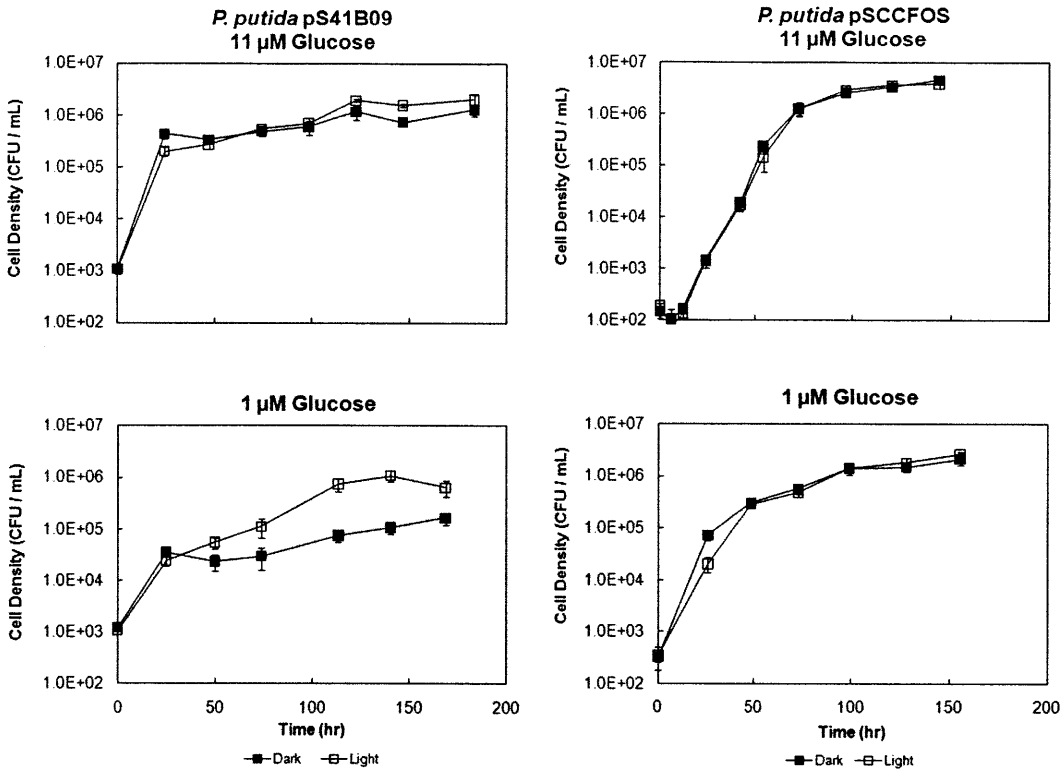

Figure 4-5: Low DOC Growth Results of *P. putida* pS41B09. Growth of *P. putida* pS41B09 in M9 media with A) 11 uM glucose and B) 1 uM glucose was as described in the methods section. Growth curve for the negative control strain *P. putida* pSCCFOS are shown under identical conditions of C) 11 uM glucose and D) 1 uM glucose.

P. putida pS55B11 was tested for a light-based growth effect. The PR on pS55B11 is predicted to be a green variant based on the glutamate residue at the tuning position (McCarren and DeLong, 2007). Otherwise, the gene cluster contains *crtEIBY* and *blh* and shows a high degree of similarity to that of the PRPS in pSJ2B6. To determine if retinal limitation exists in the system, the system was tested with and without exogenous retinal addition. Methanol, which did not demonstrate appreciable effects on *P. putida* pSJ2B6 growth under conditions tested (data not shown), served as the vehicle for the retinal to eliminate the carbon source effects of ethanol (data not shown) and was added to the experiments without retinal addition. Unlike any of the other strains tested, at 11 uM glucose *P. putida* pS55B11 demonstrated a pronounced decrease for growth in the light compared to the dark. The addition of retinal increased CFU for both the light and the dark growths conditions, however the detrimental effect of light was observed regardless of the addition of exogenous retinal (Figure 4-6). Under these growth conditions with *P. putida* pS55B11, no growth advantage was conferred by light. Additional growth conditions were not evaluated.

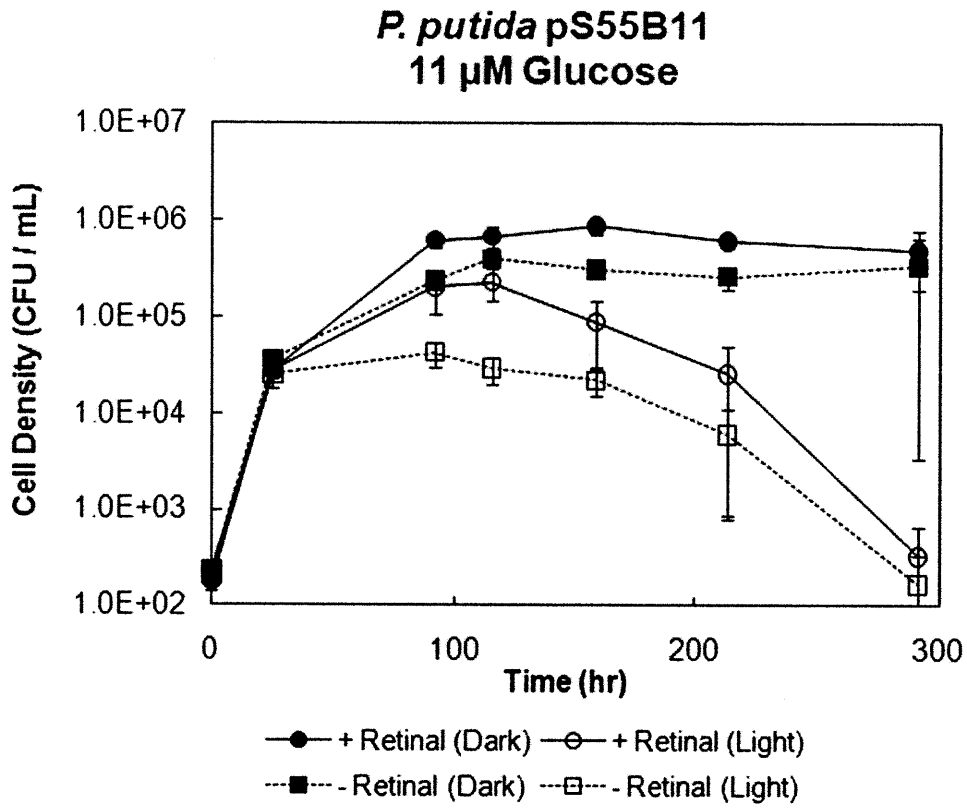

Figure 4-6: Low DOC Growth Results of *P. putida* pS55B11 with and without Retinal Addition.

The status of each of the host-vector combinations is summarized in Table 4-5. Three PRPS-containing strains of *P. putida* were not tested for light-dependent growth effects. pS31A08 was not tested due to concerns about strain health. pSHF10_25F10 was not prioritized for testing due to its similarity to pSHF10_19P19 (Man et al., 2003). pS60D04 was not tested as it does not contain a PR gene. While evidence for transcription was found for all of the *P. atlantica* strains containing a PR gene, the light dependence of low DOC growth was not evaluated for the *P. atlantica* strains during this study.

Table 4-5: Results of PRPS Host-Vector Survey

	P. putida pSCCFOS	*P. atlantica* pSCCFOS	*P. putida* pSJ2B6	*P. atlantica* pSJ2B6	*P. putida* pSHF10_19P19	*P. atlantica* pSHF10_19P19	*P. putida* pSHF10_25F10	*P. atlantica* pSHF10_25F10	*P. putida* pS41B09	*P. atlantica* pS41B09	*P. putida* pS55B11	*P. atlantica* pS55B11	*P. putida* pS31A08	*P. atlantica* pS31A08	*P. putida* pS60D04	*P. atlantica* pS60D04
Exconjugants Produced	X	X	X	X	X	X	X	X	X	X	X	X	X		X	X
Exconjugants Verified	X	X	X	X	X	X	X	X	X	X	X	X	X			
Evidence of PR Transcription	n/a	n/a	X	X	X	X	X	X	X	X	X	X				
Light-Dependent Growth Effect	None Observed	N.D.	Increase [glucose] < 1100 uM	N.D.	Increase [glucose] = 1.1 uM	N.D.	N.D.	N.D.	Increase [glucose] = 1.1 uM	N.D.	Decrease	N.D.	N.D.		N.D.	N.D.

X = Accomplished; n/a = Not Applicable; N.D. = Not Determined

Discussion

Eight vectors were incorporated in *Pseudomonas putida* and *Pseduoalteromonas atlantica* to survey the performance of PRPS variants in multiple hosts. Six of the vectors contain proteorhodopsin, and they represent five unique photosystems spanning the range from only a PR, to PR with *crtEIBY* with *blh*, to PR with *crtEIBY* with *blh* and *idi*. While representatives were present from various rhodopsin phenotypes including blue PR, green PR, and xanthorhodopsin, the diversity of PRPS observed in the marine environment far exceeds what was evaluated in this study.

Five photosystem constructs were successfully transferred to both hosts, however the pS31A08 PRPS could only be incorporated into *P. putida*. For the other five PRPS constructs, evidence of transcription was observed in both hosts. Given the variety of the locations and orientations of the PRPS in the vectors, it seems unlikely that the transcription observed is entirely the result of read-through from the promoters on the vector backbone. Thus, it would seem that regulatory regions within the PRPS are responsible for expression. The regulation of genes in the PRPS is not well-understood. Some studies from native systems indicate constitutive expression of the PR (Martinez et al., 2007) while other studies have revealed increased expression in the light (Giovannoni et al., 2005a) and yet others have demonstrated increased expression in the dark (Kimura et al., 2011). While numerous studies have related the importance of carbon availability on the effect of PR (Steindler et al., 2011), no reports have demonstrated differential expression resulting from carbon concentration (Gomez-Consarnau et al., 2007; Martinez et al., 2007; Gomez-Consarnau et al., 2010; Steindler et al., 2011). These results indicate that much is still to be learned about the strategies for regulation of PR expression.

Following up on the observed growth effects of a PRPS in *P. putida* reported in Chapter 3, three vectors possessing two unique photosystems (pSHF10_19P19/pSJ2B6 and pS41B09) have demonstrated have a light-dependent growth yield increase. Common to all of

these systems was an observed dependence on the concentration of carbon. However, the various constructs displayed differences in the observed magnitude of the effect and the carbon concentration at which the effect was present; an increased yield was observed for *P. putida* pSJ2B6 at a glucose concentration of 100 uM, while the glucose concentration below 10 uM was required for a significant effect in *P. putida* pSHF10_19P19 and *P. putida* pS41B09. In addition, the maximum observed ratio of light to dark yield was greater than ten for *P. putida* pSJ2B6 (16.0 ± 3.8), while this value was around six for the other constructs (6.5 ± 2.3 for pS41B09, 5.3 ± 1.3 for pSHF10_19P19). These numbers point to possible differences in net efficiencies of the PRPS. Since the photosystems are identical for pSHF10_19P19 and pSJ2B6 and they are nearly identical in the vector junction at the 5' end of the PRPS (Figure 4-1), the expression of the photosystems is probably quite similar. This points to differences in the remaining portion of the environmental DNA contained on the large insert of pSHF10_19P19 as a likely cause for the differences in the response to light. One possibility is the burden or toxicity associated with the expression the genes contained on the remaining 34 kb. This would be consistent with the similarities in response observed between *P. putida* pSHF10_19P19 and *P. putida* pS41B09.

The differences between *P. putida* pSJ2B6 and *P. putida* pSCCFOS implicate the PRPS in whole as the cause of the light-based increase in growth yield (Chapter 3). However, direct evidence relating this effect directly to the proton pumping action of the PR has not yet been demonstrated. Likewise, the expression of a functional proton pump from pS41B09 has not been confirmed. pS41B09 contains two rhodopsin proteins; PR#1 aligns closely to other PR and is predicted to be a blue variant based on the tuning residue (Riedel et al., 2010), and PR#2 is most similar to xanthorhodopsin from *Salinibacter ruber* (Man et al., 2003). However, the absence of the Schiff-base forming lysine residue raises questions about the functionality of PR#2 (McCarren and DeLong, 2007). Thus, follow up experiments are required to confirm that PR function is responsible for the growth effects seen in all constructs, to identify if one or both of

the rhodopsins of pS41B09 is the cause of the growth yield increase, and to determine if burden of unnecessary DNA results in a diminished effect.

As described above, only pSJ2B6 and pSHF10_19P19 constructs contain the PRPS on the end of the insert DNA. All other PRPS are located directly in the middle of the insert, and as a result, native regulation from within the environmental insert is likely the reason for expression in all of these systems. Since a positive effect was observed in pS41B09, differences in expression level caused by substantial transcription of the PRPS from the promoters for the *cat* and *lacZ* genes upstream of the PR do not seem relevant. Testing pSHF10_25F10, which would likely be controlled solely by internal regulatory regions, is a possible way to explore this issue. Since other genes present on the insert may confound the results, a negative result for the pSHF10_25F10 would not indicate that expression of PR from the gene cluster is the issue. However, a positive result would likely indicate that the expression from internal regulator regions is sufficient. Pending the results seen in this system, the role of expression levels and metabolite utilization for the onset of the observed growth increase as discussed in Chapter 3 could be evaluated.

The final strain tested, *P. putida* pS55B11 does not show the light-based increase observed in the other PRPS-containing strains of *P. putida*. In fact, *P. putida* pS55B11 shows decreased growth in the light which occurs with and without the addition of exogenous retinal. While there is a possibility that the methanol vehicle was the cause of the decreased growth in the light, this does not seem likely as previous experiments with methanol did not demonstrate a detrimental effect on growth in the light or dark (data not shown). The pS55B11 vector is quite large (in excess of 20 kb larger than the other photosystems tested). It is quite plausible that the extra genes on the vector are causing the increased sensitivity to the light observed for this construct. The PRPS should be isolated and confirmed for functionality in the *E. coli* over expression system. Then, a direct comparison of growth curves could be made to determine if the

phenotypic differences exist because of the genes outside the PRPS or because of the some property of the PRPS itself. The pS55B11 photosystem is similar to the pSHF10_10P19 photosystem with two primary differences. First, the PR of pS55B11 is predicted to be a green variant opposed to the blue variant in pSHF10_19P19. In general, green variants display fast photocycle kinetics (McCarren and DeLong, 2007), so as long as a functional photosystem is formed it is likely to be just as effective at proton pumping if not more. Second, the pS55B11 PRPS lacks the *idi* gene, which is not strictly necessary for retinal synthesis, but has been demonstrated to increase production of isoprenoids (Man et al., 2003). However, this gene was not required for the positive effect observed in pS41B09 and is not likely to be contributing to the negative response observed in pS55B11, which is reinforced by the similarities of the growth with and without retinal.

The proven context of the *P. putida* MBD1 host provides the opportunity to explore additional photosystems to understand functional differences that may arise due to variations in the PR and retinal synthesis genes. Other vector constructs already conjugated into *P. putida* could be explored further to provide additional information. For instance, pSHF10_25F10 is very similar to HF10_19P19 and should be able to confirm the result of pSJ2B6 and pSHF10_19P19, pending suitable expression from the middle region of the insert. The pS31A08 and the pS60D04 vectors would allow decoupling of the PR from the carotenoid synthesis genes to pinpoint the source of the observed effects. However, difficulty in generating the pS31A08 exconjugant and the excessive size of the inserts introduces confounding factors into the analysis of the experimental results.

A better approach to studying variability in the system components may be to introduce the decoupled retinal synthesis and PR genes into the host independently. Using precise deletions generated by lambda red one-step gene replacement recombination techniques (Kajiwara et al., 1997) gives a means to finely control the PRPS components with minimal effect to the non-

targeted genes. This approach could be used to delete the PR gene from the PRPS of the pSJ2B6 system to verify that the rhodopsin is responsible for the observed phenotype. Alternatively, using a retinal synthesis system pieced together from the individual components [Michael Lee unpublished work (DeLong Lab, MIT), (Datsenko and Wanner, 2000)] could also be used as a retinal production background for testing alternative PR variants. This testing can expand beyond PR sequences to other ion-pumping rhodopsins including the proton pumps xanthorhodopsin, actinorhodopsin, and bacteriorhodopsin as well as other ion pumps such as the chloride translocating halorhodopsin. The genetic systems available to *P. putida* allow for a chromosomal incorporation of one component (Kim et al., 2008) and complementation of the other component using a plasmid system (Martinez et al., 2004). Similar to studying variants in the PR, differences in the retinal synthesis gene cluster can be tested using variations in the genetic constructs.

Testing the effect of the PRPS in alternate hosts, such as the *P. atlantica* exconjugant strains, will provide more information about the importance of the metabolic and physiological background on PRPS utilization. *P. atlantica* pSJ2B6 provides an optimal starting point for these studies because of the complete photosystem and the lack confounding variables. As with *P. putida*, transcription was observed in *P. atlantica*, but retinal synthesis and integral membrane protein were not able to be verified. *P. atlantica* provides an opportunity to study the PRPS in a marine bacteria to continue developing our understanding of how this ubiquitous light-harvesting complex influences microbial physiology and ecology.

Conclusion

In this work, we demonstrated the successful incorporation of five PRPS-containing constructs into *Pseudomonas putida* and *Pseudoalteromonas atlantica*, and we presented evidence for transcription of the PR for each of the five PRPS in both hosts. Growth of *P. putida* in low DOC media with two constructs, pSHF10_19P19 and pS41B09, demonstrated the same qualitative light-dependent growth yield increase observed for *P. putida* pSJ2B6 (Chapter 3, this

thesis). The result of *P. putida* pS41B09 demonstrates that the *idi* gene encoding the isopentenyl diphosphate isomerase is not required for the observed light-based growth effect and that expression from regulatory regions native to the PRPS is likely sufficient to produce the observed light-dependent growth effect. The *P. putida* system provides a platform for evaluating the functional differences of a wide variety of PRPS constructs or PR variants.

Chapter 5: Conclusion

Rhodopsin-based phototrophy presents an opportunity for harnessing vastly abundant solar energy with the use of a relatively simple biological system. Unlike the complicated photosystems of oxygenic photosynthesis which require multi-protein complexes, multiple cofactors, and numerous support proteins and biosynthetic pathways, rhodopsin phototrophy only requires a single membrane protein and one relatively simple small molecule cofactor (Bagdasarian et al., 1981; Lushnikov et al., 1985; Olekhnovich and Fomichev, 1994). The cost for this simplicity is efficiency and reducing potential. However, for conditions in which reducing potential is not needed, the simplicity and the minimal burden of photosystem synthesis and maintenance may justify the lower energetic efficiency.

A completely functional rhodopsin photosystem can be formed using as few as six genes, *crtEIBY*, *blh*, and the PR gene (Oesterhelt and Stoeckenius, 1971; Beja et al., 2000b). In this thesis, I described the subcloning and functional characterization of a seven gene PRPS, including the unnecessary isopentenyl isomerase (*idi*). These seven genes were sufficient to form a functional photosystem when overexpressed in *E. coli* (Chapter 2 this work). The absorbance spectrum of membranes with the retinylidene protein confirmed the PR to be a blue variant as expected (Sabehi et al., 2005; Martinez et al., 2007). The isolated PRPS also confirmed all of the attributes previously described for the for the large-insert metagenomic clone from which it was isolated (Martinez et al., 2007), including retinal synthesis, light-driven proton pumping, and photophosphorylation.

Proteorhodopsin expression has been demonstrated in several hosts. Expression in *E. coli* originally confirmed the expected function of PR (Martinez et al., 2007) and continues to be the choice organism for checking function of PR variants (Beja et al., 2000b). Functional PR has

also been demonstrated in *Shewanella oneidensis* (Sabehi et al., 2003; Giovannoni et al., 2005a; Sabehi et al., 2005; Gomez-Consarnau et al., 2007; Martinez et al., 2007; Gomez-Consarnau et al., 2010). In this thesis work, transcription of PR has been demonstrated in *Pseudomonas putida* and *Pseudoalteromonas atlantica* (Chapters 3 and 4) extending the range of gamma-proteobacteria hosts. Additional studies are needed to evaluate the full breadth of diversity of strains which can express the PR.

The PRPS clearly plays an important ecological role. The abundance of PR in the marine environment (Hunt et al., 2010; Johnson et al., 2010) and the diversity of taxa harboring the PRPS (Sabehi et al., 2003; Venter et al., 2004; Sharma et al., 2006; McCarren and DeLong, 2007) suggest a physiological function of profound importance. The modularity and mobility of the PRPS and high rates of horizontal gene transfer indicate that the benefits of PRPS are easily acquired by a range of hosts (de la Torre et al., 2003; Frigaard et al., 2006; McCarren and DeLong, 2007). Although the empirical evidence for the utility of the photosystem is apparent from metagenomic analysis, microbial physiology studies are needed to evaluate the mechanisms leading to the advantage conferred by the PR.

Similar to the phototrophic role of bacteriorhodopsin in *Halobacterium salinarum* (Sabehi et al., 2005; Sharma et al., 2006; Martinez et al., 2007; McCarren and DeLong, 2007), the energetic benefits of the photosystem have been clearly demonstrated for heterotrophic marine isolates which display improved growth (Oesterhelt and Krippahl, 1973; Oesterhelt and Stoeckenius, 1973; Danon and Stoeckenius, 1974; Rogers and Morris, 1978), survival (Gomez-Consarnau et al., 2007), and ATP production and decreased respiration (Gomez-Consarnau et al., 2010). In all of the examples listed, energy limitation due the reduced capacity for respiration of organic carbon sources (either by limiting oxygen or dissolved organic carbon) is a necessity for light-based contributions from the rhodopsin photosystems; conditions in which ample carbon and oxygen are present, corresponding to rapid growth rates, do not show utility from the PRPS.

Rhodopsin-based phototropy obviously plays an important role for the strains which have been found harboring the photosystem, however, the question of the universal applicability of the photosystem is not as clear. Heterologous expression of PR has demonstrated that the protein is functional in heterologous hosts, pumping protons to produce proton motive force (PMF) which has been demonstrated to be suitable for the generation of ATP (Steindler et al., 2011) and powering flagellar motility (Martinez et al., 2007) and transport systems (Walter et al., 2007). However, the physiological utilization of this extra energy supplied from the PRPS for the purpose of conferring a fitness advantage has been more elusive. Extended survival has been demonstrated (Johnson et al., 2010) which is presumably caused by the supply of ATP during times of depletion. Increased substrate uptake was demonstrated (Walter et al., 2007; Johnson et al., 2010) which could also serve a competitive advantage. However, for photoheterotrophy to be broadly applicable to biotechnological metabolic engineering applications, the energy derived from light must be applied to increase the yield of carbon compounds. As observed with environmental isolates, limitations to respiratory energy are common to all scenarios in which the PRPS function is observed and clearly beneficial to the host organism (Johnson et al., 2010). In addition, for many of the assays employed for observing the effects of the PRPS in heterologous hosts, high levels of expression are also required, posing a potential problem for the balance between burden from expression and benefit from generated PMF.

Despite lack of inducible control of expression and confirmation of the retinylidene protein, growth of PRPS-containing *P. putida* in minimal media with low dissolved organic carbon demonstrated a light-dependent increase in growth yield (Chapter 3 this work). A control strain without the PRPS did not demonstrate any light-dependent growth effects, but did display a higher yield than the PRPS-containing strain when grown in the dark. Growth in the light with the PRPS essentially recovered the growth deficit related the PRPS observed for dark cultures. The light-based growth effect was dependent on the concentration of dissolved organic carbon in

the growth media. With the PRPS at low carbon concentrations, a 10-fold increase in growth yield was observed in the light over the dark; at glucose concentrations of 1.1 mM, this effect was eliminated. This result further substantiates previously observed dependencies for low carbon concentrations (Martinez et al., 2007; Walter et al., 2007; Hunt et al., 2010), low respiration rates, or low growth rates (Gomez-Consarnau et al., 2007) for rhodopsin-based improvements to growth yield. Obviously, the interaction between PR and respiratory proton pumping is important for the physiological effects from PR. Additional studies are needed to understand how the factors of PR expression levels, growth rate, and respiration rate individually contribute to this effect.

A preliminary survey of PRPS-containing vectors from marine metagenomic libraries in *P. putida* demonstrated the light-based growth yield increase for two additional photosystems including a different PRPS lacking the *idi* gene, proving that the observed effect does not require this isomerase (Chapter 4 this work). Systems demonstrating the light-dependent yield effect displayed different carbon concentration thresholds. This may indicate differences in the cost-benefit ratio of the constructs which contain differences in genes unrelated to the PRPS. Regardless of the reason for the differences between the photosystems, this work demonstrates an opportunity to explore the large space of variants in PR and retinal synthesis genes. Expanding the set of available tools will become increasingly important as work in the field moves into optimization and application of the technology.

Additional work is needed to elucidate the exact nature of and mechanisms responsible for the observed growth yield effect. The system is now well-situated to investigate the flux of the metabolic pathways used by the host organism and the possible redistribution of carbon flux to facilitate the increased growth yield (Rogers and Morris, 1978). With an understanding of the stoichiometry and flux of pathways utilized with various substrates and under various growth conditions, it will be possible to understand the limitations overcome by PR which result the relevant physiological phenotypes. This will lead to the development of schemes and strategies in

which the energy captured by PR from light can be directed into the production of valuable products.

The PRPS provides interesting prospects for biotechnological application. However, target products will need to be carefully selected to utilize the specific benefits from PR. The product should be limited in yield production due to an energy limitation within the cell. To increase productivity from cell yield limitation, the products should be produced during low carbon growth conditions making it likely to be a secondary metabolite of stationary phase. Applications involving the conversion of an expensive substrate in which yield is critical would be good targets if the cell maintenance carbon requirements can be limited by the activity of the PR. Efforts in this area may require substantial engineering to produce a strain with suitable pathways for the production of the target compound and the utilization of the PRPS. Carbon fixation pathways would be tremendously interesting targets, but as the PR does not generate reducing potential, a readily available source of electron donor would be required.

In many situations, the higher efficiency and reducing potential generation of oxygenic photosynthetic systems may be preferred to the PRPS. However, specific instances in which the product pathway is not compatible with the conditions of photosynthesis may be well-suited using the PRPS. For example, the use of nitrogenase or hydrogenase enzymes requires a strict anaerobic condition which is not feasible in environments with active oxygenic photosynthesis (Fuhrer et al., 2005). The simplicity and mobility of the photosystem would also suggest applications with very specific requirements for the host; if the host cannot be changed, as would be the case for a compound with highly specific metabolic requirements or toxicity to other strains, moving the PRPS into the host strain could provide the ability to harness light energy where oxygenic photosynthesis cannot.

The discovery of proteorhodopsin nearly 12 years ago uncovered a process of profound importance to marine microbes (Vignais et al., 1985). Since that time, much has been learned

about the structure, function, and physiological effects of PR. Studies using PR as a tool (Beja et al., 2000b) will contribute to our understanding of basic cellular process interacting with proton motive force and membrane potential. As the understanding of this simple photosystem and its interaction with cellular energy metabolism continue to growth, so will the opportunities for using the PRPS to harvest solar radiation for driving biotechnological applications.

References Cited

Agranoff, B.W., Eggerer, H., Henning, U., and Lynen, F. (1959) Isopentenol Pyrophosphate Isomerase. *Journal of the American Chemical Society* **81**: 1254-1255.

Akagawamatsushita, M., Matsuo, M., Koga, Y., and Yamasato, K. (1992) Alteromonas-Atlantica Sp-Nov and Alteromonas-Carrageenovora Sp-Nov, Bacteria That Decompose Algal Polysaccharides. *International Journal of Systematic Bacteriology* **42**: 621-627.

Alshuth, T., Stockburger, M., Hegemann, P., and Oesterhelt, D. (1985) Structure of the Retinal Chromophore in Halorhodopsin - a Resonance Raman-Study. *Febs Letters* **179**: 55-59.

Altschul, S.F., Gish, W., Miller, W., Myers, E.W., and Lipman, D.J. (1990) Basic local alignment search tool. *J Mol Biol* **215**: 403-410.

Amann, R., Fuchs, B., Giovannoni, S.J., Ferriera, S., Johnson, J., Kravitz, S. et al. (2008) Direct Sequence Submission: marine gamma proteobacterium HTCC2148. In: GenBank: Accession # NZ_DS999223.

Amsden, J.J., Kralj, J.M., Bergo, V.B., Spudich, E.N., Spudich, J.L., and Rothschild, K.J. (2008) Different structural changes occur in blue- and green-proteorhodopsins during the primary photoreaction. *Biochemistry* **47**: 11490-11498.

Anderson, A.J., and Dawes, E.A. (1990) Occurrence, metabolism, metabolic role, and industrial uses of bacterial polyhydroxyalkanoates. *Microbiol Rev* **54**: 450-472.

Andersson, M., Malmerberg, E., Westenhoff, S., Katona, G., Cammarata, M., Wohri, A.B. et al. (2009) Structural dynamics of light-driven proton pumps. *Structure* **17**: 1265-1275.

Anton, J., Oren, A., Benlloch, S., Rodriguez-Valera, F., Amann, R., and Rossello-Mora, R. (2002) Salinibacter ruber gen. nov., sp. nov., a novel, extremely halophilic member of the Bacteria from saltern crystallizer ponds. *Int J Syst Evol Microbiol* **52**: 485-491.

Atamna-Ismaeel, N., Sabehi, G., Sharon, I., Witzel, K.P., Labrenz, M., Jurgens, K. et al. (2008) Widespread distribution of proteorhodopsins in freshwater and brackish ecosystems. *ISME J* **2**: 656-662.

Ausubel, F.M. (1987) *Current protocols in molecular biology*. Brooklyn, N.Y.

Media, Pa.: Greene Pub. Associates ;

J. Wiley, order fulfillment.

Baba, T., Ara, T., Hasegawa, M., Takai, Y., Okumura, Y., Baba, M. et al. (2006) Construction of Escherichia coli K-12 in-frame, single-gene knockout mutants: the Keio collection. *Mol Syst Biol* **2**: 2006 0008.

Bae, Y.S., Yang, J., Jin, S., Lee, S.Y., and Park, C.H. (1999) Optical CDMA system using bacteriorhodopsin for optical data storage. *Biotechnol Prog* **15**: 971-973.

Bagdasarian, M., Lurz, R., Ruckert, B., Franklin, F.C., Bagdasarian, M.M., Frey, J., and Timmis, K.N. (1981) Specific-purpose plasmid cloning vectors. II. Broad host range, high copy number, RSF1010-derived vectors, and a host-vector system for gene cloning in Pseudomonas. *Gene* **16**: 237-247.

Balashov, S.P., Imasheva, E.S., and Lanyi, J.K. (2006) Induced chirality of the light-harvesting carotenoid salinixanthin and its interaction with the retinal of xanthorhodopsin. *Biochemistry* **45**: 10998-11004.

Balashov, S.P., Imasheva, E.S., Wang, J.M., and Lanyi, J.K. (2008) Excitation energy-transfer and the relative orientation of retinal and carotenoid in xanthorhodopsin. *Biophys J* **95**: 2402-2414.

Balashov, S.P., Imasheva, E.S., Boichenko, V.A., Anton, J., Wang, J.M., and Lanyi, J.K. (2005) Xanthorhodopsin: a proton pump with a light-harvesting carotenoid antenna. *Science* **309**: 2061-2064.

Bamberg, E., Tittor, J., and Oesterhelt, D. (1993) Light-driven proton or chloride pumping by halorhodopsin. *Proc Natl Acad Sci U S A* **90**: 639-643.

Bartlett, D.H., Wright, M.E., and Silverman, M. (1988) Variable expression of extracellular polysaccharide in the marine bacterium Pseudomonas atlantica is controlled by genome rearrangement. *Proc Natl Acad Sci U S A* **85**: 3923-3927.

Bassler, B., Clifton, S.W., Fulton, L., Delehaunty, K., Fronick, C., Harrison, M. et al. (2007) Direct Sequence Submission: Vibrio harveyi ATCC BAA-1116. In: GenBank: Accession # NC_009784.

Beja, O., Spudich, E.N., Spudich, J.L., Leclerc, M., and DeLong, E.F. (2001) Proteorhodopsin phototrophy in the ocean. *Nature* **411**: 786-789.

Beja, O., Koonin, E.V., Aravind, L., Taylor, L.T., Seitz, H., Stein, J.L. et al. (2002) Comparative genomic analysis of archaeal genotypic variants in a single population and in two different oceanic provinces. *Appl Environ Microbiol* **68**: 335-345.

Beja, O., Suzuki, M.T., Koonin, E.V., Aravind, L., Hadd, A., Nguyen, L.P. et al. (2000a) Construction and analysis of bacterial artificial chromosome libraries from a marine microbial assemblage. *Environ Microbiol* **2**: 516-529.

Beja, O., Aravind, L., Koonin, E.V., Suzuki, M.T., Hadd, A., Nguyen, L.P. et al. (2000b) Bacterial rhodopsin: evidence for a new type of phototrophy in the sea. *Science* **289**: 1902-1906.

Belas, R., Bartlett, D., and Silverman, M. (1988) Cloning and Gene Replacement Mutagenesis of a Pseudomonas atlantica Agarase Gene. *Appl Environ Microbiol* **54**: 30-37.

Bender, C.L., Rangaswamy, V., and Loper, J. (1999) POLYKETIDE PRODUCTION BY PLANT-ASSOCIATED PSEUDOMONADS1. *Annual Review of Phytopathology* **37**: 175-196.

Bennett, P.M., Grinsted, J., and Richmond, M.H. (1977) Transposition of TnA does not generate deletions. *Mol Gen Genet* **154**: 205-211.

Berg, H.C. (2003) The rotary motor of bacterial flagella. *Annu Rev Biochem* **72**: 19-54.

Berg, H.C., Manson, M.D., and Conley, M.P. (1982) Dynamics and energetics of flagellar rotation in bacteria. *Symp Soc Exp Biol* **35**: 1-31.

Bergey, D.H., and Holt, J.G. (1984) *Bergey's manual of systematic bacteriology*. Baltimore: Williams & Wilkins.

Bergo, V., Amsden, J.J., Spudich, E.N., Spudich, J.L., and Rothschild, K.J. (2004) Structural changes in the photoactive site of proteorhodopsin during the primary photoreaction. *Biochemistry* **43**: 9075-9083.

Bergo, V.B., Sineshchekov, O.A., Kralj, J.M., Partha, R., Spudich, E.N., Rothschild, K.J., and Spudich, J.L. (2009) His-75 in proteorhodopsin, a novel component in light-driven proton translocation by primary pumps. *J Biol Chem* **284**: 2836-2843.

Beuttler, H., Hoffmann, J., Jeske, M., Hauer, B., Schmid, R.D., Altenbuchner, J., and Urlacher, V.B. (2011) Biosynthesis of zeaxanthin in recombinant Pseudomonas putida. *Appl Microbiol Biotechnol* **89**: 1137-1147.

Beytia, E.D., and Porter, J.W. (1976) Biochemistry of polyisoprenoid biosynthesis. *Annu Rev Biochem* **45**: 113-142.

Bielawski, J.P., Dunn, K.A., Sabehi, G., and Beja, O. (2004) Darwinian adaptation of proteorhodopsin to different light intensities in the marine environment. *Proc Natl Acad Sci U S A* **101**: 14824-14829.

Bierman, M., Logan, R., O'Brien, K., Seno, E.T., Rao, R.N., and Schoner, B.E. (1992) Plasmid cloning vectors for the conjugal transfer of DNA from Escherichia coli to Streptomyces spp. *Gene* **116**: 43-49.

Blankenship, R.E. (1992) Origin and early evolution of photosynthesis. *Photosynth Res* **33**: 91-111.

Blattner, F.R., Plunkett, G., 3rd, Bloch, C.A., Perna, N.T., Burland, V., Riley, M. et al. (1997) The complete genome sequence of Escherichia coli K-12. *Science* **277**: 1453-1462.

Bogomolni, R.A., and Spudich, J.L. (1982) Identification of a third rhodopsin-like pigment in phototactic Halobacterium halobium. *Proc Natl Acad Sci U S A* **79**: 6250-6254.

Bogomolni, R.A., Stoeckenius, W., Szundi, I., Perozo, E., Olson, K.D., and Spudich, J.L. (1994) Removal of transducer HtrI allows electrogenic proton translocation by sensory rhodopsin I. *Proc Natl Acad Sci U S A* **91**: 10188-10192.

Boichenko, V.A., Wang, J.M., Anton, J., Lanyi, J.K., and Balashov, S.P. (2006) Functions of carotenoids in xanthorhodopsin and archaerhodopsin, from action spectra of photoinhibition of cell respiration. *Biochim Biophys Acta* **1757**: 1649-1656.

Bott, R.R.B.C.A., Jensen, R.B.H., Kelemen, B.R.M.P.C.A., Ward, I.I.D.E.L.A.C.A., and Whited, G.M.B.C.A. (2008) Composition Comprising Various Proteorhodopsins and/or Bacteriorhodopsins and Use Thereof. In. US.

Bowman, J., Ferriera, S., Johnson, J., Kravitz, S., Halpern, A., Remington, K.A. et al. (2006) Direct Sequence Submission: Psychroflexus torquis ATCC 700755. In: GenBank: Accession # AAPR01000000.

Brenner, M. (2006) Engineering Microorgansims for Energy Production. In. Energy, U.S.D.o. (ed). McLean, Virginia: MITRE Corporation, pp. 1-92.

Brock, T.D., and Petersen, S. (1976) Some effects of light on the viability of rhodopsin-containing halobacteria. *Arch Microbiol* **109**: 199-200.

Caballero, A., Esteve-Nunez, A., Zylstra, G.J., and Ramos, J.L. (2005) Assimilation of nitrogen from nitrite and trinitrotoluene in Pseudomonas putida JLR11. *J Bacteriol* **187**: 396-399.

Campbell, B.J., Waidner, L.A., Cottrell, M.T., and Kirchman, D.L. (2008) Abundant proteorhodopsin genes in the North Atlantic Ocean. *Environ Microbiol* **10**: 99-109.

Capaldi, R.A., and Aggeler, R. (2002) Mechanism of the F(1)F(0)-type ATP synthase, a biological rotary motor. *Trends Biochem Sci* **27**: 154-160.

Che, A., Shetty, R., and Knight, T. (2008). Preparing electrocompetent cells [OpenWetWare (wiki)]. URL http://openwetware.org/wiki/Knight:Preparing_electrocompetent_cells

Copeland, A., Lucas, S., Lapidus, A., Barry, K., Detter, J.C., Glavina Del Rio, T. et al. (2006) Direct Sequence Submission: Pseudoalteromonas atlantica T6c. In: GenBank: Accession # NC_008228.

Costa-Ramos, C., and Rowley, A.F. (2004) Effect of extracellular products of Pseudoalteromonas atlantica on the edible crab Cancer pagurus. *Appl Environ Microbiol* **70**: 729-735.

Cottrell, M.T., and Kirchman, D.L. (2009) Photoheterotrophic microbes in the Arctic Ocean in summer and winter. *Appl Environ Microbiol* **75**: 4958-4966.

Courtois, S., Cappellano, C.M., Ball, M., Francou, F.X., Normand, P., Helynck, G. et al. (2003) Recombinant environmental libraries provide access to microbial diversity for drug discovery from natural products. *Appl Environ Microbiol* **69**: 49-55.

Cunningham, F.X., Jr., Sun, Z., Chamovitz, D., Hirschberg, J., and Gantt, E. (1994) Molecular structure and enzymatic function of lycopene cyclase from the cyanobacterium Synechococcus sp strain PCC7942. *Plant Cell* **6**: 1107-1121.

Dagley, S. (1971) Catabolism of aromatic compounds by micro-organisms. *Adv Microb Physiol* **6**: 1-46.

Danon, A., and Stoeckenius, W. (1974) Photophosphorylation in Halobacterium halobium. *Proc Natl Acad Sci U S A* **71**: 1234-1238.

Datsenko, K.A., and Wanner, B.L. (2000) One-step inactivation of chromosomal genes in Escherichia coli K-12 using PCR products. *Proc Natl Acad Sci U S A* **97**: 6640-6645.

de la Torre, J.R., Christianson, L.M., Beja, O., Suzuki, M.T., Karl, D.M., Heidelberg, J., and DeLong, E.F. (2003) Proteorhodopsin genes are distributed among divergent marine bacterial taxa. *Proc Natl Acad Sci U S A* **100**: 12830-12835.

Dejonghe, W., Boon, N., Seghers, D., Top, E.M., and Verstraete, W. (2001) Bioaugmentation of soils by increasing microbial richness: missing links. *Environ Microbiol* **3**: 649-657.

del Castillo, T., and Ramos, J.L. (2007) Simultaneous catabolite repression between glucose and toluene metabolism in Pseudomonas putida is channeled through different signaling pathways. *J Bacteriol* **189**: 6602-6610.

del Castillo, T., Ramos, J.L., Rodriguez-Herva, J.J., Fuhrer, T., Sauer, U., and Duque, E. (2007) Convergent peripheral pathways catalyze initial glucose catabolism in Pseudomonas putida: genomic and flux analysis. *J Bacteriol* **189**: 5142-5152.

DeLong, E.F., Preston, C.M., Mincer, T., Rich, V., Hallam, S.J., Frigaard, N.U. et al. (2006) Community genomics among stratified microbial assemblages in the ocean's interior. *Science* **311**: 496-503.

Delong, E.F.C.M.A., and Beja, O.M. (2009) Light-driven energy generation using proteorhodopsin. In. US.

Delong, E.F.M.C.A., and Beja, O.M.C.A. (2003) Light-driven energy generation using proteorhodopsin. In. US.

Devroe, E.J.M.M.A., Berry, D.A.B.M.A., Afeyan, N.B.L.M.A., Robertson, D.E.B.M.A., Skraly, F.A.W.M.A., and Ridley, C.P.A.M.A. (2009) Engineered Light-Harvesting Organisms. In. US.

Dioumaev, A.K., Wang, J.M., Balint, Z., Varo, G., and Lanyi, J.K. (2003) Proton transport by proteorhodopsin requires that the retinal Schiff base counterion Asp-97 be anionic. *Biochemistry* **42**: 6582-6587.

Dioumaev, A.K., Brown, L.S., Shih, J., Spudich, E.N., Spudich, J.L., and Lanyi, J.K. (2002) Proton transfers in the photochemical reaction cycle of proteorhodopsin. *Biochemistry* **41**: 5348-5358.

Drachev, L.A., Kaulen, A.D., Ostroumov, S.A., and Skulachev, V.P. (1974a) Electrogenesis by bacteriorhodopsin incorporated in a planar phospholipid membrane. *FEBS Lett* **39**: 43-45.

Drachev, L.A., Jasaitis, A.A., Kaulen, A.D., Kondrashin, A.A., Liberman, E.A., Nemecek, I.B. et al. (1974b) Direct measurement of electric current generation by cytochrome oxidase, H+-ATPase and bacteriorhodopsin. *Nature* **249**: 321-324.

Eilers, H., Pernthaler, J., and Amann, R. (2000) Succession of pelagic marine bacteria during enrichment: a close look at cultivation-induced shifts. *Appl Environ Microbiol* **66**: 4634-4640.

Eisenberg, R.C., and Dobrogosz, W.J. (1967) Gluconate metabolism in Escherichia coli. *J Bacteriol* **93**: 941-949.

Espinosa-Urgel, M., Salido, A., and Ramos, J.L. (2000) Genetic analysis of functions involved in adhesion of Pseudomonas putida to seeds. *J Bacteriol* **182**: 2363-2369.

Fernandez, M., Duque, E., Pizarro-Tobias, P., Van Dillewijn, P., Wittich, R.M., and Ramos, J.L. (2009) Microbial responses to xenobiotic compounds. Identification of genes that allow Pseudomonas putida KT2440 to cope with 2,4,6-trinitrotoluene. *Microb Biotechnol* **2**: 287-294.

Flett, F., Mersinias, V., and Smith, C.P. (1997) High efficiency intergeneric conjugal transfer of plasmid DNA from Escherichia coli to methyl DNA-restricting streptomycetes. *FEMS Microbiol Lett* **155**: 223-229.

Franklin, F.C., Bagdasarian, M., Bagdasarian, M.M., and Timmis, K.N. (1981) Molecular and functional analysis of the TOL plasmid pWWO from Pseudomonas putida and cloning of genes for the entire regulated aromatic ring meta cleavage pathway. *Proc Natl Acad Sci U S A* **78**: 7458-7462.

Friedrich, T., Geibel, S., Kalmbach, R., Chizhov, I., Ataka, K., Heberle, J. et al. (2002) Proteorhodopsin is a light-driven proton pump with variable vectoriality. *J Mol Biol* **321**: 821-838.

Frigaard, N.U., Martinez, A., Mincer, T.J., and DeLong, E.F. (2006) Proteorhodopsin lateral gene transfer between marine planktonic Bacteria and Archaea. *Nature* **439**: 847-850.

Fuhrer, T., Fischer, E., and Sauer, U. (2005) Experimental identification and quantification of glucose metabolism in seven bacterial species. *J Bacteriol* **187**: 1581-1590.

Fuhrman, J.A., Schwalbach, M.S., and Stingl, U. (2008) Proteorhodopsins: an array of physiological roles? *Nat Rev Microbiol* **6**: 488-494.

Fujisaki, S., Nishino, T., Katsuki, H., Hara, H., Nishimura, Y., and Hirota, Y. (1989) Isolation and characterization of an Escherichia coli mutant having temperature-sensitive farnesyl diphosphate synthase. *J Bacteriol* **171**: 5654-5658.

Fung, D.C., and Berg, H.C. (1995) Powering the flagellar motor of Escherichia coli with an external voltage source. *Nature* **375**: 809-812.

Gabel, C.V., and Berg, H.C. (2003) The speed of the flagellar rotary motor of Escherichia coli varies linearly with protonmotive force. *Proc Natl Acad Sci U S A* **100**: 8748-8751.

Gauthier, G., Gauthier, M., and Christen, R. (1995) Phylogenetic analysis of the genera Alteromonas, Shewanella, and Moritella using genes coding for small-subunit rRNA sequences and division of the genus Alteromonas into two genera, Alteromonas (emended) and Pseudoalteromonas gen. nov., and proposal of twelve new species combinations. *Int J Syst Bacteriol* **45**: 755-761.

Gertz, E.M., Yu, Y.K., Agarwala, R., Schaffer, A.A., and Altschul, S.F. (2006) Composition-based statistics and translated nucleotide searches: improving the TBLASTN module of BLAST. *BMC Biol* **4**: 41.

Giovannoni, S.J., Hayakawa, D.H., Tripp, H.J., Stingl, U., Givan, S.A., Cho, J.C. et al. (2008) The small genome of an abundant coastal ocean methylotroph. *Environ Microbiol* **10**: 1771-1782.

Giovannoni, S.J., Bibbs, L., Cho, J.C., Stapels, M.D., Desiderio, R., Vergin, K.L. et al. (2005a) Proteorhodopsin in the ubiquitous marine bacterium SAR11. *Nature* **438**: 82-85.

Giovannoni, S.J., Cho, J.C., Ferriera, S., Johnson, J., Kravitz, S., Halpern, A. et al. (2006a) Direct Sequence Submission: gamma proteobacterium HTCC2207. In: GenBank: Accession # CH672396.

Giovannoni, S.J., Cho, J.C., Ferriera, S., Johnson, J., Kravitz, S., Halpern, A. et al. (2006b) Direct Sequence Submission: alpha proteobacterium HTCC2255. In: GenBank: Accession # NZDS022282.

Giovannoni, S.J., Tripp, H.J., Givan, S., Podar, M., Vergin, K.L., Baptista, D. et al. (2005b) Genome streamlining in a cosmopolitan oceanic bacterium. *Science* **309**: 1242-1245.

Giuliano, G., Pollock, D., and Scolnik, P.A. (1986) The gene crtI mediates the conversion of phytoene into colored carotenoids in Rhodopseudomonas capsulata. *J Biol Chem* **261**: 12925-12929.

Gomez-Consarnau, L., Gonzalez, J.M., Coll-Llado, M., Gourdon, P., Pascher, T., Neutze, R. et al. (2007) Light stimulates growth of proteorhodopsin-containing marine Flavobacteria. *Nature* **445**: 210-213.

Gomez-Consarnau, L., Akram, N., Lindell, K., Pedersen, A., Neutze, R., Milton, D.L. et al. (2010) Proteorhodopsin phototrophy promotes survival of marine bacteria during starvation. *PLoS Biol* **8**: e1000358.

Gonzalez, J.M., Fernandez-Gomez, B., Fernandez-Guerra, A., Gomez-Consarnau, L., Sanchez, O., Coll-Llado, M. et al. (2008) Genome analysis of the proteorhodopsin-containing marine bacterium Polaribacter sp. MED152 (Flavobacteria). *Proc Natl Acad Sci U S A* **105**: 8724-8729.

Gorenflo, V., Schmack, G., Vogel, R., and Steinbuchel, A. (2001) Development of a process for the biotechnological large-scale production of 4-hydroxyvalerate-containing polyesters and characterization of their physical and mechanical properties. *Biomacromolecules* **2**: 45-57.

Gosmann, B., and Rehm, H.J. (1986) Oxygen-Uptake of Microorganisms Entrapped in Ca-Alginate. *Applied Microbiology and Biotechnology* **23**: 163-167.

Gottschalk, G. (1986) *Bacterial metabolism*. New York: Springer-Verlag.

Gourdon, P., Alfredsson, A., Pedersen, A., Malmerberg, E., Nyblom, M., Widell, M. et al. (2008) Optimized in vitro and in vivo expression of proteorhodopsin: a seven-transmembrane proton pump. *Protein Expr Purif* **58**: 103-113.

Greated, A., Lambertsen, L., Williams, P.A., and Thomas, C.M. (2002) Complete sequence of the IncP-9 TOL plasmid pWW0 from Pseudomonas putida. *Environ Microbiol* **4**: 856-871.

Greene, R.V., MacDonald, R.E., and Perrault, G.J. (1980) Action spectra determined with tunable dye laser light for light-induced proton efflux and uptake in membrane vesicles of Halobacterium halobium. *J Biol Chem* **255**: 3245-3247.

Groleau, D., and Yaphe, W. (1977) Enzymatic hydrolysis of agar: purification and characterization of beta-neoagarotetraose hydrolase from Pseudomonas atlantica. *Can J Microbiol* **23**: 672-679.

Guiney, D.G., and Yakobson, E. (1983) Location and nucleotide sequence of the transfer origin of the broad host range plasmid RK2. *Proc Natl Acad Sci U S A* **80**: 3595-3598.

Hagstrom, A., Ferriera, S., Johnson, J., Kravitz, S., Beeson, K., Sutton, G. et al. (2007) Direct Sequence Submission: flavobacteria bacterium BAL38. In: GenBank: Accession # AAXX01000000.

Hagstrom, A.J., Ferriera, S., Johnson, J., Kravitz, S., Halpern, A., Remington, K. et al. (2006) Direct Sequence Submission: Photobacterium sp. SKA34. In: GenBank: Accession # NZ_AAOU00000000.

Hahn, F.M., Hurlburt, A.P., and Poulter, C.D. (1999) Escherichia coli open reading frame 696 is idi, a nonessential gene encoding isopentenyl diphosphate isomerase. *J Bacteriol* **181**: 4499-4504.

Hanahan, D. (1983) Studies on transformation of Escherichia coli with plasmids. *J Mol Biol* **166**: 557-580.

Hansen, L.H., Sorensen, S.J., and Jensen, L.B. (1997) Chromosomal insertion of the entire Escherichia coli lactose operon, into two strains of Pseudomonas, using a modified mini-Tn5 delivery system. *Gene* **186**: 167-173.

Hao, W., and Fong, H.K. (1999) The endogenous chromophore of retinal G protein-coupled receptor opsin from the pigment epithelium. *J Biol Chem* **274**: 6085-6090.

Haupts, U., Haupts, C., and Oesterhelt, D. (1995) The photoreceptor sensory rhodopsin I as a two-photon-driven proton pump. *Proc Natl Acad Sci U S A* **92**: 3834-3838.

Haywood, G.W., Anderson, A.J., and Dawes, E.A. (1989) A survey of the accumulation of novel polyhydroxyalkanoates by bacteria. *Biotechnology Letters* **11**: 471-476.

Hempelmann, F., Holper, S., Verhoefen, M.K., Woerner, A.C., Kohler, T., Fiedler, S.A. et al. (2011) His75-Asp97 cluster in green proteorhodopsin. *J Am Chem Soc* **133**: 4645-4654.

Henderson, R. (1975) The structure of the purple membrane from Halobacterium halobium: analysis of the X-ray diffraction pattern. *J Mol Biol* **93**: 123-138.

Henderson, R., and Unwin, P.N. (1975) Three-dimensional model of purple membrane obtained by electron microscopy. *Nature* **257**: 28-32.

Henn, M.R., Young, S., Jaffe, D.B., Gnerre, S., Berlin, A., Heiman, D. et al. (2008) Direct Sequence Submission. In: GenBank.

Hibbing, M.E., Fuqua, C., Parsek, M.R., and Peterson, S.B. (2010) Bacterial competition: surviving and thriving in the microbial jungle. *Nat Rev Microbiol* **8**: 15-25.

Hoff, W.D., Jung, K.H., and Spudich, J.L. (1997) Molecular mechanism of photosignaling by archaeal sensory rhodopsins. *Annu Rev Biophys Biomol Struct* **26**: 223-258.

Hubbard, J.S., Rinehart, C.A., and Baker, R.A. (1976) Energy coupling in the active transport of amino acids by bacteriohodopsin-containing cells of Halobacterium holobium. *J Bacteriol* **125**: 181-190.

Huber, R., Kohler, T., Lenz, M.O., Bamberg, E., Kalmbach, R., Engelhard, M., and Wachtveitl, J. (2005) pH-dependent photoisomerization of retinal in proteorhodopsin. *Biochemistry* **44**: 1800-1806.

Hunt, K.A., Flynn, J.M., Naranjo, B., Shikhare, I.D., and Gralnick, J.A. (2010) Substrate-level phosphorylation is the primary source of energy conservation during anaerobic respiration of Shewanella oneidensis strain MR-1. *J Bacteriol* **192**: 3345-3351.

Imasheva, E.S., Balashov, S.P., Wang, J.M., Dioumaev, A.K., and Lanyi, J.K. (2004) Selectivity of retinal photoisomerization in proteorhodopsin is controlled by aspartic acid 227. *Biochemistry* **43**: 1648-1655.

Imasheva, E.S., Balashov, S.P., Wang, J.M., Smolensky, E., Sheves, M., and Lanyi, J.K. (2008) Chromophore interaction in xanthorhodopsin--retinal dependence of salinixanthin binding. *Photochem Photobiol* **84**: 977-984.

Imasheva, E.S., Shimono, K., Balashov, S.P., Wang, J.M., Zadok, U., Sheves, M. et al. (2005) Formation of a long-lived photoproduct with a deprotonated Schiff base in proteorhodopsin, and its enhancement by mutation of Asp227. *Biochemistry* **44**: 10828-10838.

Ingledew, W.J., and Poole, R.K. (1984) The respiratory chains of Escherichia coli. *Microbiol Rev* **48**: 222-271.

Iwamoto, M., Shimono, K., Sumi, M., and Kamo, N. (1999) Positioning proton-donating residues to the Schiff-base accelerates the M-decay of pharaonis phoborhodopsin expressed in Escherichia coli. *Biophysical Chemistry* **79**: 187-192.

Jensen, R.B.H., Kelemen, B.R.M.P.C.A., Ward, I.I.D.E.L.A.C.A., and Asato, A.E.W.H.I. (2008) Photochromic Material Comprising a Proteorhodopsin Apoprotein and a Retinal Analog. In. US.

Jensen, R.B.M.V.C.A., and Kelemen, B.M.P.C.A. (2005) Proteorhodopsin mutants with improved optical characteristics. In. US.

Jensen, R.B.M.V.C.A., Kelemen, B.R.M.P.C.A., McAuliffe, J.C.S.C.A., and Smith, W.C.T.C.A. (2004) Optical information carrier comprising immobilized proteorhodopsin. In. US.

Jensen, R.B.M.V.C.A., Kelemen, B.R.M.P.C.A., McAuliffe, J.C.S.C.A., and Smith, W.C.T.C.A. (2009) Method For Preparing Solid Materials Comprising Immobilized Proteorhodopsin. In. US.

Johnson, E.T., Baron, D.B., Naranjo, B., Bond, D.R., Schmidt-Dannert, C., and Gralnick, J.A. (2010) Enhancement of survival and electricity production in an engineered bacterium by light-driven proton pumping. *Appl Environ Microbiol* **76**: 4123-4129.

Juchem, T., Sanio, M., and Hampp, N. (2002) Bacteriorhodopsin modules for data processing with incoherent light. *Opt Lett* **27**: 1607-1609.

Jung, J.Y., Choi, A.R., Lee, Y.K., Lee, H.K., and Jung, K.H. (2008) Spectroscopic and photochemical analysis of proteorhodopsin variants from the surface of the Arctic Ocean. *FEBS Lett* **582**: 1679-1684.

Kajiwara, S., Fraser, P.D., Kondo, K., and Misawa, N. (1997) Expression of an exogenous isopentenyl diphosphate isomerase gene enhances isoprenoid biosynthesis in Escherichia coli. *Biochem J* **324 (Pt 2)**: 421-426.

Kanehisa, M., and Goto, S. (2000) KEGG: kyoto encyclopedia of genes and genomes. *Nucleic Acids Res* **28**: 27-30.

Karl, D.M., and Lukas, R. (1996) The Hawaii Ocean Time-series (HOT) program: Background, rationale and field implementation. *Deep-Sea Research Part Ii-Topical Studies in Oceanography* **43**: 129-156.

Kayushin, L.P., and Skulachev, V.P. (1974) Bacteriorhodopsin as an electrogenic proton pump: reconstitution of bacteriorhodopsin proteoliposomes generating delta psi and delta pH. *FEBS Lett* **39**: 39-42.

Kelly, F.X., Dapsis, K.J., and Lauffenburger, D.A. (1988) Effect of Bacterial Chemotaxis on Dynamics of Microbial Competition. *Microbial Ecology* **16**: 115-131.

Kim, S.Y., Waschuk, S.A., Brown, L.S., and Jung, K.H. (2008) Screening and characterization of proteorhodopsin color-tuning mutations in Escherichia coli with endogenous retinal synthesis. *Biochim Biophys Acta* **1777**: 504-513.

Kimura, H., Young, C.R., Martinez, A., and Delong, E.F. (2011) Light-induced transcriptional responses associated with proteorhodopsin-enhanced growth in a marine flavobacterium. *ISME J* **5**: 1641-1651.

Klippel, B., Lochner, A., Bruce, D.C., Davenport, K.W., Detter, C., Goodwin, L.A. et al. (2011) Complete genome sequences of Krokinobacter sp. strain 4H-3-7-5 and Lacinutrix sp. strain 5H-3-7-4, polysaccharide-degrading members of the family Flavobacteriaceae. *J Bacteriol* **193**: 4545-4546.

Klyszejko, A.L., Shastri, S., Mari, S.A., Grubmuller, H., Muller, D.J., and Glaubitz, C. (2008) Folding and assembly of proteorhodopsin. *J Mol Biol* **376**: 35-41.

Koh, E.Y., Atamna-Ismaeel, N., Martin, A., Cowie, R.O., Beja, O., Davy, S.K. et al. (2010) Proteorhodopsin-bearing bacteria in Antarctic sea ice. *Appl Environ Microbiol* **76**: 5918-5925.

Kralj, J.M., Spudich, E.N., Spudich, J.L., and Rothschild, K.J. (2008a) Raman spectroscopy reveals direct chromophore interactions in the Leu/Gln105 spectral tuning switch of proteorhodopsins. *J Phys Chem B* **112**: 11770-11776.

Kralj, J.M., Hochbaum, D.R., Douglass, A.D., and Cohen, A.E. (2011) Electrical spiking in Escherichia coli probed with a fluorescent voltage-indicating protein. *Science* **333**: 345-348.

Kralj, J.M., Bergo, V.B., Amsden, J.J., Spudich, E.N., Spudich, J.L., and Rothschild, K.J. (2008b) Protonation state of Glu142 differs in the green- and blue-absorbing variants of proteorhodopsin. *Biochemistry* **47**: 3447-3453.

Krebs, R.A., Alexiev, U., Partha, R., DeVita, A.M., and Braiman, M.S. (2002) Detection of fast light-activated H+ release and M intermediate formation from proteorhodopsin. *BMC Physiol* **2**: 5.

Kuhstoss, S., Richardson, M.A., and Rao, R.N. (1991) Plasmid cloning vectors that integrate site-specifically in Streptomyces spp. *Gene* **97**: 143-146.

Kung, M.C., Devault, D., Hess, B., and Oesterhelt, D. (1975) Photolysis of Bacterial Rhodopsin. *Biophysical Journal* **15**: 907-911.

Kuzuyama, T., and Seto, H. (2003) Diversity of the biosynthesis of the isoprene units. *Nat Prod Rep* **20**: 171-183.

Lail, K., Sikorski, J., Saunders, E., Lapidus, A., Glavina Del Rio, T., Copeland, A. et al. (2010) Complete genome sequence of Spirosoma linguale type strain (1). *Stand Genomic Sci* **2**: 176-185.

Lakatos, M., Lanyi, J.K., Szakacs, J., and Varo, G. (2003) The photochemical reaction cycle of proteorhodopsin at low pH. *Biophys J* **84**: 3252-3256.

Lami, R., Cottrell, M.T., Campbell, B.J., and Kirchman, D.L. (2009) Light-dependent growth and proteorhodopsin expression by Flavobacteria and SAR11 in experiments with Delaware coastal waters. *Environ Microbiol.*

Lanyi, J.K. (1986) Halorhodopsin: a light-driven chloride ion pump. *Annu Rev Biophys Biophys Chem* **15**: 11-28.

Lanyi, J.K. (1995) Bacteriorhodopsin as a model for proton pumps. *Nature* **375**: 461-463.

Lanyi, J.K. (2006) Proton transfers in the bacteriorhodopsin photocycle. *Biochim Biophys Acta* **1757**: 1012-1018.

Lanyi, J.K., and MacDonald, R.E. (1979) Light-induced transport in Halobacterium halobium. *Methods Enzymol* **56**: 398-407.

Latrach Tlemcani, L., Corroler, D., Barillier, D., and Mosrati, R. (2008) Physiological states and energetic adaptation during growth of Pseudomonas putida mt-2 on glucose. *Arch Microbiol* **190**: 141-150.

Lauro, F.M., McDougald, D., Thomas, T., Williams, T.J., Egan, S., Rice, S. et al. (2009) The genomic basis of trophic strategy in marine bacteria. *Proc Natl Acad Sci U S A* **106**: 15527-15533.

Leedjarv, A., Ivask, A., and Virta, M. (2008) Interplay of different transporters in the mediation of divalent heavy metal resistance in Pseudomonas putida KT2440. *J Bacteriol* **190**: 2680-2689.

Lemke, H.D., and Oesterhelt, D. (1981) Lysine 216 is a binding site of the retinyl moiety in bacteriorhodopsin. *FEBS Lett* **128**: 255-260.

Lenz, M.O., Huber, R., Schmidt, B., Gilch, P., Kalmbach, R., Engelhard, M., and Wachtveitl, J. (2006) First steps of retinal photoisomerization in proteorhodopsin. *Biophys J* **91**: 255-262.

Litvin, F.F., Boichenko, V.A., Balashov, S.P., and Dubrovakii, V.T. (1977) [Photoinduced inhibition and stimulation of respiration in cells of Halobacterium halobiums kinetics, action spectra, relationship to photoinduction of deltapH]. *Biofizika* **22**: 1062-1071.

Lozier, R.H., Bogomolni, R.A., and Stoeckenius, W. (1975) Bacteriorhodopsin: a light-driven proton pump in Halobacterium Halobium. *Biophys J* **15**: 955-962.

Lucas, S., Han, J., Lapidus, A., Bruce, D., Goodwin, L., Pitluck, S. et al. (2011) Direct Sequence Submission: Haliscomenobacter hydrossis DSM 1100. In: GenBank: Accession # NC_015510.

Luecke, H., Schobert, B., Richter, H.T., Cartailler, J.P., and Lanyi, J.K. (1999) Structure of bacteriorhodopsin at 1.55 A resolution. *J Mol Biol* **291**: 899-911.

Luecke, H., Schobert, B., Stagno, J., Imasheva, E.S., Wang, J.M., Balashov, S.P., and Lanyi, J.K. (2008) Crystallographic structure of xanthorhodopsin, the light-driven proton pump with a dual chromophore. *Proc Natl Acad Sci U S A* **105**: 16561-16565.

Luengo, J.M., Garcia, J.L., and Olivera, E.R. (2001) The phenylacetyl-CoA catabolon: a complex catabolic unit with broad biotechnological applications. *Mol Microbiol* **39**: 1434-1442.

Lushnikov, A.A., Andreevskaya, E.A., Lukashova, L.I., Lobach, J.B., and Domaradskij, I.V. (1985) Shuttle vector for Escherichia coli, Pseudomonas putida, and Pseudomonas aeruginosa. *Basic Life Sci* **30**: 657-662.

MacDonald, R.E., and Lanyi, L.K. (1975) Light-induced leucine transport in Halobacterium halobium envelope vesicles: a chemiosmotic system. *Biochemistry* **14**: 2882-2889.

MacDonald, R.E., Greene, R.V., Clark, R.D., and Lindley, E.V. (1979) Characterization of the light-driven sodium pump of Halobacterium halobium. Consequences of sodium efflux as the primary light-driven event. *J Biol Chem* **254**: 11831-11838.

MacNeil, I.A., Tiong, C.L., Minor, C., August, P.R., Grossman, T.H., Loiacono, K.A. et al. (2001) Expression and isolation of antimicrobial small molecules from soil DNA libraries. *J Mol Microbiol Biotechnol* **3**: 301-308.

Man-Aharonovich, D., Sabehi, G., Sineshchekov, O.A., Spudich, E.N., Spudich, J.L., and Beja, O. (2004) Characterization of RS29, a blue-green proteorhodopsin variant from the Red Sea. *Photochem Photobiol Sci* **3**: 459-462.

Man, D., Wang, W., Sabehi, G., Aravind, L., Post, A.F., Massana, R. et al. (2003) Diversification and spectral tuning in marine proteorhodopsins. *EMBO J* **22**: 1725-1731.

Maresca, J.A., Graham, J.E., Wu, M., Eisen, J.A., and Bryant, D.A. (2007) Identification of a fourth family of lycopene cyclases in photosynthetic bacteria. *Proc Natl Acad Sci U S A* **104**: 11784-11789.

Martinez, A., Bradley, A.S., Waldbauer, J.R., Summons, R.E., and DeLong, E.F. (2007) Proteorhodopsin photosystem gene expression enables photophosphorylation in a heterologous host. *Proc Natl Acad Sci U S A* **104**: 5590-5595.

Martinez, A., Kolvek, S.J., Yip, C.L., Hopke, J., Brown, K.A., MacNeil, I.A., and Osburne, M.S. (2004) Genetically modified bacterial strains and novel bacterial artificial chromosome shuttle vectors for constructing environmental libraries and detecting heterologous natural products in multiple expression hosts. *Appl Environ Microbiol* **70**: 2452-2463.

Martinez, A.A.M.A., and Delong, E.F.C.M.A. (2009) Heterologous Expression Of Proteorhodopsin Photosystem. In. US.

Matsuno-Yagi, A., and Mukohata, Y. (1980) ATP synthesis linked to light-dependent proton uptake in a rad mutant strain of Halobacterium lacking bacteriorhodopsin. *Arch Biochem Biophys* **199**: 297-303.

McCarren, J., and DeLong, E.F. (2007) Proteorhodopsin photosystem gene clusters exhibit co-evolutionary trends and shared ancestry among diverse marine microbial phyla. *Environ Microbiol* **9**: 846-858.

Meijnen, J.P., de Winde, J.H., and Ruijssenaars, H.J. (2008) Engineering Pseudomonas putida S12 for efficient utilization of D-xylose and L-arabinose. *Appl Environ Microbiol* **74**: 5031-5037.

Mendelsohn, R., Verma, A.L., Bernstein, H.J., and Kates, M. (1974) Structural studies of bacteriorhodopsin from Halobacterium cutirubrum by resonance Raman spectroscopy. *Can J Biochem* **52**: 774-781.

Michel, H., and Oesterhelt, D. (1976) Light-induced changes of the pH gradient and the membrane potential in H. halobium. *FEBS Lett* **65**: 175-178.

Michel, H., and Oesterhelt, D. (1980) Three-dimensional crystals of membrane proteins: bacteriorhodopsin. *Proc Natl Acad Sci U S A* **77**: 1283-1285.

Miller, C.D., Pettee, B., Zhang, C., Pabst, M., McLean, J.E., and Anderson, A.J. (2009) Copper and cadmium: responses in Pseudomonas putida KT2440. *Lett Appl Microbiol* **49**: 775-783.

Misawa, N., Nakagawa, M., Kobayashi, K., Yamano, S., Izawa, Y., Nakamura, K., and Harashima, K. (1990) Elucidation of the Erwinia uredovora carotenoid biosynthetic pathway by functional analysis of gene products expressed in Escherichia coli. *J Bacteriol* **172**: 6704-6712.

Molina, L., Ramos, C., Duque, E., Ronchel, M.C., Garcia, J.M., Wyke, L., and Ramos, J.L. (2000) Survival of Pseudomonas putida KT2440 in soil and in the rhizosphere of plants under greenhouse and environmental conditions. *Soil Biology & Biochemistry* **32**: 315-321.

Mongodin, E.F., Nelson, K.E., Daugherty, S., Deboy, R.T., Wister, J., Khouri, H. et al. (2005) The genome of Salinibacter ruber: convergence and gene exchange among hyperhalophilic bacteria and archaea. *Proc Natl Acad Sci U S A* **102**: 18147-18152.

Morrice, L.M., McLean, M.W., Long, W.F., and Williamson, F.B. (1983a) Beta-agarases I and II from Pseudomonas atlantica. Substrate specificities. *Eur J Biochem* **137**: 149-154.

Morrice, L.M., McLean, M.W., Williamson, F.B., and Long, W.F. (1983b) beta-agarases I and II from Pseudomonas atlantica. Purifications and some properties. *Eur J Biochem* **135**: 553-558.

Morris, R.M., Rappe, M.S., Connon, S.A., Vergin, K.L., Siebold, W.A., Carlson, C.A., and Giovannoni, S.J. (2002) SAR11 clade dominates ocean surface bacterioplankton communities. *Nature* **420**: 806-810.

Mullis, K., Faloona, F., Scharf, S., Saiki, R., Horn, G., and Erlich, H. (1986) Specific enzymatic amplification of DNA in vitro: the polymerase chain reaction. *Cold Spring Harb Symp Quant Biol* **51 Pt 1**: 263-273.

Nakano, Y., Yoshida, Y., Yamashita, Y., and Koga, T. (1995) Construction of a series of pACYC-derived plasmid vectors. *Gene* **162**: 157-158.

Nelson, K.E., Weinel, C., Paulsen, I.T., Dodson, R.J., Hilbert, H., Martins dos Santos, V.A. et al. (2002) Complete genome sequence and comparative analysis of the metabolically versatile Pseudomonas putida KT2440. *Environ Microbiol* **4**: 799-808.

Neumann, K., Verhoefen, M.K., Weber, I., Glaubitz, C., and Wachtveitl, J. (2008) Initial reaction dynamics of proteorhodopsin observed by femtosecond infrared and visible spectroscopy. *Biophys J* **94**: 4796-4807.

Nwachukwu, S.U. (2001) Bioremediation of sterile agricultural soils polluted with crude petroleum by application of the soil bacterium, Pseudomonas putida, with inorganic nutrient supplementations. *Curr Microbiol* **42**: 231-236.

Oesterhelt, D., and Stoeckenius, W. (1971) Rhodopsin-like protein from the purple membrane of Halobacterium halobium. *Nat New Biol* **233**: 149-152.

Oesterhelt, D., and Stoeckenius, W. (1973) Functions of a new photoreceptor membrane. *Proc Natl Acad Sci U S A* **70**: 2853-2857.

Oesterhelt, D., and Hess, B. (1973) Reversible photolysis of the purple complex in the purple membrane of Halobacterium halobium. *Eur J Biochem* **37**: 316-326.

Oesterhelt, D., and Krippahl, G. (1973) Light inhibition of respiration in Halobacterium halobium. *FEBS Lett* **36**: 72-76.

Oesterhelt, D., and Schuhman, L. (1974) Reconstitution of Bacteriorhodopsin. *Febs Letters* **44**: 262-265.

Oesterhelt, D., Meentzen, M., and Schuhmann, L. (1973) Reversible dissociation of the purple complex in bacteriorhodopsin and identification of 13-cis and all-trans-retinal as its chromophores. *Eur J Biochem* **40**: 453-463.

Oesterhelt, D., Schuhman, L., and Gruber, H. (1974) Light-Dependent Reaction of Bacteriorhodopsin with Hydroxylamine in Cell-Suspensions of Halobacterium-Halobium - Demonstration of an Apo-Membrane. *Febs Letters* **44**: 257-261.

Oesterhelt, D., Brauchle, C., and Hampp, N. (1991) Bacteriorhodopsin: a biological material for information processing. *Q Rev Biophys* **24**: 425-478.

Oh, H.M., Kwon, K.K., Kang, I., Kang, S.G., Lee, J.H., Kim, S.J., and Cho, J.C. (2010) Complete genome sequence of "Candidatus Puniceispirillum marinum" IMCC1322, a representative of the SAR116 clade in the Alphaproteobacteria. *J Bacteriol* **192**: 3240-3241.

Olekhnovich, I.N., and Fomichev, Y.K. (1994) Controlled-expression shuttle vector for pseudomonads based on the trpIBA genes of Pseudomonas putida. *Gene* **140**: 63-65.

Olivera, E.R., Carnicero, D., Jodra, R., Minambres, B., Garcia, B., Abraham, G.A. et al. (2001) Genetically engineered Pseudomonas: a factory of new bioplastics with broad applications. *Environ Microbiol* **3**: 612-618.

Partha, R., Krebs, R., Caterino, T.L., and Braiman, M.S. (2005) Weakened coupling of conserved arginine to the proteorhodopsin chromophore and its counterion implies structural differences from bacteriorhodopsin. *Biochim Biophys Acta* **1708**: 6-12.

Peck, R.F., Echavarri-Erasun, C., Johnson, E.A., Ng, W.V., Kennedy, S.P., Hood, L. et al. (2001) brp and blh are required for synthesis of the retinal cofactor of bacteriorhodopsin in Halobacterium salinarum. *J Biol Chem* **276**: 5739-5744.

Phillips, A.T., and Mulfinger, L.M. (1981) Cyclic adenosine 3',5'-monophosphate levels in Pseudomonas putida and Pseudomonas aeruginosa during induction and carbon catabolite repression of histidase synthesis. *J Bacteriol* **145**: 1286-1292.

Polivka, T., Balashov, S.P., Chabera, P., Imasheva, E.S., Yartsev, A., Sundstrom, V., and Lanyi, J.K. (2009) Femtosecond carotenoid to retinal energy transfer in xanthorhodopsin. *Biophys J* **96**: 2268-2277.

Ramos, J.-L. (2004) *Pseudomonas*. Boston: Kluwer Academic/Plenum.

Ramos, J.L., Wasserfallen, A., Rose, K., and Timmis, K.N. (1987) Redesigning metabolic routes: manipulation of TOL plasmid pathway for catabolism of alkylbenzoates. *Science* **235**: 593-596.

Ramos, J.L., Duque, E., Godoy, P., and Segura, A. (1998) Efflux pumps involved in toluene tolerance in Pseudomonas putida DOT-T1E. *J Bacteriol* **180**: 3323-3329.

Ranaghan, M.J., Schwall, C.T., Alder, N.N., and Birge, R.R. (2011) Green proteorhodopsin reconstituted into nanoscale phospholipid bilayers (nanodiscs) as photoactive monomers. *J Am Chem Soc* **133**: 18318-18327.

Ranaghan, M.J., Shima, S., Ramos, L., Poulin, D.S., Whited, G., Rajasekaran, S. et al. (2010) Photochemical and thermal stability of green and blue proteorhodopsins: implications for protein-based bioelectronic devices. *J Phys Chem B* **114**: 14064-14070.

Rappe, M., Ferriera, S., Johnson, J., Kravitz, S., Beeson, K., Sutton, G. et al. (2009) Direct Sequence Submission: alpha proteobacterium HIMB114. In: GenBank: Accession # GG704932.

Reckel, S., Gottstein, D., Stehle, J., Lohr, F., Verhoefen, M.K., Takeda, M. et al. (2011) Solution NMR Structure of Proteorhodopsin. *Angew Chem Int Ed Engl.*

Regenhardt, D., Heuer, H., Heim, S., Fernandez, D.U., Strompl, C., Moore, E.R., and Timmis, K.N. (2002) Pedigree and taxonomic credentials of Pseudomonas putida strain KT2440. *Environ Microbiol* **4**: 912-915.

Reyrat, J.M., Pelicic, V., Gicquel, B., and Rappuoli, R. (1998) Counterselectable markers: untapped tools for bacterial genetics and pathogenesis. *Infect Immun* **66**: 4011-4017.

Rich, V.I., Konstantinidis, K., and DeLong, E.F. (2008) Design and testing of 'genome-proxy' microarrays to profile marine microbial communities. *Environ Microbiol* **10**: 506-521.

Riedel, T., Tomasch, J., Buchholz, I., Jacobs, J., Kollenberg, M., Gerdts, G. et al. (2010) Constitutive expression of the proteorhodopsin gene by a flavobacterium strain representative of the proteorhodopsin-producing microbial community in the North Sea. *Appl Environ Microbiol* **76**: 3187-3197.

Rodriguez-Valera, F., Nieto, J.J., and Ruiz-Berraquero, F. (1983) Light as an energy source in continuous cultures of bacteriorhodopsin-containing halobacteria. *Appl Environ Microbiol* **45**: 868-871.

Rogers, P.J., and Morris, C.A. (1978) Regulation of Bacteriorhodopsin Synthesis by Growth-Rate in Continuous Cultures of Halobacterium-Halobium. *Archives of Microbiology* **119**: 323-325.

Rohmer, M., Seemann, M., Horbach, S., Bringer-Meyer, S., and Sahm, H. (1996) Glyceraldehyde 3-Phosphate and Pyruvate as Precursors of Isoprenic Units in an Alternative Non-mevalonate Pathway for Terpenoid Biosynthesis. *Journal of the American Chemical Society* **118**: 2564-2566.

Rondon, M.R., August, P.R., Bettermann, A.D., Brady, S.F., Grossman, T.H., Liles, M.R. et al. (2000) Cloning the soil metagenome: a strategy for accessing the genetic and functional diversity of uncultured microorganisms. *Appl Environ Microbiol* **66**: 2541-2547.

Rusch, D.B., Halpern, A.L., Sutton, G., Heidelberg, K.B., Williamson, S., Yooseph, S. et al. (2007) The Sorcerer II Global Ocean Sampling expedition: northwest Atlantic through eastern tropical Pacific. *PLoS Biol* **5**: e77.

Sabehi, G., Beja, O., Suzuki, M.T., Preston, C.M., and DeLong, E.F. (2004) Different SAR86 subgroups harbour divergent proteorhodopsins. *Environ Microbiol* **6**: 903-910.

Sabehi, G., Massana, R., Bielawski, J.P., Rosenberg, M., Delong, E.F., and Beja, O. (2003) Novel Proteorhodopsin variants from the Mediterranean and Red Seas. *Environ Microbiol* **5**: 842-849.

Sabehi, G., Loy, A., Jung, K.H., Partha, R., Spudich, J.L., Isaacson, T. et al. (2005) New insights into metabolic properties of marine bacteria encoding proteorhodopsins. *PLoS Biol* **3**: e273.

Sambrook, J., Fritsch, E.F., and Maniatis, T. (1989) *Molecular cloning : a laboratory manual.* Cold Spring Harbor, N.Y.: Cold Spring Harbor Laboratory.

Sandmann, G., and Misawa, N. (1992) New functional assignment of the carotenogenic genes crtB and crtE with constructs of these genes from Erwinia species. *FEMS Microbiol Lett* **69**: 253-257.

Sanger, F., Nicklen, S., and Coulson, A.R. (1977) DNA sequencing with chain-terminating inhibitors. *Proc Natl Acad Sci U S A* **74**: 5463-5467.

Sasaki, J., Brown, L.S., Chon, Y.S., Kandori, H., Maeda, A., Needleman, R., and Lanyi, J.K. (1995) Conversion of bacteriorhodopsin into a chloride ion pump. *Science* **269**: 73-75.

Sauer, B. (1994) Site-specific recombination: developments and applications. *Curr Opin Biotechnol* **5**: 521-527.

Sauer, U., Canonaco, F., Heri, S., Perrenoud, A., and Fischer, E. (2004) The soluble and membrane-bound transhydrogenases UdhA and PntAB have divergent functions in NADPH metabolism of Escherichia coli. *J Biol Chem* **279**: 6613-6619.

Schmid, A., Dordick, J.S., Hauer, B., Kiener, A., Wubbolts, M., and Witholt, B. (2001) Industrial biocatalysis today and tomorrow. *Nature* **409**: 258-268.

Schmies, G., Luttenberg, B., Chizhov, I., Engelhard, M., Becker, A., and Bamberg, E. (2000) Sensory rhodopsin II from the haloalkaliphilic natronobacterium pharaonis: light-activated proton transfer reactions. *Biophys J* **78**: 967-976.

Seki, T., Isono, K., Ozaki, K., Tsukahara, Y., Shibata-Katsuta, Y., Ito, M. et al. (1998) The metabolic pathway of visual pigment chromophore formation in Drosophila melanogaster--all-trans (3S)-3-hydroxyretinal is formed from all-trans retinal via (3R)-3-hydroxyretinal in the dark. *Eur J Biochem* **257**: 522-527.

Seow, K.T., Meurer, G., Gerlitz, M., Wendt-Pienkowski, E., Hutchinson, C.R., and Davies, J. (1997) A study of iterative type II polyketide synthases, using bacterial genes cloned from soil DNA: a means to access and use genes from uncultured microorganisms. *J Bacteriol* **179**: 7360-7368.

Shand, R.F., and Betlach, M.C. (1991) Expression of the Bop Gene-Cluster of Halobacterium-Halobium Is Induced by Low Oxygen-Tension and by Light. *Journal of Bacteriology* **173**: 4692-4699.

Sharma, A.K., Spudich, J.L., and Doolittle, W.F. (2006) Microbial rhodopsins: functional versatility and genetic mobility. *Trends Microbiol* **14**: 463-469.

Sharma, A.K., Sommerfeld, K., Bullerjahn, G.S., Matteson, A.R., Wilhelm, S.W., Jezbera, J. et al. (2009) Actinorhodopsin genes discovered in diverse freshwater habitats and among cultivated freshwater Actinobacteria. *ISME J* **3**: 726-737.

Shi, L., Lake, E.M., Ahmed, M.A., Brown, L.S., and Ladizhansky, V. (2009) Solid-state NMR study of proteorhodopsin in the lipid environment: secondary structure and dynamics. *Biochim Biophys Acta* **1788**: 2563-2574.

Simoni, R.D., and Postma, P.W. (1975) The energetics of bacterial active transport. *Annu Rev Biochem* **44**: 523-554.

Slamovits, C.H., Okamoto, N., Burri, L., James, E.R., and Keeling, P.J. (2011) A bacterial proteorhodopsin proton pump in marine eukaryotes. *Nat Commun* **2**: 183.

Spudich, J.L., Zacks, D.N., and Bogomolni, R.A. (1995) Microbial sensory rhodopsins: Photochemistry and function. *Israel Journal of Chemistry* **35**: 495-513.

Spudich, J.L., Yang, C.S., Jung, K.H., and Spudich, E.N. (2000) Retinylidene proteins: structures and functions from archaea to humans. *Annu Rev Cell Dev Biol* **16**: 365-392.

Stein, J.L., Marsh, T.L., Wu, K.Y., Shizuya, H., and DeLong, E.F. (1996) Characterization of uncultivated prokaryotes: isolation and analysis of a 40-kilobase-pair genome fragment from a planktonic marine archaeon. *J Bacteriol* **178**: 591-599.

Steindler, L., Schwalbach, M.S., Smith, D.P., Chan, F., and Giovannoni, S.J. (2011) Energy starved Candidatus Pelagibacter ubique substitutes light-mediated ATP production for endogenous carbon respiration. *PLoS One* **6**: e19725.

Stingl, U., Desiderio, R.A., Cho, J.C., Vergin, K.L., and Giovannoni, S.J. (2007) The SAR92 clade: an abundant coastal clade of culturable marine bacteria possessing proteorhodopsin. *Appl Environ Microbiol* **73**: 2290-2296.

Stoeckenius, W., and Kunau, W.H. (1968) Further Characterization of Particulate Fractions from Lysed Cell Envelopes of Halobacterium Halobium and Isolation of Gas Vacuole Membranes. *Journal of Cell Biology* **38**: 337-&.

Stuart, J.A.C.C.T. (2008) Binary Optical Compound and Method of Manufacture. In. US.

Timmis, K.N. (2002) Pseudomonas putida: a cosmopolitan opportunist par excellence. *Environ Microbiol* **4**: 779-781.

Uhlinger, D.J., and White, D.C. (1983) Relationship Between Physiological Status and Formation of Extracellular Polysaccharide Glycocalyx in Pseudomonas atlantica. *Appl Environ Microbiol* **45**: 64-70.

Unden, G., and Bongaerts, J. (1997) Alternative respiratory pathways of Escherichia coli: energetics and transcriptional regulation in response to electron acceptors. *Biochim Biophys Acta* **1320**: 217-234.

United States. Office of the Federal Register., and National Archives (U.S.) (1982) Federal register. In *Certified host-vector systems*. Washington, D.C.: [Office of the Federal Register, National Archives and Records Service Supt. of Docs., U.S. G.P.O., p. 17197.

Varo, G., Brown, L.S., Needleman, R., and Lanyi, J.K. (1996) Proton transport by halorhodopsin. *Biochemistry* **35**: 6604-6611.

Varo, G., Brown, L.S., Lakatos, M., and Lanyi, J.K. (2003) Characterization of the photochemical reaction cycle of proteorhodopsin. *Biophys J* **84**: 1202-1207.

Varo, G., Brown, L.S., Sasaki, J., Kandori, H., Maeda, A., Needleman, R., and Lanyi, J.K. (1995) Light-driven chloride ion transport by halorhodopsin from Natronobacterium pharaonis. 1. The photochemical cycle. *Biochemistry* **34**: 14490-14499.

Venter, J.C., Remington, K., Heidelberg, J.F., Halpern, A.L., Rusch, D., Eisen, J.A. et al. (2004) Environmental genome shotgun sequencing of the Sargasso Sea. *Science* **304**: 66-74.

Verhoefen, M.K., Schafer, G., Shastri, S., Weber, I., Glaubitz, C., Mantele, W., and Wachtveitl, J. (2011) Low temperature FTIR spectroscopy provides new insights in the pH-dependent proton pathway of proteorhodopsin. *Biochim Biophys Acta* **1807**: 1583-1590.

Vicente, M., and Canovas, J.L. (1973a) Glucolysis in Pseudomonas putida: physiological role of alternative routes from the analysis of defective mutants. *J Bacteriol* **116**: 908-914.

Vicente, M., and Canovas, J.L. (1973b) Regulation of the glucolytic enzymes in Pseudomonas putida. *Arch Mikrobiol* **93**: 53-64.

Vignais, P.M., Colbeau, A., Willison, J.C., and Jouanneau, Y. (1985) Hydrogenase, nitrogenase, and hydrogen metabolism in the photosynthetic bacteria. *Adv Microb Physiol* **26**: 155-234.

Voet, D., and Voet, J.G. (2004) *Biochemistry*. New York: J. Wiley & Sons.

Walter, J.M., Greenfield, D., and Liphardt, J. (2010) Potential of light-harvesting proton pumps for bioenergy applications. *Curr Opin Biotechnol* **21**: 265-270.

Walter, J.M., Greenfield, D., Bustamante, C., and Liphardt, J. (2007) Light-powering Escherichia coli with proteorhodopsin. *Proc Natl Acad Sci U S A* **104**: 2408-2412.

Wang, G.Y., Graziani, E., Waters, B., Pan, W., Li, X., McDermott, J. et al. (2000) Novel natural products from soil DNA libraries in a streptomycete host. *Org Lett* **2**: 2401-2404.

Wang, W.W., Sineshchekov, O.A., Spudich, E.N., and Spudich, J.L. (2003) Spectroscopic and photochemical characterization of a deep ocean proteorhodopsin. *J Biol Chem* **278**: 33985-33991.

Wang, Z., Xiong, G., and Lutz, F. (1995) Site-specific integration of the phage phi CTX genome into the Pseudomonas aeruginosa chromosome: characterization of the functional integrase gene located close to and upstream of attP. *Mol Gen Genet* **246**: 72-79.

Ward, P.G., Goff, M., Donner, M., Kaminsky, W., and O'Connor, K.E. (2006) A two step chemo-biotechnological conversion of polystyrene to a biodegradable thermoplastic. *Environ Sci Technol* **40**: 2433-2437.

Weber, F.J., Ooijkaas, L.P., Schemen, R.M., Hartmans, S., and de Bont, J.A. (1993) Adaptation of Pseudomonas putida S12 to high concentrations of styrene and other organic solvents. *Appl Environ Microbiol* **59**: 3502-3504.

Wolff, E.K., Bogomolni, R.A., Scherrer, P., Hess, B., and Stoeckenius, W. (1986) Color discrimination in halobacteria: spectroscopic characterization of a second sensory receptor covering the blue-green region of the spectrum. *Proc Natl Acad Sci U S A* **83**: 7272-7276.

Xiao, Y., Partha, R., Krebs, R., and Braiman, M. (2005) Time-resolved FTIR spectroscopy of the photointermediates involved in fast transient H+ release by proteorhodopsin. *J Phys Chem B* **109**: 634-641.

Yamada, K., Kawanabe, A., and Kandori, H. (2010) Importance of alanine at position 178 in proteorhodopsin for absorption of prevalent ambient light in the marine environment. *Biochemistry* **49**: 2416-2423.

Yao, B., Lei, M., Ren, L., Menke, N., Wang, Y., Fischer, T., and Hampp, N. (2005a) Polarization multiplexed write-once-read-many optical data storage in bacteriorhodopsin films. *Opt Lett* **30**: 3060-3062.

Yao, B., Ren, Z., Menke, N., Wang, Y., Zheng, Y., Lei, M. et al. (2005b) Polarization holographic high-density optical data storage in bacteriorhodopsin film. *Appl Opt* **44**: 7344-7348.

Yaphe, W. (1957) The use of agarase from Pseudomonas atlantica in the identification of agar in marine algae (Rhodophyceae). *Can J Microbiol* **3**: 987-993.

Yaphe, W., and Morgan, K. (1959) Enzymic hydrolysis of fucoidin by Pseudomonas atlantica and Pseudomonas carrageenovora. *Nature* **183**: 761-762.

Yoshitsugu, M., Shibata, M., Ikeda, D., Furutani, Y., and Kandori, H. (2008) Color change of proteorhodopsin by a single amino acid replacement at a distant cytoplasmic loop. *Angew Chem Int Ed Engl* **47**: 3923-3926.

Zhao, M., Chen, F., and Jiao, N. (2009) Genetic diversity and abundance of flavobacterial proteorhodopsin in China seas. *Appl Environ Microbiol* **75**: 529-533.